

MODEL HAMILTONIANS FOR THE CALCULATION
OF ATOMIC AND MOLECULAR SPECTROSCOPY

By

JOHN DAVID BAKER

A DISSERTATION PRESENTED TO THE GRADUATE SCHOOL
OF THE UNIVERSITY OF FLORIDA IN PARTIAL FULFILLMENT
OF THE REQUIREMENTS FOR THE DEGREE OF
DOCTOR OF PHILOSOPHY

UNIVERSITY OF FLORIDA

1991

ACKNOWLEDGMENTS

I would like to thank first and foremost my wife, Rebecca, for her understanding and support that was crucial to the success of this work. Secondly, I would like to thank Tennessee Eastman for the financial support that accelerated this project. A special thanks goes to my committee who have struggled with me to get many recommendations and resumes in the mail. I thank my advisor, Dr. Zerner, for allowing me the freedom I desire to explore my own ideas while supporting me in the process. This, I feel, is truly unique in the academic business and I certainly realize the personal sacrifice he has made to allow his guys this privilege. And finally, I would like to thank the guys in the clubhouse who put up with my songs and occasional bouts of sarcasm.

TABLE OF CONTENTS

ACKNOWLEDGMENTS	ii
ABSTRACT	v
CHAPTERS	
1. INTRODUCTION	1
Motivation	1
Time Dependent Perturbation Theory	5
Molecular Response to Radiation	7
The Reporting of Theoretically Calculated Spectral Probabilities	13
2. GENERAL THEORY	20
The Hartree-Fock Equations	20
The Roothaan Equations	27
The Calculation of Electronic Spectra	31
Singlet Excitations with a Finite Basis	41
3. THE INDO/RPA METHOD	44
Theory	44
Benzene and Pyridine	51
Naphthalene and Quinoline	58
The Diazines	61
The RPA for Extended Systems	65
4. THE UV-VIS SPECTRA OF FREE BASE AND MAGNESIUM PORPHIN	70
Motivation	70
Results	73
Discussion	76

5. THE INDO/RPA CALCULATION OF NMR CHEMICAL SHIELDING	79
The Concept of Chemical Shift	79
Theory	82
Localization and Integral Evaluation	93
Reduced Linear Equations	97
Diamagnetic Shielding in Molecules	101
The INDO/RPA Method for Chemical Shift	104
6. A CHARGE DEPENDENT HAMILTONIAN FOR ATOMIC PROPERTIES	109
Impetus	109
Atomic Parameterization	111
A New Atomic Parameterization	115
Analysis	121
7. A DENSITY PARTITIONED HAMILTONIAN FOR MOLECULAR ELECTRONIC SPECTRA	141
Density Partitioning	141
Atomic Hamiltonian	145
Molecular Hamiltonian	149
Modified SCF Procedure	151
Results	153
8. CONCLUSIONS	156
Spectroscopy	156
Development of a Better Model	158
BIBLIOGRAPHY	161
BIOGRAPHICAL SKETCH	169

Abstract of Dissertation Presented to the Graduate School
of the University of Florida in Partial Fulfillment of the
Requirements for the Degree of Doctor of Philosophy

MODEL HAMILTONIANS FOR THE CALCULATION
OF ATOMIC AND MOLECULAR SPECTROSCOPY

By

JOHN DAVID BAKER

May, 1991

Chairman: Michael C. Zerner
Major Department: Chemistry

Semiempirical models appropriate for the calculation of atomic and molecular spectroscopy for large systems were developed. Through equation of motion (EOM) constraints, equivalent to the random phase approximation (RPA), electronic transitions and oscillator strengths are calculated directly. The RPA formalism is demonstrated to give accurate transition energies for electronic excitations. The EOM constraints guarantee equivalence between calculated oscillator strengths in differing formalisms. Although this provision is only true for a complete basis, considerable improvement in predicting oscillator strengths that compare with experiment, and differing formalisms, is demonstrated for a considerably smaller basis.

The computational tools associated with the RPA were applied to the calculation of the electronic spectra of free base and magnesium porphin. The ability of the RPA formalism to predict accurate oscillator strengths and selectively correlate transition energies has allowed direct corroboration of the experimental spectra associated with these molecules. The RPA formalism is also used for the calculation of isotropic nuclear magnetic resonance (NMR) chemical shift. The method is capable of demonstrating the inductive effects associated with electron-withdrawing substituents and is capable of differentiating types of bonding environments. The prediction of paramagnetic substituent effects, however, was found to be deficient due to the small size of the basis utilized.

Minimal basis set (MBS) formalisms are restricted in their ability to predict accurate results for properties. In order to maximize the capability of model Hamiltonians and maintain the efficiency of such MBS formalisms, a complete charge-dependent intermediate neglect of differential overlap (INDO) Hamiltonian appropriate for the calculation of molecular spectra was developed and examined. The new model is capable of accurately describing the local chemical potential of atoms in molecules, and surpasses the current INDO/S model in the prediction of carbonyl excitation energies. A procedure for the acquisition of atomic and molecular parameters was developed that makes use of readily available experimental data. Simplified parameter functions were developed which allow more information to be incorporated into the model with less effort than previously.

CHAPTER 1 INTRODUCTION

Motivation

Chemistry is the study of interactions at the atomic and molecular level. These interactions can be between the atoms that constitute a molecule, between molecules or between a molecule and its environment. Quantum chemistry dedicates itself to the task of predicting observables associated with these interactions. One specific area of study is the interaction of matter with long wavelength radiation. Molecules react to short-lived pulses of radiation in many ways depending on the frequency of the radiation. High-energy radiation may result in dissociation or ionization. Low-energy radiation may result in orientational changes of a molecule. In all cases, however, specific molecules respond to radiation of differing wavelength very uniquely and can be characterized by their specific ability to interact with radiation of a given frequency.

The range of wavelength associated with visible and ultraviolet light usually corresponds to electronic transitions in molecules. Light of a set wavelength may be absorbed by the material resulting in a new electronic state. This absorption will take place with a given probability which is again a function of the molecule of interest. In addition, the probability for which a molecule absorbs

radiation of fixed wavelength but opposite polarization may differ. The qualitative and quantitative prediction of these types of interactions has been prominent in quantum chemistry from its inception. While quantum mechanics can in principle yield exact results for all molecular interactions, the difficulty in obtaining these solutions has led workers to seek approximate solutions. Early Hückel theory models are successful in predicting the qualitative nature of molecular absorptions of visible and ultraviolet light for planar conjugated systems [1]. More exact models such as that of Pariser, Parr and Pople (PPP) for conjugated systems were developed and the agreement between theory and experiment was extended to the accurate prediction of transition energies [2–4]. Hückel theory was also extended to nonplanar systems [5].

Modern approximate methods usually involve the use of well-characterized experimental data for small systems to fit quantum mechanical models that can be extrapolated to much larger systems. The spectroscopic parameterization of the Intermediate Neglect of Differential Overlap (INDO/S) model Hamiltonian has been very successful in the prediction of properties associated with electronic transitions [6, 7]. The use of the INDO/S Hamiltonian for the prediction of electronic transition moments and properties has been primarily a state-oriented approach. In other words, electronic states are calculated directly yielding transition energies as differences in state energies and transition probabilities as transition amplitudes between states.

In this work a transition-oriented approach is developed with the INDO/S model Hamiltonian and compared to the more traditional state-oriented approach. Through the use of polarization propagator (PP) techniques [8], transition energies and probability amplitudes can be calculated directly without the need to describe the individual states. If exact state functions can be found then both the state—and transition-oriented approaches are equivalent. For almost all cases, however, approximate state solutions are employed and methods that are capable of giving the most consistent solution to a given property must be exploited. A consistent approach to the calculation of molecular response to electromagnetic radiation will involve an equitable treatment of transition moments as calculated in both the dipole length and dipole velocity formalisms. This consistency requirement will be sufficient to derive the equations associated with the Random Phase Approximation (RPA) [9, 10]. In this way a balanced treatment of transition amplitudes can be achieved.

Many properties are computationally related to the transition energies and moments associated with electronic excitations. Such properties are usually associated with the response of the total energy of a molecule to an external perturbation such as a constant magnetic field [11, 12]. These properties are often expressed as a perturbative expansion of the total energy and truncated at some order. For a small perturbation the expansion can be truncated at second order which usually involves a formal sum over all transition moments and associated

energies. Computational tools used must not become prohibitively expensive as the size of the system becomes larger regardless of the Hamiltonian used. For properties that involve a formal sum over all the states of a system, the techniques necessary to calculate individual state transition moments become too difficult. The method of reduced linear equations [13] as recently employed in the calculation of molecular polarizabilities [14] meets the criteria of expediency for sum over state properties. This technique is used in the calculation of Nuclear Magnetic Resonance (NMR) shielding tensors at the RPA level of theory for large compounds which would not be possible otherwise [15].

Accurate ab initio calculations with the RPA for small systems has yielded excellent results but ab initio techniques are often too computationally intensive for large molecules. If quantum chemistry is to be predictive for the majority of chemical systems model Hamiltonians will continue to be a necessary tool. It is therefore prudent to develop and characterize the basic structure of model Hamiltonians and the content of the parameters in such models. To this end the basic form of the atomic parameters in the INDO model are examined. In conjunction with recent developments in density functional theory [16] this examination suggests generalization and improvement of the current Hamiltonian used for electronic spectra.

Time Dependent Perturbation Theory

If a molecule is subjected to a short duration of long wavelength radiation the response of the molecule to such radiation can be treated as a time dependent perturbation. Stationary state solutions (Ψ_i^0) to the time dependent Schrödinger equation

$$\hat{H}^0 \Psi^0 = -\frac{\hbar}{i} \frac{\partial \Psi^0}{\partial t} \quad (1-1)$$

for time independent Hamiltonians (\hat{H}^0) can be expressed as,

$$\Psi_i^0(q, t) = \exp(-iE_i^0 t/\hbar) \psi_i(q) \quad (1-2)$$

where E_i^0 is the total energy of stationary state i . The ψ_i are orthonormal functions of space and spin coordinates (q) only and are eigenfunctions of \hat{H}^0 .

For a time dependent potential energy perturbation (\hat{H}') Equation (1-1) becomes

$$(\hat{H}^0 + \hat{H}') \Psi = -\frac{\hbar}{i} \frac{\partial \Psi}{\partial t} . \quad (1-3)$$

For a fixed point in time, solutions to Equation (1-3) can be expressed as a linear combination of Ψ_i^0 since they are eigenfunctions of the Hermitian operator \hat{H}^0 and thus form a complete set. For different points in time the coefficients of the expansion will in general be different; therefore, solutions for Equation (1-3) of the form

$$\Psi = \sum_j a_j(t) \Psi_j^0(q, t) = \sum_j a_j(t) \exp(-iE_j^0 t/\hbar) \psi_j(q) \quad (1-4)$$

must be sought. Substitution of Equation (1-4) into Equation (1-3) yields,

$$\begin{aligned} \sum_j [E_j^0 a_j(t) + \hat{H}' a_j(t)] \exp(-iE_j^0 t/\hbar) \psi_j(q) = \\ \sum_j [E_j^0 a_j(t) - \frac{\hbar}{i} \frac{da_j(t)}{dt}] \exp(-iE_j^0 t/\hbar) \psi_j(q). \end{aligned} \quad (1-5)$$

Utilizing the orthonormality of ψ_i one obtains,

$$\sum_j a_j(t) \exp(-iE_j^0 t/\hbar) \langle \psi_k | \hat{H}' | \psi_j \rangle = -\frac{\hbar}{i} \frac{da_k(t)}{dt} \exp(-iE_k^0 t/\hbar) \quad (1-6)$$

so that Equation (1-3) becomes a series of differential equations in time for the coefficients in Equation (1-4) without loss of generality [17].

$$\frac{da_k(t)}{dt} = -\frac{i}{\hbar} \sum_j a_j(t) \exp[i(E_k^0 - E_j^0)t/\hbar] \langle \psi_k | \hat{H}' | \psi_j \rangle \quad (1-7)$$

For a system in state m in the absence of a time dependent perturbation we can choose initial conditions such that $a_m \approx 1$ and $a_{n \neq m} \approx 0$. For a perturbation applied at time 0 of sufficiently short duration that the coefficients are close to their initial values we can approximate Equation (1-7) as

$$\frac{da_k(t)}{dt} \approx -\frac{i}{\hbar} \exp[i(E_k^0 - E_m^0)t/\hbar] \langle \psi_k | \hat{H}' | \psi_m \rangle \quad (1-8)$$

and integrate from $t=0$ to t' to obtain an approximate expression for the coefficients.

$$\begin{aligned} \int_0^{t'} da_k(t) &\approx -\frac{i}{\hbar} \int_0^{t'} \exp[i(E_k^0 - E_m^0)t/\hbar] \langle \psi_k | \hat{H}' | \psi_m \rangle dt \\ a_k(t') &\approx a_k(0) - \frac{i}{\hbar} \int_0^{t'} \exp[i(E_k^0 - E_m^0)t/\hbar] \langle \psi_k | \hat{H}' | \psi_m \rangle dt \end{aligned} \quad (1-9)$$

If the perturbation ceases after t' then the final state function can be expressed as Equation (1-4) with constant $a_k(t')$. This result is a superposition of eigenstates of the unperturbed Hamiltonian. The probability of observing the system in state n with energy E_n^0 after the perturbation is then [18],

$$P_n = |a_n(t') \exp(-iE_n^0 t'/\hbar)|^2 = |a_n(t')|^2 \quad (1-10)$$

The effect of the perturbation is a transition from the initial state m to final state n with probability P_n .

Molecular Response to Radiation

Electromagnetic radiation consists of both electric (E) and magnetic (B) fields that can interact with the electrons within a molecule. The classical potential energy of interaction between these fields and a system of n identically charged particles (q) can be written as [19],

$$E_p = -q \sum_{i=1}^n \left(\vec{E} \cdot \vec{r}_i + \vec{B} \cdot \frac{\vec{r}_i \times \vec{p}_i}{2m_i c} \right) = -\vec{E} \cdot \vec{d} - \vec{B} \cdot \vec{\mu} \quad (1-11)$$

where the position, momentum and mass are represented by r , p and m , respectively, and c is the speed of light. The second equality expresses the interaction energy in terms of the system dipole and magnetic moments, respectively. If a classical description of the electromagnetic fields is maintained and we replace

the dipole and magnetic moments with their quantum mechanical operators the interaction energy becomes for electrons of charge $-e$

$$\hat{H}' = \sum_{i=1}^n \left(e\vec{E} \cdot \vec{r}_i + \vec{B} \cdot \frac{-ie\hbar\vec{r}_i \times \vec{\nabla}_i}{2mc} \right) = \sum_{i=1}^n \left(e\vec{E} \cdot \vec{r}_i + \vec{B} \cdot \frac{e\hat{L}_i}{2mc} \right) . \quad (1-12)$$

In the above L is the angular momentum operator.

The space and time variations of the electromagnetic fields of transverse plane waves in a vacuum can be expressed in a right-handed coordinate system $(\hat{e}_1, \hat{e}_2, \hat{e}_3)$ with propagation along \hat{e}_3 as

$$\begin{aligned} \vec{E}(\vec{r}, t) &= (E_1\hat{e}_1 + E_2\hat{e}_2) \exp(ik\hat{e}_3 \cdot \vec{r} - i\omega t) \\ \vec{B}(\vec{r}, t) &= \hat{e}_3 \times \vec{E} \end{aligned} \quad (1-13)$$

The magnitude of the wave vector is denoted k and has dimensions of reciprocal wavelength. The variation in coordinate for an electron in a molecule is of the order of Ångstroms while the wavelength of radiation in the ultraviolet region is of the order of thousands of Ångstroms; therefore, the spatial variation of the electromagnetic field can be neglected to obtain [20]

$$\begin{aligned} \vec{E}(\vec{r}, t) &= (E_1\hat{e}_1 + E_2\hat{e}_2) \exp(-i\omega t) = \vec{E}_r \exp(-i\omega t) \\ \vec{B}(\vec{r}, t) &= (E_1\hat{e}_2 - E_2\hat{e}_1) \exp(-i\omega t) = \vec{B}_r \exp(-i\omega t) . \end{aligned} \quad (1-14)$$

The terms E_1 and E_2 are, in general, complex.

Two special cases are of interest, that of linear and circularly polarized radiation. Let E_1 be real and E_2 purely imaginary and of equal magnitude as

E_1 . Through the use of the identity $\exp(i\theta) = \cos \theta + i \sin \theta$ the real component of the fields can be expressed

$$\begin{aligned}\vec{E}_{\text{L}}(\vec{r}, t) &= E_1(\hat{e}_1 \cos \omega t \pm \hat{e}_2 \sin \omega t) \\ \vec{B}_{\text{L}}(\vec{r}, t) &= E_1(\hat{e}_2 \cos \omega t \mp \hat{e}_1 \sin \omega t)\end{aligned}\tag{1-15}$$

The upper sign designates left circularly polarized light as the rotation of the polarization vector is counterclockwise as observed towards the origin from the positive axis of propagation. The lower sign designates right circular polarization. The electric and magnetic vectors maintain mutual orthogonality. Linearly polarized radiation can be expressed as an average of pure left and right circular polarizations.

Combining Equations (1-11) and (1-15) the interaction Hamiltonian of interest is obtained.

$$\begin{aligned}\hat{H}'_{\text{L}} &= -E_1[(\hat{e}_1 \cdot \vec{d} + \hat{e}_2 \cdot \vec{\mu}) \cos \omega t \pm (\hat{e}_2 \cdot \vec{d} - \hat{e}_1 \cdot \vec{\mu}) \sin \omega t] \\ \hat{H}'_{\text{L}} &= -E_1(\hat{H}_1 \cos \omega t \pm \hat{H}_2 \sin \omega t)\end{aligned}\tag{1-16}$$

where \hat{H}_1 and \hat{H}_2 are independent of time. Defining $\omega_{km} \equiv (E_k^0 - E_m^0)/\hbar$ Equation (1-9) becomes

$$\begin{aligned}
 a_{k_L}(t') &= a_k(0) + \frac{iE_1}{\hbar} \int_0^{t'} \exp(i\omega_{km}t) \cos \omega t \langle \psi_k | \hat{H}_1 | \psi_m \rangle dt \\
 &\quad \pm \frac{iE_1}{\hbar} \int_0^{t'} \exp(i\omega_{km}t) \sin \omega t \langle \psi_k | \hat{H}_2 | \psi_m \rangle dt \\
 a_{k_R}(t') &= a_k(0) + \langle \psi_k | \hat{H}_1 | \psi_m \rangle \frac{iE_1}{\hbar} \int_0^{t'} \exp(i\omega_{km}t) \cos \omega t dt \\
 &\quad \pm \langle \psi_k | \hat{H}_2 | \psi_m \rangle \frac{iE_1}{\hbar} \int_0^{t'} \exp(i\omega_{km}t) \sin \omega t dt
 \end{aligned} \tag{1-17}$$

The sine and cosine terms can be written as exponentials

$$\begin{aligned}
 \cos \omega t &= \frac{1}{2} (\exp(i\omega t) + \exp(-i\omega t)) \\
 \sin \omega t &= \frac{i}{2} (\exp(-i\omega t) - \exp(i\omega t))
 \end{aligned} \tag{1-18}$$

and the explicit integration over time performed [19].

$$\begin{aligned}
 a_{k_L}(t') &= a_k(0) \\
 &+ \langle \psi_k | \hat{H}_1 | \psi_m \rangle \frac{iE_1}{2\hbar} \left[\frac{\exp[it'(\omega_{km} + \omega)] - 1}{\omega_{km} + \omega} + \frac{\exp[it'(\omega_{km} - \omega)] - 1}{\omega_{km} - \omega} \right] \\
 &\mp \langle \psi_k | \hat{H}_2 | \psi_m \rangle \frac{E_1}{2\hbar} \left[\frac{\exp[it'(\omega_{km} - \omega)] - 1}{\omega_{km} - \omega} - \frac{\exp[it'(\omega_{km} + \omega)] - 1}{\omega_{km} + \omega} \right]
 \end{aligned} \tag{1-19}$$

Equation (1-19) was derived on the premise that t' is small; therefore, the only cases for which a_k becomes of appreciable magnitude is if ω approaches $\pm\omega_{km}$. Since

$$\lim_{\theta \rightarrow 0} \frac{\exp(it'\theta) - 1}{\theta} = it' \tag{1-20}$$

the expression does not become infinite [18]. If $E_k^0 \rangle E_m^0$ then the case of $\omega = \omega_{km}$ corresponds to an absorption of radiation to go from state m to state k . For the opposite case we obtain the probability of stimulated emission from a higher state to a lower state. The probability for absorption for $k \neq m$ is then given by Equation (1-10) recalling the initial conditions on a_k .

$$\begin{aligned}
 P_{k_L} = a_{k_L}(t') a_{k_L}^*(t') &= P_{k_L}(\hat{H}_1, \hat{H}_2) \times P_k(E_1, t') = \\
 &\{ |\langle \psi_k | \hat{H}_1 | \psi_m \rangle|^2 + |\langle \psi_k | \hat{H}_2 | \psi_m \rangle|^2 \\
 &\mp i [\langle \psi_k | \hat{H}_1 | \psi_m \rangle \langle \psi_k | \hat{H}_2 | \psi_m \rangle^* - \langle \psi_k | \hat{H}_1 | \psi_m \rangle^* \langle \psi_k | \hat{H}_2 | \psi_m \rangle] \} \\
 &\times \frac{E_1^2}{4\hbar^2} \left[\frac{2 - \exp[it'(\omega_{km} - \omega)] - \exp[-it'(\omega_{km} - \omega)]}{(\omega_{km} - \omega)^2} \right]
 \end{aligned} \tag{1-21}$$

The time dependent portion of the probability can be simplified to yield

$$P_{k_L} = P_{k_L}(\hat{H}_1, \hat{H}_2) \times \frac{E_1^2}{\hbar^2} \left[\frac{\sin^2[.5(\omega_{km} - \omega)t']}{(\omega_{km} - \omega)^2} \right] \tag{1-22}$$

For a source of radiation that has equal portions of left and right circularly polarized light we can define two different types of absorption processes. The average of left and right polarizations ($P_{k_{lin}} \equiv P_k = .5(P_{k_L} + P_{k_R})$) yields linear polarization and the absorption process is the total response of the material to the perturbation. The remaining component corresponds to the difference in absorption between left and right polarizations ($P_{k_{diff}} \equiv P_{k_{CD}} = .5(P_{k_L} - P_{k_R})$). This

is known as circular dichroism [21]. The spatial components of the probability of absorptions becomes,

$$\begin{aligned}
 P_k(\hat{H}_1, \hat{H}_2) &= |\langle \psi_k | \hat{H}_1 | \psi_m \rangle|^2 \\
 &= |\langle \psi_k | \hat{e}_1 \cdot \vec{d} | \psi_m \rangle|^2 + |\langle \psi_k | \hat{e}_2 \cdot \vec{\mu} | \psi_m \rangle|^2 \\
 &= |\hat{e}_1 \cdot \vec{d}_{km}|^2 + |\hat{e}_2 \cdot \vec{\mu}_{km}|^2
 \end{aligned} \tag{1-23}$$

and

$$\begin{aligned}
 P_{kCD}(\hat{H}_1, \hat{H}_2) &= -\frac{1}{2}i[\langle \psi_k | \hat{H}_1 | \psi_m \rangle \langle \psi_k | \hat{H}_2 | \psi_m \rangle^* - \langle \psi_k | \hat{H}_1 | \psi_m \rangle^* \langle \psi_k | \hat{H}_2 | \psi_m \rangle] \\
 &= -i[(\hat{e}_1 \cdot \vec{d}_{km})(\hat{e}_1 \cdot \vec{\mu}_{km}) + (\hat{e}_2 \cdot \vec{d}_{km})(\hat{e}_2 \cdot \vec{\mu}_{km})]
 \end{aligned} \tag{1-24}$$

Assuming that the energy for the absorption process is supplied by the external radiation of frequency ν then

$$\begin{aligned}
 \omega_{km} - \omega &= (E_k^0 - E_m^0 - h\nu)/\hbar = 2\pi(E_k^0 - E_m^0 - h\nu)/h \\
 &= 2\pi(\nu_{km} - \nu)
 \end{aligned} \tag{1-25}$$

Normal radiation is not composed of a single frequency but is better described by a frequency distribution. The magnitude of the field E_1 is related to the radiation per unit volume (U_1) via $U_1 = (E_1)^2/8\pi$ which is also in general a function of the frequency [22]. Let $u_1(\nu)d\nu$ be the electromagnetic radiation per unit volume for frequency ν in the differential range ν to $\nu + d\nu$. In terms of probability per unit frequency the field dependent portion of the transition probability becomes [18]

$$P_k(E_1, t', d\nu) = \frac{8\pi}{h^2} u_1(\nu) \frac{\sin^2[\pi(\nu_{km} - \nu)t']}{(\nu_{km} - \nu)^2} d\nu \tag{1-26}$$

Only for ν close to ν_{km} does the frequency dependence of the probability have appreciable magnitude. The frequency of visible light is on the order of 10^{15} cycles per second or Hertz (Hz). We can therefore approximate $u_1(\nu)$ to be constant in the region of ν_{km} and integrate over all frequencies to obtain, via $\int_{-\infty}^{\infty} dx \sin^2(ax)/x^2 = a\pi$,

$$P_k(E_1, t') = P_k(\nu_{km}, t') = \frac{2\pi}{\hbar^2} u_1(\nu_{km}) t' \quad (1-27)$$

The probability per unit time is obtained by dividing by t' .

Thus far we have only been dealing with radiation that is propagating along a specific axis. For isotropic radiation ($u_1 = u_2 = u_3 = u/3$) we have to sum the probabilities over all orientations to obtain the total probability of absorption. The final expressions for the probability of absorption of a single molecule to go from state m to state k per unit time is

$$\begin{aligned} P_k &= [|\vec{d}_{km}|^2 + |\vec{\mu}_{km}|^2] \frac{2\pi}{3\hbar^2} u(\nu_{km}) \\ P_{kCD} &= -2i[\vec{d}_{km} \cdot \vec{\mu}_{km}] \frac{2\pi}{3\hbar^2} u(\nu_{km}) \end{aligned} \quad (1-28)$$

The Reporting of Theoretically Calculated Spectral Probabilities

The total probability per unit time for the absorption of a system of N molecules is simply N times the single molecule probability. There are two parts of the transition probability that are characteristic of the molecule and not a

function of time or the radiation field in this treatment. The first is the frequency or energy of the transition. The second is the proportionality constant that is a function of the transition matrix elements of the dipole and magnetic moment operators. The probability for absorption can be formulated as a proportionality constant times the density of the radiation times the number of molecules. The proportionality constant then becomes [18]

$$\begin{aligned} B_{mk} &= [|\vec{d}_{km}|^2 + |\vec{\mu}_{km}|^2] \frac{2\pi}{3\hbar^2} \\ B_{mk_{CD}} &= -2i[\vec{d}_{km} \cdot \vec{\mu}_{km}] \frac{2\pi}{3\hbar^2} \end{aligned} \quad (1-29)$$

The problem that must be addressed theoretically, therefore, is the attainment of the transition energies and the transition moments themselves.

The transition moments have been expressed as matrix elements between wave functions of the total time independent Hamiltonian operator.

$$\hat{H}^0 = \sum_i^{N_T} -\frac{\hbar^2}{2m_i} \nabla_i^2 + \sum_{i,j(i)}^{N_T} \frac{q_i q_j}{r_{ij}} \quad (1-30)$$

These state functions therefore include both the nuclear as well as the electronic components. In this treatment the electronic portion of these transition moments is of interest. The mass of the proton is approximately 1836 times the mass of the electron; therefore it is reasonable to assume that the electronic motion can be treated separately from the nuclear motion. In other words, since the electronic motion should be very fast with respect to the nuclear motion the nuclei can be treated as fixed with respect to the electronic motion and treated as a potential

field. This is commonly known as the Born-Oppenheimer approximation [17, 23].

For n electrons and M nuclei the Hamiltonian for fixed nuclei becomes

$$\hat{H}_{\text{el}}^0 = \left[- \sum_i^n \frac{\hbar^2}{2m_e} \vec{\nabla}_i^2 + \sum_i^n e^2 \left(\sum_{j \neq i} \frac{1}{r_{ij}} - \sum_{\alpha}^M \frac{Z_{\alpha}}{r_{i\alpha}} \right) \right] + \sum_{\alpha, \beta}^M \frac{e^2 Z_{\alpha} Z_{\beta}}{r_{\alpha\beta}} \quad (1-31)$$

Solutions to Equation (1-31) for arbitrary nuclear positions then defines a potential energy function ($V(r_i)$) from which the nuclear motion Hamiltonian (\hat{H}_N^0) can be defined.

$$\begin{aligned} \hat{H}^0 &= \sum_{\alpha}^M -\frac{\hbar^2}{2m_{\alpha}} \vec{\nabla}_{\alpha}^2 + \hat{H}_{\text{el}}^0 \Rightarrow \\ \hat{H}_N^0 &= \sum_{\alpha}^M -\frac{\hbar^2}{2m_{\alpha}} \vec{\nabla}_{\alpha}^2 + V(r_i) \end{aligned} \quad (1-32)$$

Under the Born-Oppenheimer approximation the Hamiltonian operator is partitioned between the electronic and nuclear motion. Therefore the state functions for the total Hamiltonian can be expressed as a product of nuclear and electronic functions in which the electronic wave function depends parametrically on the coordinates of the nuclei.

$$\psi_k = \psi_{\text{el}_k}(r_i, \{r_{\alpha}\}) \psi_{N_k}(r_{\alpha}) \quad (1-33)$$

Transition elements for perturbation operators such as dipole then become

$$\begin{aligned} \langle \psi_k | \vec{d} | \psi_m \rangle &= \langle \psi_{\text{el}_k} \psi_{N_k} | \vec{d} | \psi_{\text{el}_m} \psi_{N_m} \rangle \\ &= \langle \psi_{N_k} | \langle \psi_{\text{el}_k} | \vec{d}_e | \psi_{\text{el}_m} \rangle | \psi_{N_m} \rangle + \langle \psi_{\text{el}_k} | \langle \psi_{N_k} | \vec{d}_N | \psi_{N_m} \rangle | \psi_{\text{el}_m} \rangle \\ &= \langle \psi_{N_k} | \langle \psi_{\text{el}_k} | \vec{d}_e | \psi_{\text{el}_m} \rangle | \psi_{N_m} \rangle, \quad k \neq m \end{aligned} \quad (1-34)$$

The nuclear contribution to the dipole operator vanishes for transitions between electronic states and will not be considered further.

If for given initial nuclear and electronic state m and specific electronic state k , $\langle \psi_{elk} | \vec{d} | \psi_{elm} \rangle$ is treated as an average electronic moment for all excited nuclear states, k' , the electronic integral can be removed and the squared matrix element written

$$|\vec{d}_{km}|^2 = |\langle \psi_{elk} | \vec{d} | \psi_{elm} \rangle|^2 \times \langle \psi_{N_{k'}} | \psi_{N_m} \rangle \langle \psi_{N_m} | \psi_{N_{k'}} \rangle \quad (1-35)$$

For a given electronic transition from state m to k many possible nuclear transitions are possible. The squared overlap between nuclear state functions is known as the Franck-Condon factor for the electronic transition. The nuclear states correspond to various vibrational and rotational states for the molecule. The Frank-Condon factors then give the relative intensities of electronic transitions as divided among the various final nuclear states [18]. Considering that the $\psi_{N_{m'}}$ are eigenfunctions of a Hermitian operator corresponding to electronic state m , they form a complete set of orthonormal functions and therefore the total electronic transition probability over all final nuclear states is

$$\begin{aligned} \sum_{m'} |\vec{d}_{km}|^2 &= |\langle \psi_{elk} | \vec{d} | \psi_{elm} \rangle|^2 \times \sum_{m'} \langle \psi_{N_{k'}} | \psi_{N_{m'}} \rangle \langle \psi_{N_{m'}} | \psi_{N_{k'}} \rangle \\ &= |\langle \psi_{elk} | \vec{d} | \psi_{elm} \rangle|^2 \times \langle \psi_{N_{k'}} | \psi_{N_{k'}} \rangle = |\langle \psi_{elk} | \vec{d} | \psi_{elm} \rangle|^2 \end{aligned} \quad (1-36)$$

Therefore the total probability of an electronic transition under the Born-Oppenheimer approximation can be expressed at the average electronic state

probability. This average is usually further approximated as the value obtained between electronic states at a fixed geometry.

With the approximations to the transition moments presented above, the theoretical problem is reduced to the determination of the state functions and energies of the electronic Hamiltonian for a molecule. The frequency of a transition is obtained from the difference in state energies and the probabilities of interest are found as straightforward integrations of the perturbation operators over the electronic state functions. The total probability for electronic transitions is proportional to the sum of both dipole and magnetic moments. For dipole allowed transitions the magnetic moments are usually 10^{-4} those of the dipole transition moments and are usually neglected.

Consider a three dimensional harmonic oscillator of the same mass and charge of an electron initially in its ground vibrational state with vibrational frequency the same as that of the electronic transition in question. The proportionality constant for a change of one vibrational quantum number from the ground state is given by [18]

$$B_{01} = \frac{\pi e^2}{\nu_{km} m h} = \frac{\pi e^2}{E_{km} m} \quad (1-37)$$

The convention for reporting total electronic absorption probabilities is in the form of oscillator strengths which is defined as the ratio of the electronic proportionality

constant to that of the pure harmonic oscillator described above. The result is a dimensionless constant usually designated f_ν^r .

$$\begin{aligned} f_\nu^r &= \frac{4\pi\nu_{km}m}{3\hbar e^2} |\vec{d}_{km}|^2 = \frac{2E_{km}m}{3\hbar^2 e^2} |\vec{d}_{km}|^2 \\ &= \frac{2E_{km}m}{3\hbar^2} |\langle\psi_k|\sum_i \vec{r}_i|\psi_m\rangle|^2 \end{aligned} \quad (1-38)$$

The “r” indicates the use of the dipole length operator to calculate the transition matrix elements [24].

For circular dichroism the proportionality constant can be rewritten

$$\begin{aligned} B_{mkCD} &= -2i[\vec{d}_{km} \cdot \vec{\mu}_{km}] \frac{2\pi}{3\hbar^2} = R_{mk}^r \frac{4\pi}{3\hbar^2} \\ R_{mk}^r &= -i\langle\psi_k|\vec{d}|\psi_m\rangle\langle\psi_k|\vec{\mu}|\psi_m\rangle \\ &= \frac{e^2\hbar}{2mc} \langle\psi_m|\sum_i \vec{r}_i|\psi_k\rangle\langle\psi_m|\sum_i \vec{r}_i \times \vec{\nabla}_i|\psi_k\rangle \end{aligned} \quad (1-39)$$

R_{mk}^r is known as the rotary strength of the electronic transition from state m to k. Rotary strength has both sign and magnitude since it represents the difference between the probabilities of absorption for left and right polarized light [21, 25]. For equal absorption of left and right circularly polarized radiation the rotary strength would be zero even though the total oscillator strength could be substantial. As with oscillator strength rotary strength is proportional to the total electronic probability averaged over all final nuclear states.

Oscillator strength is a dimensionless quantity but some system of units must be used in order to account for the magnitude of rotary strength [26]. The most

commonly used system is cgs units. Rotary strength in cgs units becomes

$$R_{mk}^r(\text{cgs}) = 4.45458 \times 10^{-30} \langle \psi_m | \sum_i^n \vec{r}_i | \psi_k \rangle \langle \psi_m | \sum_i^n \vec{r}_i \times \vec{\nabla}_i | \psi_k \rangle \quad (1-40)$$

It is customary in quantum mechanical calculations to use atomic units to calculate transition energies and moments. In atomic units $\hbar = e = m = 1$. The atomic unit of energy is the Hartree and the atomic unit of length is the Bohr. Using atomic units to calculate transition moments and energies, oscillator strength and rotary strength becomes

$$f_{\nu}^r = \frac{2E_{km}(\text{au})}{3} |\langle \psi_m | \sum_i^n \vec{r}_i | \psi_k \rangle|^2 \quad (1-41)$$

$$R_{mk}^r(\text{cgs}) = 235.7262 \times 10^{-40} \langle \psi_m | \sum_i^n \vec{r}_i | \psi_k \rangle \langle \psi_m | \sum_i^n \vec{r}_i \times \vec{\nabla}_i | \psi_k \rangle$$

Common units for reporting transition energies are electron volts and reciprocal centimeters ($1 \text{ au} = 27.212 \text{ eV} = 219474.6 \text{ cm}^{-1}$). The conversion constant for rotary strength from cgs to SI units is 1.19×10^6 .

CHAPTER 2 GENERAL THEORY

The Hartree-Fock Equations

In order to determine the electronic transition moments and energies for a molecule it is necessary to determine in some fashion the eigenfunctions and energies of the electronic Hamiltonian. In atomic units the electronic Hamiltonian becomes

$$\hat{H}^0 = - \sum_i^n \frac{\vec{\nabla}_i^2}{2} + \sum_i^n \left(\sum_{j \neq i} \frac{1}{r_{ij}} - \sum_{\alpha}^M \frac{Z_{\alpha}}{r_{i\alpha}} \right) + V_{\text{nucl.}} \quad (2-1)$$

The first term is the electron kinetic energy operator. The second sum contains the potential energy of repulsion of the electrons and the potential energy of attraction between the electrons and nuclei. The final term is the nuclear potential energy and is a constant for fixed geometry regardless of electronic state. Since we are interested in differences in electronic states this term is dropped. We seek solutions to Equation (2-1) of the form

$$\hat{H}^0 |\psi_j\rangle = E_j |\psi_j\rangle \quad (2-2)$$

The eigenstates ψ_j are functions of the electronic coordinates and spin. The nonrelativistic Hamiltonian used in this treatment is not a function of the spin

coordinates of the electrons. Since electrons are spin 1/2 and therefore fermions the eigenstates for a system of electrons must be antisymmetric with respect to the interchange of the coordinates of any two particles [17]. It is necessary therefore to seek solutions that have the property

$$\psi_j(q_1, q_2, \dots) = -\psi_j(q_2, q_1, \dots) \quad (2-3)$$

where q_1 is the space and spin coordinate for electron one.

According to the variation principle, for an arbitrary well behaved normalized wave function, $|\Phi\rangle$, the expectation value for the Hamiltonian of a system is an upper bound to the exact ground state energy. In other words

$$E_0 \leq \langle \Phi | \hat{H}^0 | \Phi \rangle \quad (2-4)$$

If $|\Phi\rangle$ contains adjustable parameters they can be varied so that $E = \langle \Phi | \hat{H}^0 | \Phi \rangle$ is a minimum and thus $|\Phi\rangle$ becomes the best possible approximation to the ground state wave function and E the best possible approximation to the exact ground state energy. The calculated energy (E) only becomes the exact if $|\Phi\rangle$ is the exact wave function [19].

In general it is not possible to solve Equation (2-2) for more than two electrons. It becomes necessary to seek expedient approximations that allow generalized methods of solution. The most common such approximation is the molecular orbital or Hartree-Fock (HF) approximation [23]. In the HF

approximation ψ_j is expressed as the best possible determinant of one-electron spin orbitals. Since a determinant changes sign when two rows or columns are transposed, which in this case represents a single electron function, the fermion property of antisymmetry is attained whereas a simple product of spin orbitals would not have this property. For n electrons

$$\begin{aligned} |\psi_j\rangle &\approx |\phi_1(q_1)\phi_2(q_2)\cdots\phi_m(q_m)\cdots\phi_n(q_n)\rangle \\ &= \frac{1}{\sqrt{n!}} \sum_{i=1}^{n!} (-1)^{p_i} \hat{P}_i \phi_1(q_1)\phi_2(q_2)\cdots\phi_m(q_m)\cdots\phi_n(q_n) \end{aligned} \quad (2-5)$$

and is known as a Slater determinant. The symbol \hat{P}_i is the permutation operator for the electron labels and the sum is over all $n!$ permutations. The number of single label interchanges necessary to restore the i 'th permutation to the initial order is denoted p_i . The $1/\sqrt{n!}$ factor is the normalization constant so that $\langle\psi_j|\psi_j\rangle = 1$.

Utilizing the variational principle with a Slater determinant of orthonormal spin orbitals yields

$$E_0 \leq E = \langle\psi_0|\hat{H}^0|\psi_0\rangle \quad (2-6)$$

The calculated energy becomes a function of the molecular orbitals that make up the determinant. The remaining discussion is restricted to closed shell determinants. Insertion of Equation (2-1) into (2-6) and integrating over space and

spin yields

$$\begin{aligned}
 E &= \sum_{i=1}^n \int \phi_i^*(q_1) \left[-\frac{\vec{\nabla}_1^2}{2} - \sum_{\alpha=1}^M \frac{Z_\alpha}{r_{1\alpha}} \right] \phi_i(q_1) dq_1 \\
 &+ \frac{1}{2} \sum_{i,j=1}^n \int \int \phi_i^*(q_1) \phi_j^*(q_2) \frac{1}{r_{ij}} [\phi_i(q_1) \phi_j(q_2) - \phi_j(q_1) \phi_i(q_2)] dq_1 dq_2 \\
 &= \sum_{i=1}^n \langle \phi_i | \hat{h} | \phi_i \rangle + \frac{1}{2} \sum_{i,j=1}^n [\langle \phi_i \phi_j | \phi_i \phi_j \rangle - \langle \phi_i \phi_j | \phi_j \phi_i \rangle] \\
 &= \sum_{i=1}^n \langle \phi_i | \hat{h} | \phi_i \rangle + \frac{1}{2} \sum_{i,j=1}^n \langle \phi_i \phi_j | | \phi_i \phi_j \rangle
 \end{aligned} \tag{2-7}$$

The operator \hat{h} is a one-electron operator consisting of kinetic energy and nuclear electronic attraction. The i 'th term is usually denoted h_{ii} . The two terms relating to the electron repulsion are known as the coulomb (J_{ij}) and exchange (K_{ij}) integrals respectively. The exchange integral is the direct result of using a determinantal form for the wave function and would be absent if the wave function were a simple product. In simplified notation Equation (2-7) becomes

$$\begin{aligned}
 E &= \sum_{i=1}^n \langle i | \hat{h} | i \rangle + \frac{1}{2} \sum_{i,j=1}^n \langle ij | | ij \rangle \\
 &= \sum_{i=1}^n h_{ii} + \frac{1}{2} \sum_{i,j=1}^n [J_{ij} - K_{ij}]
 \end{aligned} \tag{2-8}$$

In order to obtain the best possible solution to Equation (2-8) the spin orbitals are varied under the constraint of maintaining orthonormality. Let ϵ_{ij} be a set of

Lagrange multipliers so that the Lagrange variational expression becomes

$$\begin{aligned} L &= E - \sum_{ij} \epsilon_{ji} [\langle i|j \rangle - \delta_{ij}] \\ \delta L &= \delta \left\{ E - \sum_{ij} \epsilon_{ji} [\langle i|j \rangle - \delta_{ij}] \right\} = 0 \end{aligned} \quad (2-9)$$

Differentiating the orbitals and rearranging terms yields

$$\begin{aligned} & \sum_{i=1}^n \int dq_1 \delta \phi_i^*(1) \left\{ \hat{h}(1) \phi_i(1) + \sum_{j=1}^n \left[\int dq_2 \phi_j^*(2) \frac{1}{r_{ij}} \phi_j(2) \right] \phi_i(1) \right. \\ & \quad \left. - \sum_{j=1}^n \left[\int dq_2 \phi_j^*(2) \frac{1}{r_{ij}} \hat{P}_{12} \phi_j(2) \right] \phi_i(1) \right\} + \text{complex conjugate} \\ &= \sum_{i=1}^n \int dq_1 \delta \phi_i^*(1) \left\{ \sum_{j=1}^n \epsilon_{ji} \phi_j(1) \right\} + \text{complex conjugate} \end{aligned} \quad (2-10)$$

The terms in brackets are known as the coulomb and exchange operators respectively. The variation of the spin orbital is arbitrary so Equation (2-10) must hold term by term or

$$\left\{ \hat{h}(1) + \sum_{j=1}^n [\hat{J}_j - \hat{K}_j] \right\} \phi_i(1) = \hat{f}(1) \phi_i(1) = \sum_{j=1}^n \epsilon_{ji} \phi_j(1) \quad (2-11)$$

where the first equality defines the one-electron Fock operator. Multiplying by ϕ_k and integrating one obtains $\langle \phi_k | \hat{f} | \phi_i \rangle = \epsilon_{ki}$. The Lagrange multipliers are matrix elements of the Fock operator in the basis of the spin orbitals. Since the Fock operator is invariant to a unitary transformation and the matrix of Lagrange multipliers is Hermitian it is possible to choose the ϕ_i so that the matrix of Lagrange multipliers is diagonal. That set of ϕ_i and ϵ_i are known as the

canonical Hartree-Fock equations. The solution of the HF equations reduces to the determination of the eigenvalues and eigenfunctions of the Fock operator.

$$\hat{f}|\phi_i\rangle = \varepsilon_i|\phi_i\rangle \quad (2-12)$$

with the Fock operator defined in Equation (2-11). Since the Fock operator itself is a function of the spin orbitals the methods for the solution of Equation (2-12) are in general iterative in nature.

The energy minimization that led to Equation (2-12) pertained only to the n "occupied" molecular orbitals directly associated with the electrons. Once these orbitals are determined, the Fock operator becomes a well-defined Hermitian operator and thus possesses a complete set of solutions. Those orbitals beyond the active occupied orbitals are known as virtual orbitals. The eigenvalue for an arbitrary canonical orbital can be expressed

$$\varepsilon_i = \langle \phi_i | \hat{f} | \phi_i \rangle = h_{ii} + \sum_{j=1}^n [J_{ij} - K_{ij}] \quad (2-13)$$

Equation (2-8) represents the total electronic energy expression for n electrons. As a reasonable first guess, the orbital solutions for n electrons can be used to estimate the energy for a system of $(n+1)$ or $(n-1)$ electrons. The difference in energy between an n electron state and an $(n-1)$ electron state is known as an ionization potential (IP). The difference with an n and $(n+1)$ state is known as an

electron affinity (EA). Using the orbitals obtained for an n electron system and Equation (2-8), one obtains a molecular ionization potential for arbitrary occupied orbital α and an electron affinity for arbitrary virtual orbital b .

$$\begin{aligned} E_{\alpha}(n-1) - E &= IP_{\alpha} = -\varepsilon_{\alpha} \\ E - E_b(n+1) &= EA_b = -\varepsilon_b \end{aligned} \quad (2-14)$$

Equation (2-14) is an expression of Koopmans' theorem which interprets the eigenvalues of the occupied orbitals as the negative of the IP's for those orbitals and the eigenvalues of the virtual orbitals as the negative of the EA's for those orbitals [23].

The use of the molecular orbital approximation yields an approximate ground state for a molecular system. Since the solutions for the Fock operator form a complete set the exact wave function for a system can be expressed in terms of an expansion of these solutions. From the HF ground state the occupied orbitals can be successively replaced by the virtual orbitals and classed in terms of single, double and higher replacements [27].

$$|\Psi_0\rangle = \left[C|\psi_0\rangle + \sum_{\alpha a} C_{\alpha}^a |\psi_{\alpha}^a\rangle + \frac{1}{4} \sum_{\alpha\beta ab} C_{\alpha\beta}^{ab} |\psi_{\alpha\beta}^{ab}\rangle + \dots \right] \quad (2-15)$$

The determinant generated by the replacement of occupied orbital α with virtual orbital a is denoted $|\psi_{\alpha}^a\rangle$ with corresponding expansion coefficient C_{α}^a . The coefficients of the determinants become the parameters for the use of the variational principle. Matrix elements of the Hamiltonian in the basis of determinants must

be formed to solve the problem. The matrix elements between the HF ground state and a single replacement can be expressed

$$\begin{aligned}\langle \psi_0 | \hat{H} | \psi_\alpha^a \rangle &= h_{\alpha a} + \sum_{i=1}^n \langle \alpha i | | a i \rangle = \\ \langle \phi_\alpha | \hat{f} | \phi_a \rangle &= \varepsilon_a \langle \phi_\alpha | \phi_a \rangle = 0\end{aligned}\tag{2-16}$$

The determinants formed from a single replacements do not directly interact with the HF solution for the ground state. This is an expression of Brillouin's theorem. The lowest order correction to the HF ground state is through double replacements only. The eigenvalue problem in the complete basis of determinants yields not only the exact ground state energy but also the wave functions and eigenvalues of the excited states of the system [28].

The Roothaan Equations

The Hartree-Fock equations in the previous section do not suggest a method by which to obtain the molecular orbitals that define the Fock operator. The most common way is to assume a basis set that is pertinent to the system of interest. For molecules this usually involves an atomic—like basis. Each atom in a molecule contributes a set of functions to the total basis for the solution of the HF equations. The number and type of functions that an atom can contribute is limited only to the computational resources of the researcher. The smallest basis that an atom can contribute is called the minimal basis set (MBS) and is usually that basis associated with the shell structure of an atom. Each principle quantum

number on an atom contributes a fixed number of basis functions of specific angular momentum. The molecular orbitals associated with the Fock equations become linear combinations of atomic orbitals (LCAO-MO).

$$\phi_i = \sum_{\mu=1}^N C_{\mu i} \chi_{\mu} \quad (2-17)$$

The expansion coefficients become the variational parameters. The χ_{μ} are the atomic basis functions and in general are a function of the electronic coordinates only. The total number of basis functions is N. The spin of a molecular orbital is denoted by the existence a bar over the symbol for orbitals that are spin $-1/2$. No bar is present for spin $1/2$. Alternatively, spin $-1/2$ is often denoted as β and spin $1/2$ as α . Orbitals of differing spin are orthogonal.

Placing Equation (2-17) into Equation (2-12) and multiplying by the atomic basis functions and integrating yields

$$\begin{aligned} \langle \chi_{\mu} | \hat{f} \sum_{\nu=1}^N C_{\nu i} | \chi_{\nu} \rangle &= \epsilon_i \sum_{\nu=1}^N C_{\nu i} \langle \chi_{\nu} | \chi_{\mu} \rangle \\ \sum_{\nu=1}^N C_{\nu i} \langle \chi_{\mu} | \hat{f} | \chi_{\nu} \rangle &= \epsilon_i \sum_{\nu=1}^N C_{\nu i} \langle \chi_{\mu} | \chi_{\nu} \rangle \\ \sum_{\nu=1}^N F_{\mu\nu} C_{\nu i} &= \epsilon_i \sum_{\nu=1}^N S_{\mu\nu} C_{\nu i} \end{aligned} \quad (2-18)$$

where the elements of the Fock (F) and overlap (S) matrix are defined. In terms of matrices

$$FC = SC\epsilon \quad (2-19)$$

is known as the Roothaan equation [29] and is the most used formalism for the solution of the HF system of equations. The columns of the coefficient matrix are the expansion coefficients for the molecular orbitals and ϵ is a diagonal matrix of orbital eigenvalues. For N basis functions one obtains N molecular spin orbitals, n of which are occupied and $(N-n)$ are virtual.

A determinant in which each spatial orbital is associated with both spin α and β functions and both are occupied is known as restricted Hartree-Fock (RHF) and is the most common type of calculation performed. Introduction of Equation (2-17) into the expression for the Fock operator and calculating the matrix elements of the Fock operator in Equation (2-18) for a RHF determinant yields

$$F_{\mu\nu} = h_{\mu\nu} + \sum_{i=1}^{n/2} \sum_{\sigma\tau}^N C_{\sigma i} C_{\tau i}^* [2\langle\mu\tau|\nu\sigma\rangle - \langle\mu\tau|\sigma\nu\rangle] \quad (2-20)$$

The iterative nature of the Fock equations is demonstrated in that the coefficients of the occupied orbitals must be known in order to define the Fock operator but these are the same coefficients that are sought in the calculation. The intermediate sum over the occupied orbitals and coefficients in (2-20) defines the so called density matrix $P = CnC^\dagger$. Here n represents the diagonal matrix of orbital occupancies the trace of which is the number of electrons. For an RHF determinant the spatial orbital occupancies are either 2 or 0.

$$P_{\sigma\tau} = \sum_i^{n/2} 2C_{\sigma i} C_{\tau i}^* \quad (2-21)$$

The elements of the Fock matrix become

$$F_{\mu\nu} = h_{\mu\nu} + \frac{1}{2} \sum_{\sigma\tau}^N P_{\sigma\tau} [2\langle\mu\tau|\nu\sigma\rangle - \langle\mu\tau|\sigma\nu\rangle] \quad (2-22)$$

The matrix elements of the one-electron operator in the atomic basis do not depend on the density matrix.

For real spatial atomic orbitals the overlap matrix is symmetric and can be diagonalized and real roots taken of the matrix. Let X be the transformation matrix that diagonalizes S so that $X^\dagger S X = s$.

$$S = X s X^\dagger = X s^{1/2} s^{1/2} X^\dagger = [X s^{1/2} X^\dagger] [X s^{1/2} X^\dagger] \quad (2-23)$$

If there are not any linear dependencies in S then

$$1 = [X s^{-1/2} X^\dagger] [X s^{1/2} X^\dagger] = U [X s^{1/2} X^\dagger] \quad (2-24)$$

defining the matrix $U = S^{-1/2}$. Consider the transformation of Equation (2-19).

$$\begin{aligned} U^\dagger // F1C &= F U [X s^{1/2} X^\dagger] C = [X s^{1/2} X^\dagger] [X s^{1/2} X^\dagger] C \varepsilon = S C \varepsilon \\ [U^\dagger F U] C' &= \{U^\dagger [X s^{1/2} X^\dagger]\} C' \varepsilon \\ F' C' &= C' \varepsilon \end{aligned} \quad (2-25)$$

This procedure by which the atomic basis is orthogonalized is known as symmetric or Löwdin orthogonalization [30] and the Fock procedure is reduced to the matrix eigenvalue problem $C'^\dagger F' C' = C'^\dagger C' \varepsilon = \varepsilon$.

Once the atomic basis is chosen for a problem the solution usually follows well established lines. The general algorithm is to first evaluate all the integrals in

the atomic basis. The overlap matrix is diagonalized and the transformation matrix U is formed. An initial guess for the density matrix is formed and the Fock matrix is built, transformed and diagonalized. The coefficient matrix in the atomic basis is formed by the back transformation $C = UC'$. A new density matrix can then be formed yielding a new Fock matrix and the pattern repeated. The procedure is considered converged when differences in successive density matrices are within some set threshold. This technique is known as the self-consistent-field (SCF) procedure.

The Calculation of Electronic Spectra

The Hartree-Fock procedure for a given basis provides a convenient set of orbitals from which Equation (2–15) may be variationally solved for all the electronic states of a system. The full expansion provided by all orbital replacements is known as a full configuration interaction (CI). For the special case of a complete basis set, the full CI is said to be “complete” and represents an exact solution of the problem represented by the assumed Hamiltonian. For other than very small systems, however, full CI is not feasible and some truncation is necessary at some order in the expansion. From Brillouin’s theorem the lowest order correction to the ground state comes at the inclusion of double replacements only. Since the single replacements do not mix directly with the ground state they become the basis for the lowest order approximation to singly excited states. It is

the transition moments and energies between such excited states and the ground state that are of interest here.

The expressions for oscillator and rotary strength in Chapter 1 involve matrix elements between states for the electron position and angular momentum operators. These expressions are not unique however. The commutation relation between the Hamiltonian for the system and the position operator [31] is

$$\left[\sum_{i=1}^n \vec{r}_i, \hat{H}^0 \right] = \sum_{i=1}^n \vec{\nabla}_i \quad (2-26)$$

where $\vec{\nabla}_i$ is the velocity operator for electron i . The evaluation of matrix elements between the ground and excited states of the Hamiltonian operator yields

$$\begin{aligned} \langle \psi_0 | \sum_{i=1}^n \vec{\nabla}_i | \psi_k \rangle &= \langle \psi_0 | \sum_{i=1}^n \vec{r}_i \hat{H}^0 - \hat{H}^0 \sum_{i=1}^n \vec{r}_i | \psi_k \rangle \\ &= (E_k^0 - E_0^0) \langle \psi_0 | \sum_{i=1}^n \vec{r}_i | \psi_k \rangle \\ \langle \psi_0 | \sum_{i=1}^n \vec{\nabla}_i | \psi_k \rangle &= E_{k0} \langle \psi_0 | \sum_{i=1}^n \vec{r}_i | \psi_k \rangle \end{aligned} \quad (2-27)$$

Equation (2-27) indicates that the matrix elements for the position operator can be replaced by those of the velocity operator divided by the transition energy [32, 33]. Equations (1-38) and (1-39) for oscillator and rotary strength in terms of the velocity operator become

$$\begin{aligned} f_k^r &= \frac{2E_{k0}}{3} |\langle \psi_0 | \sum_{i=1}^n \vec{r}_i | \psi_k \rangle|^2 = \\ f_k^\nabla &= \frac{2}{3E_{k0}} |\langle \psi_0 | \sum_{i=1}^n \vec{\nabla}_i | \psi_k \rangle|^2 \end{aligned} \quad (2-28)$$

and

$$\begin{aligned} R_k^r &= C_R \langle \psi_0 | \sum_{i=1}^n \vec{r}_i | \psi_k \rangle \langle \psi_0 | \sum_{i=1}^n \vec{r}_i \times \vec{\nabla}_i | \psi_k \rangle = \\ R_k^\nabla &= \frac{C_R}{E_{k0}} \langle \psi_0 | \sum_{i=1}^n \vec{\nabla}_i | \psi_k \rangle \langle \psi_0 | \sum_{i=1}^n \vec{r}_i \times \vec{\nabla}_i | \psi_k \rangle \end{aligned} \quad (2-29)$$

For exact eigenfunctions of the Hamiltonian, transition moments in both length and velocity formalisms are equivalent. Since approximate solutions to ground and excited states do not necessarily obey Equation (2-27), the equivalence of oscillator and rotary strength in Equations (2-28) and (2-29) can not be assumed. Equation (2-27) constitutes a formal constraint that must be incorporated into the calculation of approximate excited and ground states if equivalence is to be achieved.

For practical purposes the HF approximation and the HF plus doubles approximation will be considered for the ground state and singles only for the excited states [10]. Truncations at higher order are not feasible for use with large systems.

$$\begin{aligned} |\psi_0\rangle &= K_0 \left[|\psi_{\text{HF}}\rangle + \left\{ \frac{1}{4} \sum_{\alpha\beta ab} C_{\alpha\beta}^{ab} |\psi_{\alpha\beta}^{ab}\rangle \right\} \right] \\ |\psi_k\rangle &= \sum_{\gamma c} C_\gamma^c |\psi_\gamma^c\rangle \end{aligned} \quad (2-30)$$

Transition moments for a general one-electron operator \hat{O} is expressed in terms of the approximate states in Equation (2-30) as

$$\begin{aligned} \langle \psi_0 | \hat{O} | \psi_k \rangle &= \sum_{\gamma c} K_0^* C_\gamma^c \langle \psi_{\text{HF}} | \hat{O} | \psi_\gamma^c \rangle \\ &+ \left\{ \sum_{\alpha\beta\gamma abc} \frac{K_0^*}{4} C_{\alpha\beta}^{ab*} C_\gamma^c \langle \psi_{\alpha\beta}^{ab} | \hat{O} | \psi_\gamma^c \rangle \right\} \end{aligned} \quad (2-31)$$

Matrix elements for one-electron operators are identically zero if the two determinants differ by more than one orbital replacement.

$$\langle \psi_{\alpha\beta}^{ab} | \hat{O} | \psi_{\gamma}^c \rangle = \langle \psi_{\alpha\beta}^{ab} | \hat{O} | \psi_{\gamma}^c \rangle [\delta_{\alpha\gamma}^{ac} + \delta_{\alpha\gamma}^{bc} + \delta_{\beta\gamma}^{ac} + \delta_{\beta\gamma}^{bc}] \quad (2-32)$$

The indices of summation in Equation (2-31) are arbitrary so that

$$\begin{aligned} \langle \psi_0 | \hat{O} | \psi_k \rangle &= \sum_{\gamma c} K_0^* C_{\gamma}^c \langle \psi_{HF} | \hat{O} | \psi_{\gamma}^c \rangle \\ &+ \left\{ \sum_{\alpha \gamma ac} K_0^* C_{\alpha\gamma}^{ac*} C_{\gamma}^c \langle \psi_{\alpha\gamma}^{ac} | \hat{O} | \psi_{\alpha}^a \rangle \right\} \end{aligned} \quad (2-33)$$

but $\langle \psi_{\alpha\gamma}^{ac} | \hat{O} | \psi_{\alpha}^a \rangle = \langle \psi_{\gamma}^c | \hat{O} | \psi_{HF} \rangle$ yielding

$$\begin{aligned} \langle \psi_0 | \hat{O} | \psi_k \rangle &= \sum_{\gamma c} \left[K_0^* C_{\gamma}^c \langle \psi_{HF} | \hat{O} | \psi_{\gamma}^c \rangle \right. \\ &\left. + \left\{ \sum_{\alpha a} K_0^* C_{\alpha\gamma}^{ac*} C_{\gamma}^c \langle \psi_{\gamma}^c | \hat{O} | \psi_{HF} \rangle \right\} \right] \end{aligned} \quad (2-34)$$

For excitation k the following notation is adopted.

$$X_{\gamma c}^k = K_0^* C_{\gamma}^c(k), \quad Y_{\gamma c}^k = \sum_{\alpha a} K_0^* C_{\alpha\gamma}^{ac*}(k) C_{\gamma}^c(k) \quad (2-35)$$

This yields,

$$\begin{aligned} \langle \psi_0 | \hat{O} | \psi_k \rangle &= \sum_{\gamma c} \left[X_{\gamma c}^k \langle \psi_{HF} | \hat{O} | \psi_{\gamma}^c \rangle \right. \\ &\left. + \left\{ Y_{\gamma c}^k \langle \psi_{\gamma}^c | \hat{O} | \psi_{HF} \rangle \right\} \right] \end{aligned} \quad (2-36)$$

The commutation relation between the general operator \hat{O} and the Hamiltonian operator with the exact state functions [9] is according to Equation (2-27)

$$\langle \psi_0 | \hat{O} | \psi_k \rangle E_{k0} = \langle \psi_0 | [\hat{O}, \hat{H}^0] | \psi_k \rangle \quad (2-37)$$

If the commutation relation itself yields a one-electron operator as in Equation (2-26) the right hand side of Equation (2-37) becomes for the approximate states defined by Equation (2-30)

$$\begin{aligned} \text{RHS} = \sum_{\gamma^c} \left[X_{\gamma^c}^k (\langle \psi_{\text{HF}} | \hat{O} \hat{H}^0 | \psi_{\gamma^c}^c \rangle - \langle \psi_{\text{HF}} | \hat{H}^0 \hat{O} | \psi_{\gamma^c}^c \rangle) \right. \\ \left. + \left\{ Y_{\gamma^c}^k (\langle \psi_{\gamma^c}^c | \hat{O} \hat{H}^0 | \psi_{\text{HF}} \rangle - \langle \psi_{\gamma^c}^c | \hat{H}^0 \hat{O} | \psi_{\text{HF}} \rangle) \right\} \right] \end{aligned} \quad (2-38)$$

Since the eigenfunctions of the Fock operator form a complete set we can resolve the identity

$$1 = |\psi_{\text{HF}}\rangle\langle\psi_{\text{HF}}| + \{|\psi_{\gamma}^c\rangle\langle\psi_{\gamma}^c|\} + \{|\psi_{\alpha\beta}^{ab}\rangle\langle\psi_{\alpha\beta}^{ab}|\} + \dots \quad (2-39)$$

between the Hamiltonian and \hat{O} . Utilizing Brillouin's theorem and the fact that matrix elements of the Hamiltonian between two determinants that differ by more than two orbitals is zero the insertion of Equation (2-39) into (2-38) gives

$$\begin{aligned} \text{RHS} = \sum_{\gamma^c} \left[X_{\gamma^c}^k \left(\sum_{\delta^d} \langle \psi_{\text{HF}} | \hat{O} | \psi_{\delta^d}^d \rangle \langle \psi_{\delta^d}^d | \hat{H}^0 | \psi_{\gamma^c}^c \rangle \right. \right. \\ \left. - \langle \psi_{\text{HF}} | \hat{H}^0 | \psi_{\text{HF}} \rangle \langle \psi_{\text{HF}} | \hat{O} | \psi_{\gamma^c}^c \rangle - \frac{1}{4} \sum_{\delta\eta^{\text{de}}} \langle \psi_{\text{HF}} | \hat{H}^0 | \psi_{\delta\eta}^{\text{de}} \rangle \langle \psi_{\delta\eta}^{\text{de}} | \hat{O} | \psi_{\gamma^c}^c \rangle \right) \\ \left. + \left\{ Y_{\gamma^c}^k (\langle \psi_{\gamma^c}^c | \hat{O} | \psi_{\text{HF}} \rangle \langle \psi_{\text{HF}} | \hat{H}^0 | \psi_{\text{HF}} \rangle + \frac{1}{4} \sum_{\delta\eta^{\text{de}}} \langle \psi_{\gamma^c}^c | \hat{O} | \psi_{\delta\eta}^{\text{de}} \rangle \langle \psi_{\delta\eta}^{\text{de}} | \hat{H}^0 | \psi_{\text{HF}} \rangle \right. \right. \\ \left. \left. - \sum_{\delta^d} \langle \psi_{\gamma^c}^c | \hat{H}^0 | \psi_{\delta^d}^d \rangle \langle \psi_{\delta^d}^d | \hat{O} | \psi_{\text{HF}} \rangle \right\} \right] \end{aligned} \quad (2-40)$$

Defining

$$\begin{aligned} A_{\delta^d, \gamma^c} &= \langle \psi_{\delta^d}^d | \hat{H}^0 | \psi_{\gamma^c}^c \rangle - \langle \psi_{\text{HF}} | \hat{H}^0 | \psi_{\text{HF}} \rangle \delta_{\gamma^c \delta^d} \\ B_{\delta\eta^{\text{de}}, \gamma^c} &= \langle \psi_{\delta\eta}^{\text{de}} | \hat{H}^0 | \psi_{\text{HF}} \rangle \end{aligned} \quad (2-41)$$

and simplifying according to Equation (2-32) Equation (2-37) takes the form

$$\begin{aligned}
 & E_{k0} \sum_{\delta d} \left[X_{\delta d}^k \langle \psi_{HF} | \hat{O} | \psi_{\delta}^d \rangle + \{ Y_{\delta d}^k \langle \psi_{\delta}^d | \hat{O} | \psi_{HF} \rangle \} \right] \\
 &= \sum_{\gamma c} \left[X_{\gamma c}^k \sum_{\delta d} (\langle \psi_{HF} | \hat{O} | \psi_{\delta}^d \rangle A_{\delta d, \gamma c} - \langle \psi_{\delta}^d | \hat{O} | \psi_{HF} \rangle B_{\gamma c, \delta d}^*) \right. \\
 & \quad \left. + \{ Y_{\gamma c}^k \sum_{\delta d} (\langle \psi_{HF} | \hat{O} | \psi_{\delta}^d \rangle B_{\delta d, \gamma c} - \langle \psi_{\delta}^d | \hat{O} | \psi_{HF} \rangle A_{\gamma c, \delta d}) \} \right] \quad (2-42)
 \end{aligned}$$

The operator \hat{O} can in general be Hermitian as is the position operator or anti-Hermitian as is the velocity and angular momentum operators. Most calculations are performed in a basis of real orbitals in which the A and B matrices are symmetric. For Hermitian operators and real orbitals Equation (2-42) becomes

$$\begin{aligned}
 & \sum_{\gamma c} \sum_{\delta d} \langle \psi_{HF} | \hat{O}_H | \psi_{\delta}^d \rangle [(X_{\gamma c}^k - Y_{\gamma c}^k)(A_{\delta d, \gamma c} - B_{\delta d, \gamma c}) \\
 & \quad - E_{k0}(X_{\delta d}^k + Y_{\delta d}^k)\delta_{\delta \gamma}\delta_{cd}] = 0 \Rightarrow \\
 & \sum_{\gamma c} (X_{\gamma c}^k - Y_{\gamma c}^k)(A_{\delta d, \gamma c} - B_{\delta d, \gamma c}) = E_{k0}(X_{\delta d}^k + Y_{\delta d}^k) \quad (2-43)
 \end{aligned}$$

and for anti-Hermitian operators

$$\sum_{\gamma c} (X_{\gamma c}^k + Y_{\gamma c}^k)(A_{\delta d, \gamma c} + B_{\delta d, \gamma c}) = E_{k0}(X_{\delta d}^k - Y_{\delta d}^k) \quad (2-44)$$

Equations (2-43) and (2-44) thus define a set of simultaneous linear equations that must be solved in order to obtain the coefficients necessary for the calculation of transition moments for both Hermitian and anti-Hermitian operators. In matrix form they become

$$(A - B)(X - Y) = (X + Y)E_K \quad (2-45)$$

for Hermitian operators and

$$(A + B)(X + Y) = (X - Y)E_K \quad (2-46)$$

for anti-Hermitian operators. The columns of X and Y are the expansion coefficients for the excitations and E_K is a diagonal matrix of transition energies. Equations (2-45) and (2-56) are the RPA Equations [8, 11].

The first case to be considered is for excitations from the Hartree-Fock approximation to the ground state. This is obtained by setting the matrix Y identically to zero obtaining

$$(A - B)X = XE_K \quad (2-47)$$

and

$$(A + B)X = XE_K \quad (2-48)$$

which are two eigenvalue problems for X and E_K . Since A and B do not commute they do not possess a common set of solutions. Therefore transition moments calculated in different formalisms will not in general be equal. Equation (2-37) can be solved for Hermitian or anti-Hermitian operators separately, however, by the diagonalization of $(A-B)$ and $(A+B)$ respectively. If the matrix B is neglected, Equations (2-47) and (2-48) reduce to the diagonalization of A which is exactly the matrix obtained from the variational solution of the singles only configuration interaction (CIS) or also known as the Tamm-Dancoff approximation (TDA)

[34]. The TDA is the most commonly used approximation for the calculation of transition moments and energies but as seen here cannot guarantee equivalence between transition moments as calculated in different formalisms since Equations (2-27) and (2-37) do not in general hold. Only in the limit of a full CI can a variational procedure guarantee this equivalence.

The second case is the direct solution of Equations (2-45) and (2-46) which were derived on the basis of a ground state consisting Hartree-Fock and double replacements. Taking the linear sum and difference of Equations (2-45) and (2-46) yields

$$\begin{aligned} AX + BY &= XE_K \\ BX + AY &= -YE_K \end{aligned} \tag{2-49}$$

which is the linear form of the matrix equation

$$\begin{bmatrix} A & B \\ B & A \end{bmatrix} \begin{bmatrix} X \\ Y \end{bmatrix} = \begin{bmatrix} X \\ -Y \end{bmatrix} E_K \tag{2-50}$$

Since we have assumed real orbitals the matrix of A and B is real and symmetric and can be solved as [27],

$$[X^\dagger \ Y^\dagger] \begin{bmatrix} A & B \\ B & A \end{bmatrix} \begin{bmatrix} X \\ Y \end{bmatrix} = [X^\dagger \ Y^\dagger] \begin{bmatrix} X \\ -Y \end{bmatrix} E_K = [X^\dagger X - Y^\dagger Y] E_K = E_K \tag{2-51}$$

with the special normalization constraint $[X^\dagger X - Y^\dagger Y] = 1$. Direct solution of Equation (2-50) would involve the diagonalization of a matrix of twice the dimension of the number of single replacements in order to obtain the coefficients

and transition energies. The problem can be reduced to two successive diagonalizations of the same dimension as the number of single replacements. Since diagonalization scales as the cube of the dimension of the problem, two diagonalizations of dimension N are preferable to one diagonalization of dimension $2N$.

According to Ullah and Rowe [35] let $M = A + B$, $N = A - B$, $U = X + Y$ and $V = X - Y$ so that Equations (2-45) and (2-46) become

$$NV = UE_K, \quad MU = VE_K \quad (2-52)$$

The normalization constraint becomes

$$V^\dagger U = U^\dagger V = 1 \quad (2-53)$$

since with real orbitals and real coefficients

$$\begin{aligned} V^\dagger U &= (X^\dagger - Y^\dagger)(X + Y) = X^\dagger X - Y^\dagger Y + X^\dagger Y - Y^\dagger X \\ &= X^\dagger X - Y^\dagger Y + [X^\dagger Y - (X^\dagger Y)^\dagger] \\ &= X^\dagger X - Y^\dagger Y = 1 \end{aligned} \quad (2-54)$$

$$\begin{aligned} X^\dagger Y &= \frac{1}{4}[U^\dagger U - V^\dagger V - (U^\dagger V - V^\dagger U)] \\ &= \frac{1}{4}[U^\dagger U - V^\dagger V] \end{aligned}$$

If N is positive definite then $V = N^{-1}UE_K$ and

$$NMU = NVE_K = UE_K^2 \quad (2-55)$$

Equation (2-55) is similar to the Roothaan equation and an analogous treatment is sought. Let T be a unitary matrix that diagonalizes M so that $T^\dagger M T = m$, $M = T m^{1/2} m^{1/2} T^\dagger$. Equation (2-55) can be transformed

$$m^{1/2} T^\dagger // N T m^{1/2} m^{1/2} T^\dagger U = U E_K^2$$

$$[m^{1/2} T^\dagger N T m^{1/2}] [m^{1/2} T^\dagger U] = [m^{1/2} T^\dagger U] E_K^2 \quad (2-56)$$

$$N' U' = U' E_K^2$$

into a Hermitian eigenvalue problem. To obtain U the reverse transformation $U = T m^{-1/2} U'$ is performed. V can be obtained from Equation (2-52).

$$T T^\dagger // M U = M T m^{-1/2} U' = V E_K$$

$$T m^{1/2} U' = V E_K \quad (2-57)$$

$$V = T m^{1/2} U' E_K^{-1}$$

In order to obtain X and Y the normalization constraint must be taken into account.

$$U^\dagger V = [U'^\dagger m^{-1/2} T^\dagger] [T m^{1/2} U' E_K^{-1}] = 1 \quad (2-58)$$

$$U^\dagger V = U'^\dagger U' E_K^{-1} = 1$$

The normalization condition is obeyed provided the vectors in U' are scaled so that

$$U'^\dagger U' = E_K \quad (2-59)$$

With U' properly normalized and U and V obtained as above, X and Y are simply obtained from

$$X = \frac{1}{2}(U + V), \quad Y = \frac{1}{2}(U - V) \quad (2-60)$$

The use of HF plus doubles as a reference for the ground state and singles only for the excited states is successful in the maintenance of Equation (2-27) as a constraint. The resulting solutions are equal to those of the random phase approximation (RPA) or polarization propagator (PP). The RPA in a complete HF basis is the lowest level of theory in which a formal equivalence according to Equations (2-28) and (2-29) can be expected. With the RPA the transition moments and energies are obtained directly. No formal correlated ground state or excited states are explicitly formed.

Singlet Excitations with a Finite Basis

The RPA yields formally equivalent expressions for the calculation of optical properties for a complete HF basis. In practice, however, a finite basis must be chosen in which Equation (2-39) does not rigorously hold. Calculated optical properties in differing formalisms become a test for the completeness of the basis used. Often a full singles space calculation is prohibitive even in a finite basis and some truncation of the active orbitals is used to calculate transition moments and energies. If electronic excitation spectra is of primary interest usually only the lowest excited states are needed. It therefore becomes necessary to study the stability [36] and equivalence of the calculated transition energies and moments

for the lowest energy transitions as a function of the size and nature of the active space.

For this study singlet excitations from a closed shell ground state will be considered. The RPA gives two sets of transition vectors [37]. For Hermitian operators

$$\langle \psi_0 | \hat{O}_H | \psi_k \rangle = \sum_{\gamma c} \langle \psi_{HF} | \hat{O}_H | \psi_\gamma^c \rangle [X_{\gamma c}^k + Y_{\gamma c}^k] \quad (2-61)$$

and for anti-Hermitian operators

$$\langle \psi_0 | \hat{O}_A | \psi_k \rangle = \sum_{\gamma c} \langle \psi_{HF} | \hat{O}_A | \psi_\gamma^c \rangle [X_{\gamma c}^k - Y_{\gamma c}^k] \quad (2-62)$$

The singlet spin adapted excitation $|^1\psi_{\gamma c}\rangle$ in terms of spatial orbitals is

$$|^1\psi_{\gamma c}\rangle = \frac{1}{\sqrt{2}} [|^1\psi_{\gamma c}\rangle + |^1\psi_{\bar{\gamma}\bar{c}}\rangle] \quad (2-63)$$

The transition moments in Equations (2-61) and (2-62) become matrix elements of the one-electron operator in the MO basis.

$$\begin{aligned} \langle ^1\psi_{HF} | \hat{O} | ^1\psi_{\gamma c} \rangle &= \frac{1}{\sqrt{2}} [\langle ^1\psi_{HF} | \hat{O} | ^1\psi_{\gamma c} \rangle + \langle ^1\psi_{HF} | \hat{O} | ^1\psi_{\bar{\gamma}\bar{c}} \rangle] \\ &= \frac{1}{\sqrt{2}} [\langle \phi_\gamma | \hat{O} | \phi_c \rangle + \langle \bar{\phi}_\gamma | \hat{O} | \bar{\phi}_c \rangle] \\ &= \sqrt{2} \langle \phi_\gamma | \hat{O} | \phi_c \rangle \end{aligned} \quad (2-64)$$

The operators are usually evaluated in terms of the atomic basis and, after the SCF coefficients are obtained, transformed into the molecular basis.

$$\begin{aligned} \langle \phi_\gamma | \hat{O} | \phi_c \rangle &= \sum_{ij}^N C_{i\gamma}^* \langle \chi_i | \hat{O} | \chi_j \rangle C_{jc} \\ O_{\gamma c}(\text{MO}) &= [C^\dagger O(\text{AO}) C]_{\gamma c} \end{aligned} \quad (2-65)$$

The singlet spin adapted matrix elements of the TDA matrix and B matrix defined by Equation (2-41) become

$$\begin{aligned} A_{\delta d, \gamma c} &= (\varepsilon_\gamma - \varepsilon_c) \delta_{\gamma\delta} \delta_{cd} + 2\langle \gamma\delta | cd \rangle - \langle \gamma c | \delta d \rangle \\ B_{\delta d, \gamma c} &= 2\langle \gamma\delta | cd \rangle - \langle \gamma\delta | dc \rangle \end{aligned} \quad (2-66)$$

where the two-electron integrals have been suitably transformed from the atomic basis to the molecular orbital basis and the ε_i are the SCF orbital eigenvalues.

CHAPTER 3 THE INDO/RPA METHOD

Theory

Use of the LCAO—MO approximation without further simplifying assumptions creates a computational barrier. The obstacle is the evaluation of approximately $N^4/8$ two-electron integrals over the atomic basis set. N is the number of atomic basis functions. An MBS for benzene would consist of 42 basis functions and require approximately 400,000 integrals to be evaluated. Accurate calculations of molecular properties with ab initio techniques, however, often require extended basis sets. A second set of p functions on benzene increases the number of integrals to 2,400,000. Commonly used semiempirical Hamiltonians for electronic structure owe their efficiencies to reducing the number of integrals processed to N^2 . In so doing matrix multiplications and diagonalizations, both N^3 steps, dominate, at least at the HF level. In addition most semiempirical methods utilize a MBS of valence type orbitals only, further reducing N in the more complex N^3 steps. These models compensate for the reduction of integrals and small basis sets by parameterizing directly on atomic phenomena and molecular properties, and are thus often able to reproduce experiment in a more accurate fashion

than the MBS ab initio calculations on which they are modeled. A valence MBS for benzene consists of 30 basis functions and only 900 integrals.

The zero differential overlap (ZDO) approximation at the intermediate neglect of differential overlap (INDO) level is adopted for this work [6, 38–42]. The ZDO approximation assumes the differential element $\chi_\mu(1)\chi_\nu(1)d\tau_1$ to be zero unless $\mu=\nu$ where it occurs in integral evaluations. A complete description of the approximations for INDO and other levels of ZDO can be found in Sadlej [43]. The basic equations are summarized below. For INDO the ZDO approximation is applied to all two-electron integrals in which two or more centers, denoted by capital letters, are involved and all one-electron integrals associated with the SCF procedure. Certain two-center integrals will be spherically averaged in order to maintain rotational invariance. The overlap matrix becomes the unit matrix.

$$S_{\mu\nu} = \delta_{\mu\nu} \quad (3-1)$$

All one-center two-electron integrals remain and the two-center integrals are spherically averaged and symbolized by γ_{AB} .

$$\begin{aligned} \langle \mu_A \nu_B | \lambda_C \sigma_D \rangle &= \langle \mu_A \nu_B | \mu_A \nu_B \rangle \delta_{AC} \delta_{BD} \delta_{\mu\lambda} \delta_{\nu\sigma} \\ &= \gamma_{AB} \delta_{AC} \delta_{BD} \delta_{\mu\lambda} \delta_{\nu\sigma}, \quad A \neq B \end{aligned} \quad (3-2)$$

$$\langle \mu_A \nu_B | \lambda_C \sigma_D \rangle = \langle \mu_A \nu_A | \lambda_A \sigma_A \rangle \delta_{AC} \delta_{BD}, \quad A = B$$

Several cases exist for the one-electron matrix elements. Kinetic energy integrals do not contain the differential element for which the ZDO approximation

is applied so these integrals remain. If both μ and ν are on center A the matrix element is partitioned into an atomic part and a two-center part. As with the two-electron integrals all one-center integrals are kept, but with the use of a Slater basis the one-electron one-center integrals are diagonal by orbital symmetry. The core orbitals on one center have a negligible effect on the valence orbitals of a second, therefore, only the valence electrons are included in a calculation. The interaction between a core and valence electrons on a single center, however, cannot be neglected [44]. This energy of interaction scales linearly with the number of valence electrons and can be accounted for by a core-valence potential function, \hat{E}_A , that is added to the atomic portion of the one-electron matrix elements.

$$h_{\mu_A \nu_A} = \langle \mu_A | -\frac{\vec{\nabla}_1^2}{2} - \sum_{C=1}^M \frac{Z_C}{r_{1C}} + \hat{E}_A | \nu_A \rangle = \langle \mu_A | -\frac{\vec{\nabla}_1^2}{2} - \frac{Z_A}{r_{1A}} + \hat{E}_A | \nu_A \rangle \delta_{\mu\nu} - \sum_{C \neq A} Z_C \langle \mu_A | \hat{V}_C | \nu_A \rangle \delta_{\mu\nu} \quad (3-3)$$

The symbol \hat{V}_C is the potential energy of attraction for an electron to center C. The atomic one-electron one-center matrix elements are symbolized by $U_{\mu\mu}$ and are called the core integrals. Since differential overlap has been neglected between centers, the attraction of an electron on one center to the core of a second should be similar to a like repulsion. This is accomplished by setting the magnitude of the two-center nuclear attraction integral to γ_{AC} [38].

$$h_{\mu_A \nu_A} = [U_{\mu\mu} - \sum_{C \neq A} Z_C \gamma_{AC}] \delta_{\mu\nu} \quad (3-4)$$

Two-center one-electron matrix elements are not zero due to the presence of the kinetic energy operator. The two-center nuclear attraction integrals are of different type than those that occur on the diagonal of the one-electron Hamiltonian and can be neglected by the ZDO approximation. This matrix element is called a resonance integral and is symbolized by $\beta_{\mu\nu}$.

$$h_{\mu_A \nu_B} \equiv \beta_{\mu_A \nu_B}, \quad A \neq B \quad (3-5)$$

Use of the ZDO approximation reduces the Roothaan equation to

$$FC = C\varepsilon \quad (3-6)$$

which is the exact same form as the symmetrically orthogonalized equation without the ZDO approximation. Symmetric orthogonalization can be derived by the orthogonalization of a basis that maintains maximum overlap between the orthogonalized basis and the original basis [30]. The matrix elements in INDO can be viewed as if they had been evaluated directly in the orthogonal basis. In this way the coefficients determined from the INDO Fock matrix can be back transformed to the original MBS from which it is modeled. These coefficients, eigenvalues and atomic basis functions can be used to calculate properties such as transition moments and spectra. With this point of view, the

ZDO approximation then applies only to the SCF procedure and not properties that are to be calculated that rely on the SCF results. The matrix elements that remain in the INDO Hamiltonian can be evaluated directly in a basis but this approach results in a severe approximation to the full MBS calculation which is usually inadequate for the prediction of properties. Through the judicious use of experimental information the integrals are parameterized so that calculation of the same properties yields accurate results. A successful parameterization is capable of extrapolation to systems and properties for which it was not fit. Integral approximation schemes appropriate for the calculation of electronic spectra are of interest here.

Two types of parameters need to be determined. The first are the parameters that are purely atomic in nature. These are the core integrals and one-center two-electron integrals. Since all atomic integrals are kept in INDO, atomic parameters are chosen to reproduce atomic phenomena explicitly. The total energy for an atom can be written in the same form as Equation (2-8) [45]

$$E = E_c + \sum_{i=1}^{n_v} U_{ii} + \frac{1}{2} \sum_{i,j=1}^{n_v} [J_{ij} - K_{ij}] \quad (3-7)$$

E_c is the constant energy of the core electrons and n_v is the number of valence electrons. The exchange integrals, expressed in terms of Condon-Shortly integrals [46], are determined from differences in atomic state energies. The coulomb integrals are a linear combination of the spherically symmetric coulomb integral,

denoted F^0 or γ_{AA} , and the same Condon-Shortly integrals that make up the exchange integrals. According to the analysis by Pariser, F^0 is set to the ionization potential of the atom less its electron affinity [47].

$$\gamma_{AA} = F^0 = \langle ss|ss \rangle = IP - EA \quad (3-8)$$

The core terms remain and are determined as that value for which Koopmans' theorem would predict the correct orbital ionization potential.

There are two terms that must be addressed in the parameterization of two-center quantities at the INDO level of approximation. These are the two-center repulsion integrals and the one-electron bond parameters or resonance integrals. The generalized form of many two-center repulsion integrals used in semiempirical theory can be expressed as

$$\gamma_{AB}(R_{AB}) = \frac{f_g}{\left[\left(\frac{f_g}{\gamma_{AB}(0)} \right)^m + R_{AB}^m \right]^{1/m}} \quad (3-9)$$

In this equation f_g is known as the Weiss factor [7] and R_{AB} is the internuclear separation. $\gamma_{AB}(0)$ is the limit of γ_{AB} for which $R_{AB}=0$ and is usually expressed as an average of the two one-center F^0 's. The Weiss factor is set to 1.2 and m is fixed at 1 according to the prescription of Mataga-Nishimoto [48]. With f_g and m fixed no further parameters are necessary for γ_{AB} .

The INDO two-center one-electron matrix element denoted $\beta_{\mu\nu}$ is usually expressed as the average of one-center bond parameters weighted by the overlap

between two Slater orbitals and an appropriate fixed interaction factor, f_{ij} , for the type of orbitals involved. For example,

$$\beta_{\mu_A \nu_B} = \begin{cases} .5(\beta_A + \beta_B)S_{\mu\nu}, & \mu, \nu = s \\ .5(\beta_A + \beta_B)S_{\mu\nu}f_{s\sigma}, & \mu = s, \nu = p \\ .5(\beta_A + \beta_B)[f_{\sigma\sigma}g_{\sigma}S_{\sigma\sigma} + f_{\pi\pi}g_{\pi}S_{\pi\pi}], & \mu, \nu = p \end{cases} \quad (3-10)$$

The interaction factors for spectroscopic INDO [7] are

$$f_{s\sigma} = 1.0, \quad f_{\sigma\sigma} = 1.267, \quad f_{\pi\pi} = 0.585 \quad (3-11)$$

The p-p interactions are divided between pure sigma and pure pi contributions.

The Euler rotation factors are denoted by g .

Properties such as spectral transition moments involve the calculation of integrals that are not involved in the SCF procedure and have not themselves been parameterized. In order to evaluate property integrals in the assumed molecular basis, it becomes necessary to view the parameterized SCF procedure as connected to an atomic basis set through orthogonalization. The majority of INDO/S calculations performed to date involve the calculation of oscillator strength in the dipole length formalism only. The dipole integrals are restricted to one-center contributions and the SCF coefficients are maintained in the assumed orthogonalized basis. For this work all property integrals will be calculated over a Slater basis [49] and subsequently orthogonalized. This will lend to a more systematic comparison between oscillator strength as calculated in differing formalisms. Other properties such as NMR shielding involve many different

types of property integrals. Since there is currently no systematic way of parameterizing or truncating these integrals in a balanced fashion, working in a fully orthogonalized basis is the most logical point of reference to explore.

Benzene and Pyridine

The INDO/S method was originally parameterized to reproduce excitation energies for benzene and pyridine with a truncated CIS procedure. In this section the CIS and RPA methods are compared for these molecules. Oscillator strengths in both length and velocity formalisms are calculated. The effect the size of the active space has on oscillator strength and transition energies is also explored.

Benzene is of point group D_{6h} of which the highest occupied molecular orbital (HOMO) is a doubly degenerate pi orbital of E_{1g} symmetry. The lowest unoccupied molecular orbital (LUMO) is also a doubly degenerate pi orbital of E_{2u} symmetry. Single excitations from the HOMO to the LUMO generate excited states that are of B_{1u} , B_{2u} and E_{1u} symmetry. The only dipole allowed transition from the ground state is to the degenerate E_{1u} state. The experimental excitation spectra for benzene consists of three bands. The two lowest bands indicate low probability of absorption and the third has a large absorption confirming the simple analysis above. The presence of the nitrogen in pyridine reduces the symmetry of the molecule to C_{2v} . The excitations from the upper two occupied pi orbitals into the lower two unoccupied pi orbitals are all now symmetry allowed. The

split degeneracies from that of D_{6h} are small however such that there remains the same three bands as with benzene. In addition, excitations from the highest occupied nonbonding orbital on the nitrogen to the lowest unoccupied pi orbitals are also predicted. The lowest of these is allowed and the second is not. The SCF orbital eigenvalues for the outer valence region for benzene and pyridine are presented in Tables 3-1 and 3-2 and compared to the experimental orbital ionization energies. The agreement with experimental ionization potentials is reasonable with one noted exception. The nonbonded orbital is predicted to lie below the pi orbitals but is experimentally found to be nearly degenerate with the highest pi orbital. This represents the failure of Koopmans' theorem for such orbitals and not the model Hamiltonian itself. Koopmans' theorem does not take into account orbital relaxation which can be substantial for such orbitals. The model Hamiltonian correctly accounts for the experimental ordering when such effects are considered.

The calculated spectra for all configurations below $70,000\text{cm}^{-1}$ is presented in Tables 3-3 and 3-4. Both RPA and CIS give good estimates for the excitation energies. The RPA excitation energies are consistently lower than the CIS energies. It is well known that CIS dipole length oscillator strengths are usually too large and dipole velocity oscillator strengths are too small. From the form of Equation (2-28) a smaller excitation energy is necessary in order to reduce length oscillator strength in favor of velocity oscillator strength maintaining constant

Table 3-1 SCF orbital energies for benzene.

MO	Energy(AU)	EXP ^a	Symmetry(D _{6h})
12	-0.4581	-0.4222	(σ)
13	-0.4581	-0.4222	(σ)
14	-0.3291	-0.3399	E _{1g} (π)
15	-0.3291	-0.3399	E _{1g} (π)
16	0.0304	—	E _{2u} (π^*)
17	0.0304	—	E _{2u} (π^*)

^a Ref. [50]

Table 3-2 SCF orbital energies for pyridine.

MO	Energy(AU)	EXP ^a	Symmetry(C _{2v})
12	-0.4784	-0.4575	(σ)
13	-0.3709	-0.3554	A ₁ (n)
14	-0.3633	-0.3859	B ₂ (π)
15	-0.3328	-0.3601	A ₂ (π)
16	0.0151	—	B ₂ (π^*)
17	0.0290	—	A ₂ (π^*)

^a Ref. [51]

transition moments. The RPA method only guarantees equivalence in a complete basis. It is demonstrated here however, that the RPA method does a good job in balancing the two formalisms with a finite basis.

Table 3-3 Electronic excitation spectra for D_{6h} benzene.

Sym.	CIS (cm^{-1})	f_{ν}^r	f_{ν}^{∇}	RPA	f_{ν}^r	f_{ν}^{∇}	EXP ^a (osc)
$^1B_{2u}$	37797	—	—	37306	—	—	38090 (0.001)
$^1B_{1u}$	48806	—	—	48305	—	—	48972 (0.10)
$^1E_{1u}$	54644	1.020	0.222	51566	0.678	0.541	55900
$^1E_{1u}$	54644	1.020	0.222	51566	0.678	0.541	(0.69)

^a Ref. [52]

The nature of the length operator is to emphasize the long range region of the basis functions whereas the velocity operator emphasizes the region closer to the nuclei where the functions change the most. The dipole velocity oscillator strength for the lower $n-\pi^*$ transition for pyridine is larger than the length oscillator strength for both CIS and RPA. The nonbonding orbital is essentially located on the nitrogen which is more electronegative than carbon. The vicinity of the nitrogen atom is expected to gain charge and thus the electron density in the region will relax. If the assumed atomic basis took this fact into account the atomic velocity matrix elements would be diminished in favor of the length matrix elements for the pyridine nonbonding orbital. The INDO method however is based on a minimal basis formalism which does not allow atoms to become polarized in an asymmetric

Table 3-4 Electronic excitation spectra for C_{2v} pyridine.

Sym.	CIS (cm ⁻¹)	f _ν ^r	f _ν [∇]	RPA	f _ν ^r	f _ν [∇]	EXP ^a (osc)
¹ B _{2(n)}	35981	0.009	0.210	35804	0.008	0.230	34771 (0.003)
¹ A _{2(n)}	44158	—	—	44125	—	—	—
¹ B ₁	38751	0.061	0.010	38120	0.055	0.042	38350 (0.03)
¹ A ₁	49991	0.067	0.020	49230	0.099	0.083	49750 (0.2)
¹ A ₁	56282	0.732	0.037	53970	0.510	0.220	~55000
¹ B ₁	56682	0.887	0.210	54045	0.594	0.449	(1.30)

^a Ref. [52, 53]

fashion. The relaxation of all the orbitals on an atom can be accomplished however with some success and will be the subject of other chapters.

In order to do calculations for large systems some truncation of the active space must be accomplished. The effect the size of the active space has on the spectra of small systems can be studied. For benzene and pyridine no qualitative difference in the ordering of the excitation energies is noted in going from a very small space of all transitions below 55,000cm⁻¹ to a full singles space consisting of transitions above 400,000cm⁻¹. The very lowest transitions change very little

Table 3-5 Benzene $^1E_{1u}$ transition as a function of the active space.

CIS (cm^{-1})	f_{ν}^r	f_{ν}^{∇}	RPA	f_{ν}^r	f_{ν}^{∇}	Active Space (cm^{-1})
55444	1.249	0.522	52208	0.829	0.786	55000
54644	1.020	0.222	51566	0.678	0.541	65000
53060	1.041	0.259	51026	0.708	0.567	80000
53850	0.994	0.198	50854	0.677	0.512	90000
53394	0.988	0.199	50407	0.681	0.509	100000
51054	0.770	0.043	48077	0.514	0.375	130000
50848	0.776	0.051	47863	0.520	0.382	200000
50139	0.768	0.056	47097	0.523	0.394	300000
50000	.771	0.061	46929	0.528	0.402	400000 ^a

^aFull active space

after all configurations below $65,000\text{cm}^{-1}$ are included. The quantitative nature of the other excitation energies, however, systematically diminishes with increasing active space for both RPA and CIS. This is perhaps caused by excitations to the higher lying virtual orbitals calculated too low in energy when the overlap is neglected and mix too readily with the lower lying transitions. The relative magnitudes of the length versus velocity oscillator strengths remain the same for both CIS and RPA. Their absolute magnitude becomes smaller with the size of the space and reduces more rapidly for CIS than RPA. The data for the $^1E_{1u}$

Table 3-6 Pyridine 1A_1 transition as a function of the active space.

CIS (cm^{-1})	f_{ν}^r	f_{ν}^{∇}	RPA	f_{ν}^r	f_{ν}^{∇}	Active Space (cm^{-1})
57477	1.082	0.452	54674	0.717	0.646	55000
56282	0.732	0.037	53970	0.510	0.220	70000
55562	0.703	0.023	53247	0.493	0.198	85000
54426	0.645	0.001	52111	0.471	0.140	100000
52887	0.546	0.013	50392	0.382	0.122	150000
52685	0.546	0.010	50171	0.383	0.125	170000
52327	0.551	0.010	49743	0.389	0.138	240000
52074	0.564	0.005	49410	0.404	0.156	310000
51971	0.571	0.003	49267	0.411	0.164	430000 ^a

^aFull active space

excitation for benzene and the 1A_1 transition for pyridine are presented in Tables 3-5 and 3-6 for illustration. The other excitations follow the same trend.

On the basis of the above analysis the active space for the current model should be truncated in the region $65\text{--}80000\text{cm}^{-1}$ in order to maintain quantitative transition energies. All subsequent calculations will be truncated in this range unless otherwise noted.

Table 3-7 SCF orbital energies for Naphthalene and Quinoline.

MO	Energy(AU)	Energy(AU)
	Naph.	Quin.
20	—	-0.44105 π
21	-0.42976 π	-0.38831 π
22	-0.36977 π	-0.36693 π
23	-0.31545 π	-0.31520 π
24 HOMO	-0.28856 π	-0.30397 π
25	0.00043 π^*	-0.00892 π^*
26	0.02225 π^*	0.01954 π^*
27	0.05681 π^*	0.04968 π^*
28	0.08862 π^*	0.08374 π^*

Naphthalene and Quinoline

One success of the INDO/CIS method is that it extends to molecules larger than for which it was parameterized. For a model Hamiltonian this extension is not guaranteed and becomes a test of the robustness of the method. In this section the CIS and RPA methods are compared for naphthalene and quinoline which can be viewed as extending the π system of benzene and pyridine by one ring. Table 3-7 contains the higher occupied and lower unoccupied orbital eigenvalues for these molecules.

Table 3-8 Electronic excitation spectra for Naphthalene

Type	CIS (cm ⁻¹)	f_{ν}^r	f_{ν}^{∇}	RPA	f_{ν}^r	f_{ν}^{∇}	EXP ^a (osc.)
$\pi \rightarrow \pi^*$	32138	0.004	0.005	31575	0.003	0.010	32000 (0.002)
$\pi \rightarrow \pi^*$	37034	0.154	0.008	36059	0.139	0.119	37500 (0.102)
$\pi \rightarrow \pi^*$	45469	1.844	0.561	43304	1.300	1.131	47500 (1.000)
$\pi \rightarrow \pi^*$	44630	0.000	0.000	44392	0.000	0.000	—
$\pi \rightarrow \pi^*$	46153	0.000	0.000	45594	0.000	0.000	—
$\pi \rightarrow \pi^*$	48551	0.621	0.118	46749	0.416	0.352	49500 (0.300)

^a Ref. [54]

The electronic spectra of these molecules is more complicated than benzene and pyridine due to the presence of excitations from the additional pi orbitals. The calculated excitation spectra for naphthalene is reported in Table 3–8. The RPA oscillator strength values are not only nearly equivalent, but are also in line with experiment. This allows more confidence in the assignment of experimental bands based on calculation. As with benzene and pyridine the RPA transitions are systematically lower in energy than the corresponding CIS values and the CIS dipole length oscillator strength is much larger than dipole velocity.

Table 3-9 Electronic excitation spectra for Quinoline.

Type	CIS (cm ⁻¹)	f_{ν}^r	f_{ν}^{∇}	RPA	f_{ν}^r	f_{ν}^{∇}	EXP ^a (osc.)
$\pi \rightarrow \pi^*$	32467	0.027	0.002	31894	0.026	0.012	31900
$n \rightarrow \pi^*$	34312	0.007	0.181	34139	0.007	0.198	to
$\pi \rightarrow \pi^*$	37525	0.108	0.002	36788	0.106	0.071	36200 (0.116)
$\pi \rightarrow \pi^*$	43277	0.597	0.182	42148	0.724	0.622	44300
$n \rightarrow \pi^*$	45004	0.000	0.000	44968	0.000	0.000	(0.517)
$\pi \rightarrow \pi^*$	46844	0.502	0.116	45618	0.470	0.387	49300
$\pi \rightarrow \pi^*$	46997	0.858	0.278	45770	0.336	0.270	(0.743)
$\pi \rightarrow \pi^*$	48963	0.457	0.089	47582	0.157	0.135	

^a Ref. [55]

The results for quinoline are even more complicated due to the presence of excitations from the nonbonding orbital. The calculated results are presented in Table 3–9. The calculated pi excitations indicate a similar structure to naphthalene with all bands allowed. The oscillator strengths for the nonbonded excitations are like those of pyridine and a similar explanation would apply here.

The RPA performs better than the CIS method for these molecules in terms of oscillator strength. The inability of the CIS method to guarantee equivalence even in a complete basis is not grounds to reject its use for a model Hamiltonian. It is

demonstrated however, that it is not as reliable in the prediction of experimental oscillator strengths. The RPA performs as well as the CIS method for the qualitative ordering of the excitation energies and both methods do well for the quantitative prediction of excitation energies.

The Diazines

The diazines consist of a planar six membered ring containing two nitrogen atoms and, like pyridine, are isoelectronic with benzene. Two nitrogen atoms will generate two low lying nonbonding orbitals. The presence of the single nitrogen did not greatly perturb the band structure for the pi excitations of pyridine as compared to benzene. The presence of a second nitrogen in the ring perturbs the pi transition energies somewhat more but the band structure remains intact. There are now four excitations from the nonbonding orbitals most of which are not allowed and are not resolved experimentally. The calculated SCF energies and spectra may be found in Tables 3-10 through 3-13.

The RPA is very capable of reproducing the spectra of the diazines with the INDO/S Hamiltonian. For benzene, pyridine and the diazines, both CIS and RPA predict the correct order of the lowest $\pi-\pi^*$ and $n-\pi^*$ transition energies with respect to experiment. Oscillator strengths for $n-\pi^*$ transitions are systematically larger for dipole length than dipole velocity as previously observed. The highest energy $n-\pi^*$ transition is predominately from the lower nonbonding orbital. For

Table 3-10 SCF orbital energies for the Diazines.

MO	Energy(AU) 1,2-diazine	Energy(AU) 1,3-diazine	Energy(AU) 1,4-diazine
12(n)	-0.43067	-0.42097	-0.42352
13(π)	-0.38078	-0.38745	-0.40242
14(n)	-0.35278	-0.36630	-0.36475
15(π) HOMO	-0.34776	-0.34754	-0.33096
16(π^*)	0.00299	0.00554	0.00347
17(π^*)	0.01297	0.01524	0.01930
18(π^*)	0.09987	0.09927	0.10012

Table 3-11 Electronic excitation spectra for 1,2-diazine.

Type	CIS (cm ⁻¹)	f_{ν}^r	f_{ν}^{∇}	RPA	f_{ν}^r	f_{ν}^{∇}	EXP ^a (osc.)
n-> π^*	28531	0.014	0.573	28227	0.013	0.671	26649 (0.006)
	35271	0.000	0.000	35169	0.000	0.000	
	46893	0.000	0.000	46826	0.000	0.000	
	51760	0.014	0.109	51705	0.013	0.117	50865- 51503
π -> π^*	39374	0.058	0.001	38741	0.054	0.022	39500 (0.020)
	49600	0.109	0.039	48664	0.139	0.127	50000 (0.100)
	55363	0.464	0.003	53601	0.403	0.078	57300
	57635	0.910	0.260	55079	0.565	0.427	

^a Ref. [52, 53]

Table 3-12 Electronic excitation spectra for 1,3-diazine.

Type	CIS (cm ⁻¹)	f_{ν}^r	f_{ν}^{∇}	RPA	f_{ν}^r	f_{ν}^{∇}	EXP ^a (osc.)
$n \rightarrow \pi^*$	34282	0.016	0.386	34129	0.015	0.426	31073 (0.007)
	36640	0.000	0.000	36506	0.000	0.000	
	45396	0.000	0.000	45313	0.000	0.000	
	51478	0.010	0.082	51433	0.010	0.087	51143 (0.005)
$\pi \rightarrow \pi^*$	39803	0.068	0.012	39187	0.062	0.043	40310 (0.052)
	50181	0.172	0.048	49139	0.189	0.149	52340 (0.16)
R ^b	—	—	—	—	—	—	56271 (0.25)
$\pi \rightarrow \pi^*$	57530	0.652	0.078	55533	0.509	0.167	58500 (~1.)
	57594	0.626	0.011	55700	0.416	0.198	

^a Ref. [52, 53]^b Rydberg transition.

this transition the discrepancy in the calculated oscillator strengths is maintained but the magnitude of the error is diminished from that of the lowest energy transition. The two nonbonding orbitals are different in that the lower energy orbital is less localized than the higher. The hypothesis that more tightly bound orbitals will generate a larger difference in oscillator strengths holds for these molecules. In all cases studied thus far the RPA $\pi \rightarrow \pi^*$ oscillator strengths are

Table 3-13 Electronic excitation spectra for 1,4-diazine.

Type	CIS (cm ⁻¹)	f_{ν}^r	f_{ν}^{∇}	RPA	f_{ν}^r	f_{ν}^{∇}	EXP ^a (osc.)
n-> π^*	30409	0.013	0.476	30164	0.013	0.540	30875 (.01)
	39056	0.000	0.000	38857	0.000	0.000	
	40706	0.000	0.000	40652	0.000	0.000	
	54538	0.000	0.000	54534	0.000	0.000	54000
π -> π^*	36671	0.177	0.033	35609	0.146	0.108	37893- 38808 (.10)
	48358	0.232	0.024	47030	0.207	0.126	50880 (0.15)
	57694	0.253	0.081	56567	0.203	0.000	60700 (~1.)
	60653	0.857	0.256	58182	0.552	0.420	60700 (~1.)
π -> σ^*	57900						
	59305	0.000	0.000	57786	0.000	0.000	—
	60306						
R ^b	—	—	—	—	—	—	55154

^a Ref. [52, 53]^b Rydberg transition.

superior to those of CIS with respect to equivalence and experiment, and in most cases that obtained from the dipole length operator are better when compared to experiment than that obtained from the velocity operator.

The RPA for Extended Systems

One utility of modern model Hamiltonians is the ability to handle very large systems. The INDO/CIS method has proven its relevance in this regard. In this section the RPA and CIS method are compared for a series of extended aromatic hydrocarbons. The series of molecules beginning with naphthalene (two rings) and anthracene (three rings) is extended up to a linear molecule of twenty rings. The twenty ring molecule consists of 82 carbons and 44 hydrogens for a total of 372 basis functions. The density of spectroscopic states is large for all molecules beyond anthracene; however, there are two transitions that are of specific interest. The first of these is the lowest transition and gives information about the HOMO–LUMO energy gap. The second of these is the transition of maximum oscillator strength, which is polarized along the major axis of the molecule and generates a large transition dipole. Therefore as the molecule increases in length the transition dipole also increases. Data for these two transitions for the different molecules are presented in Tables 3–14 and 3–15.

As the size of the molecule increases, the ratio of RPA dipole length to dipole velocity oscillator strengths for the intense transition is almost constant whereas those of CIS are varied. This indicates that for this type of transition the RPA oscillator strengths scale properly with size whereas the CIS method does not. However the CIS method does improve with size. Both CIS and RPA dipole

Table 3-14 Lowest excitation for extended aromatic system.

# rings	CIS(cm^{-1})	f_{ν}^{r}	f_{ν}^{v}	RPA	f_{ν}^{r}	f_{ν}^{v}
2	32145	0.003	0.005	31583	0.003	0.009
3	28505	0.012	0.022	27900	0.010	0.036
4	24761	0.241	0.003	23383	0.160	0.151
5	21482	0.252	0.030	20003	0.155	0.147
6	19258	0.269	0.050	17707	0.158	0.158
10	12272	0.284	0.623	10147	0.123	0.145
20	11045	0.541	0.159	8743	0.226	0.279

Table 3-15 Most intense excitation for extended aromatic system.

# rings	CIS(cm^{-1})	f_{ν}^{r}	f_{ν}^{v}	RPA	f_{ν}^{r}	f_{ν}^{v}
2	45434	1.832	0.557	43276	1.293	1.124
3	40131	2.703	0.999	38319	1.917	1.728
4	36509	3.479	1.462	34982	2.503	2.319
5	33882	4.171	1.887	32624	3.073	2.834
6	31988	4.829	2.368	30952	3.641	3.372
10	27656	6.948	4.072	27214	5.735	5.250
20	25179	11.712	8.278	25003	10.998	9.697

length oscillator strengths scale linearly with the number of rings as can be seen in Figure 3-1. The RPA values are perfectly linear over the whole range of molecular size whereas the CIS values differ to a small degree for the smaller

molecules. The linear regressions for the oscillator strengths are

$$\begin{aligned} f_{\nu}^r(\text{RPA}) &= 0.535n + 0.344 \quad R = 0.9998 \\ f_{\nu}^r(\text{CIS}) &= 0.531n + 1.344 \quad R = 0.9945 \end{aligned} \quad (3-12)$$

$$n = \# \text{ rings}$$

The dipole length oscillator strengths scale roughly the same for the two methods with the CIS values being systematically higher than the RPA values. For the low energy transition the CIS oscillator strengths indicate no new trends. As with the other molecules studied the RPA oscillator strengths are much more consistent than those of CIS.

The excitation energies for both the RPA and CIS procedures follow predictable trends. Each line was fitted to a general exponential model in order to extrapolate the transition energies to very large systems. The modeled transition energies are

$$\begin{aligned} &\text{LOWEST TRANSITION}(\text{CM}^{-1}) \Rightarrow \\ &E(\text{RPA}) = 8612 + 28040 \exp(-.0646n^{1.625}) \\ &E(\text{CIS}) = 10910 + 25610 \exp(-.0607n^{1.654}) \\ &\text{MOST INTENSE} \Rightarrow \\ &E(\text{RPA}) = 24540 + 48420 \exp(-0.588n^{0.691}) \\ &E(\text{CIS}) = 24710 + 47110 \exp(-0.488n^{0.751}) \end{aligned} \quad (3-13)$$

Both modeled energies and transition energies can be found in Figure 3-2.

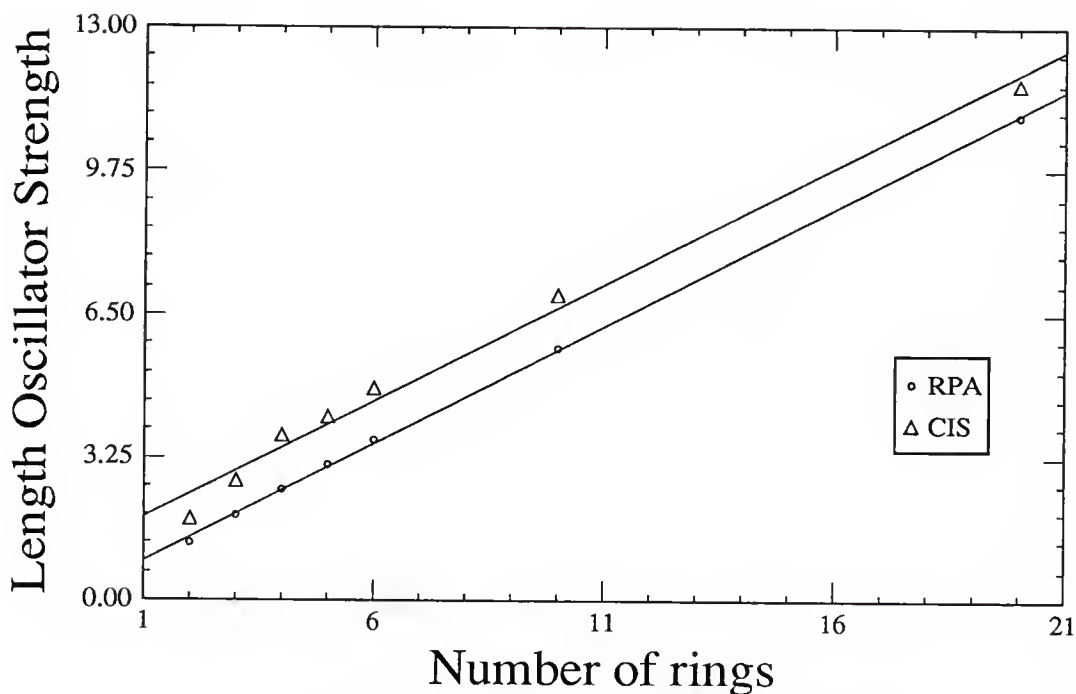


Figure 3-1 Dipole length oscillator strengths for the most intense transition.

The RPA and CIS methods scale similarly with size for a given transition. The difference between naphthalene and the extrapolated values for very large systems is roughly 21000cm^{-1} for both lines and both model calculations. The RPA excitation energies for the lowest transition are systematically smaller than the CIS values. The difference between the two levels for the larger molecules remains constant at 2000cm^{-1} . For the most intense transition the CIS and the RPA transition energies converge to the same value as the chain length is increased.

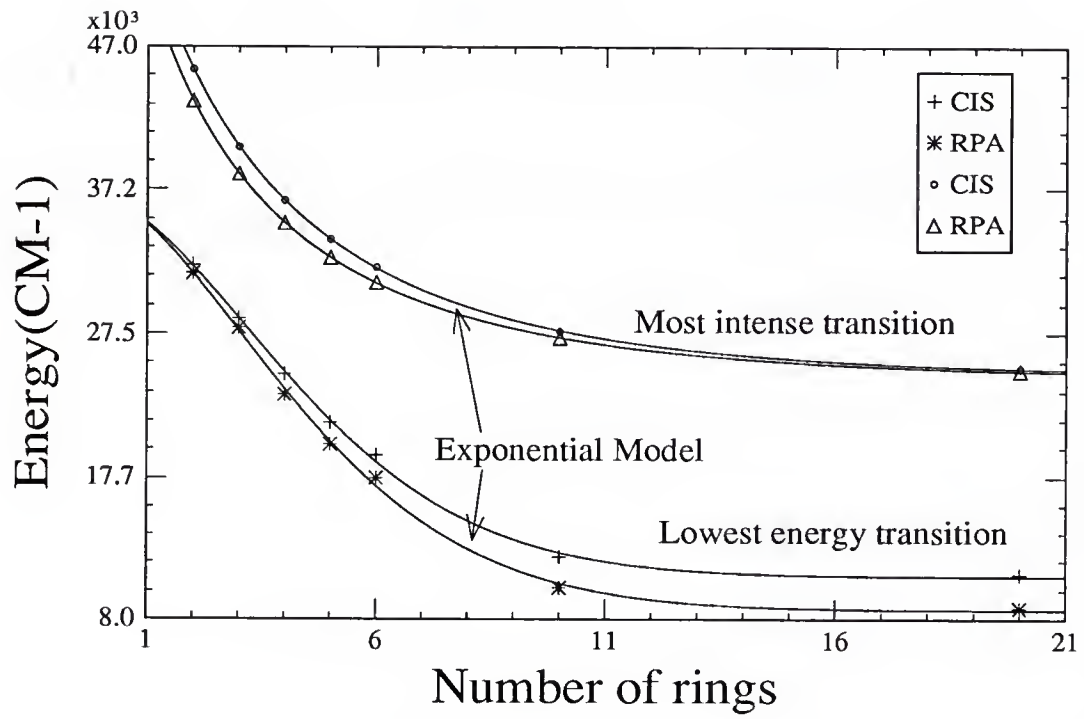


Figure 3-2 Modeled and calculated excitation energies

CHAPTER 4

THE UV-VIS SPECTRA OF FREE BASE AND MAGNESIUM PORPHIN

Motivation

Much experimental and theoretical work has gone into characterizing the electronic structure and spectroscopy of porphines [56]. These systems and their excited states are of great interest in a variety of areas, and in particular are essential in understanding the initial photochemical event in photosynthesis. The electronic spectra of porphyrin compounds are characterized by three basic regions. The so called Q bands are relatively weak and occur in the visible region. The Q bands consist of a degenerate electronic transition for divalent metalloporphines (e.g. MgP) and two separate electronic transitions for free base porphines (H₂P) separated by $\sim 3300\text{cm}^{-1}$. The intense Soret or B region occurs in the near UV and is often accompanied by a closely related N band of lower intensity. The B band for divalent metalloporphines is assumed to be a degenerate pair [57]. The higher UV bands in the third region are broad and are often of near uniform intensity.

The earliest attempts to explain the Q and B bands for H₂P were free electron models and were based on assuming specific resonance structures for porphin that involve an aromatic macrocycle of 18 π electrons [58, 59]. This simple model

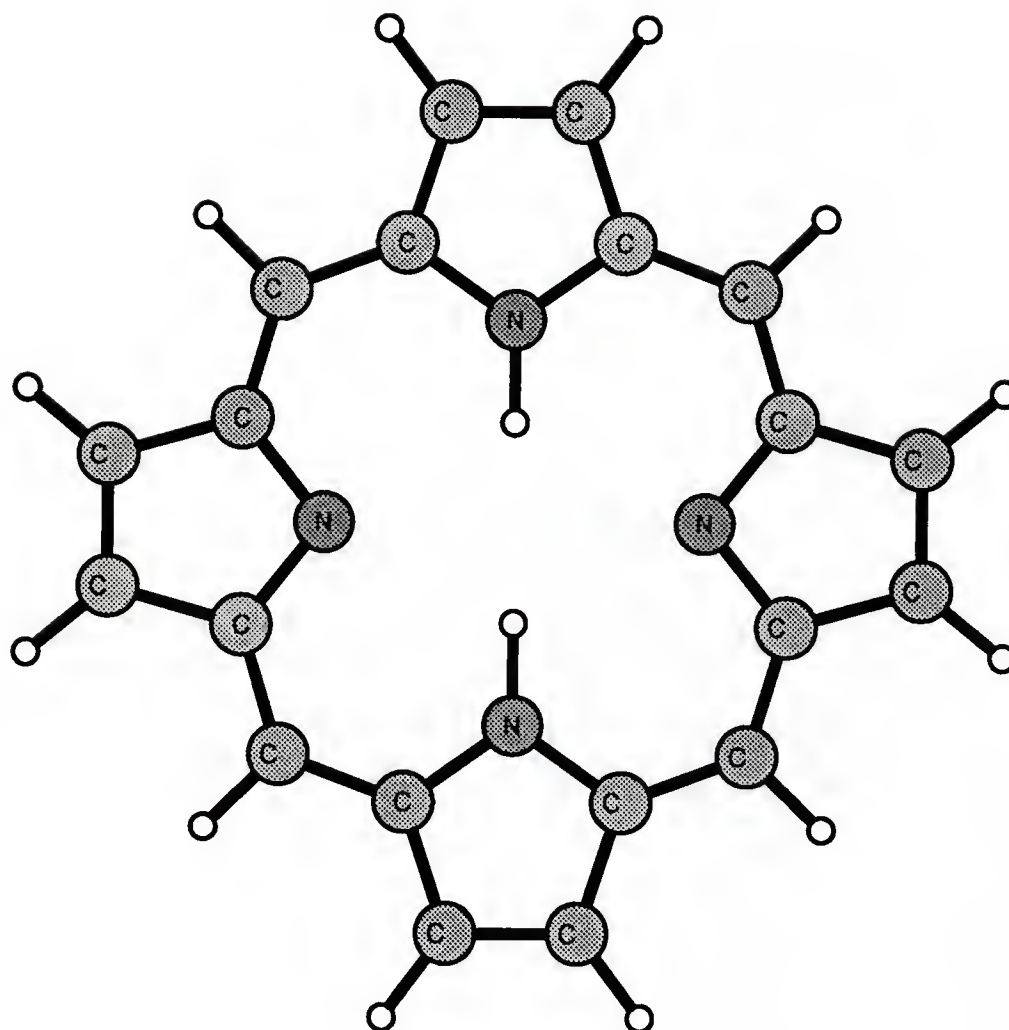


Figure 4-1 Free Base Porphine

correctly accounts for a weak band (Q) followed by a strong band (B). This 18 membered cyclic polyene can be assigned D_{18h} symmetry. Within this group excitations between the highest occupied molecular orbital e_{4u} and lowest empty

$e_{5g}(\pi^*)$ molecular orbital gives rise to states of $^1B_{1u}$, $^1B_{2u}$ and $^1E_{1u}$ symmetry. $^1B_{1u}$ and $^1B_{2u}$ lie lowest, and give rise to the observed $Q_{||}$ and Q_{\perp} peaks. The Soret band, of $^1E_{1u}$ type remains degenerate in this model. In contrast, metalloporphines can be likened to 16 membered cyclic polyenes with 18 pi electrons. In D_{16h} , the HOMO–LUMO excitations give rise to states of $^1E_{7u}$ and $^1E_{1u}$ symmetry, and both visible and Soret are predicted degenerate. Early studies determined that the two Q bands for H_2P were polarized perpendicular to each other and that the B band was of mixed polarization [60]. Low temperature studies of the B band resolved a splitting of 240cm^{-1} between equally intense transitions [61]. Hückel calculations by Gouterman using a four orbital CI model proved adequate in explaining the splitting of the Q bands and predicted that the lower Q band would be polarized parallel to the inner H-H axis [62, 63]. Further polarization studies showed this to be the case and the B band was shown to have parallel polarization at the low energy side of the band and perpendicular polarization on the high energy side of the band [64].

By 1972 extensive PPP-CI calculations had failed to reproduce the assumed B band splitting of 240cm^{-1} for H_2P [65]. The B splitting was predicted to be greater than 1500cm^{-1} and other $\pi-\pi^*$ transitions beyond the four orbital model were predicted to be part of the B and N bands now assumed to be coupled and spread over a region 3300cm^{-1} wide [66]. Sundbom suggested that $n-\pi^*$ may also contribute in this region [67]. Ab initio calculations, with scaled transition

energies, seemed to confirm the complexity of the Soret region suggesting as many as five contributing bands including $n-\pi^*$ [68].

The inability to confirm the nature of the Soret region is complicated by the fact that predicted oscillator strengths in this region do not conform to the observed spectrum without making assumptions about vibrational broadening of the B_{\perp} relative to B_{\parallel} [67, 68]. In addition, calculated oscillator strengths in both the length and velocity formalisms can differ by an order of magnitude [66]. The most commonly used dipole length formalism usually predicts oscillator strengths too large in the Soret region by a factor of two.

Encouraged by the ability of the INDO/RPA method to predict oscillator strengths in addition to excitation energies for aromatic hydrocarbons and heterocycles the spectroscopy of free base and magnesium porphyrin is reexamined in detail.

Results

CIS and RPA calculations have been performed for H_2P for several active space partitions. The number of occupied valence orbitals for H_2P are 57. Orbitals 48 and 49 are the nonbonding orbitals located on the nonprotonated pyrrole ring nitrogens and 50–64 are π . No orbitals outside of this range had significant contribution to the lowest 30 states. Transition energies and oscillator strengths

Table 4-1 Calculated and Experimental Excitation energies for H₂P.

CIS			RPA				EXP ^a
E _{<i>ν</i>} ^b	<i>f</i> _{<i>ν</i>} ^r	<i>f</i> _{<i>ν</i>} [∇]	E _{<i>ν</i>}	<i>f</i> _{<i>ν</i>} ^r	<i>f</i> _{<i>ν</i>} [∇]	Trans. ^c	E _{<i>ν</i>}
13.72	0.022	0.0001	11.81	0.020	0.021	<i>Q</i> _∥	15.94
16.58	0.033	0.001	15.92	0.033	0.029	<i>Q</i> _⊥	19.55
27.18	1.616	0.114	24.08	1.146	1.003	<i>B</i> _∥	26.85
28.42	2.411	0.306	24.44	1.228	1.224	<i>B</i> _⊥	
28.98	—	—	28.70	—	—	—	
29.52	—	—	28.98	—	—	—	29.41
32.97	1.478	0.162	31.69	0.424	0.343	<i>N</i> _∥	
33.58	—	—	33.41	—	—	—	
34.75	—	—	34.42	—	—	—	
35.64	0.366	0.063	35.30	0.169	0.115	⊥	

^a Ref. [69]^b Energies are reported in 10³cm⁻¹.^c Designations ∥ and ⊥ refer to transitions in the plane of the molecule polarized parallel or perpendicular to the inner H-H axis.

for the lowest 10 transitions for an active space of 14 occupied and 14 virtual orbitals are included in Table 4-1.

The lowest occurring n-π* for the CIS calculation is at 39637cm⁻¹ with a dipole length oscillator strength of 0.019 and for the RPA calculation 39600 and 0.019. In order to ensure that the 14x14 active space is adequate for the determination of this transition a 1060 configuration calculation was performed consisting of 53 occupied and 20 virtual orbitals. For CIS the Q, B and N

Table 4-2 Calculated and Experimental Excitation energies for MgP.

CIS			RPA				EXP ^a
E_ν ^b	f_ν^r	f_ν^∇	E_ν	f_ν^r	f_ν^∇	Trans. ^c	E_ν
15.77	0.025	0.002	14.64	0.023	0.025	Q	17.24
15.77	0.025	0.002	14.64	0.023	0.025	Q	
28.62	2.495	0.288	24.95	1.351	1.243	B	25.64
28.62	2.495	0.288	24.95	1.351	1.243	B	
28.71	—	—	28.65	—	—	CT	
29.58	—	—	28.98	—	—	$\pi \rightarrow \pi^*$	
30.46	0.032	0.049	30.41	0.030	0.055	CT	30.77
31.80	—	—	31.49	—	—	$\pi \rightarrow \pi^*$	
32.38	—	—	32.14	—	—	$\pi \rightarrow \pi^*$	
33.55	0.133	0.012	33.19	0.029	0.022	N	
33.55	0.133	0.012	33.19	0.029	0.022	N	

^a Ref. [70]^b Energies are reported in 10^3cm^{-1} .^c CT designates a charge transfer from occupied π to the Mg atom.

bands were lowered by less than 600cm^{-1} and the $n\text{-}\pi^*$ transition was lowered to 38375cm^{-1} for CIS and 38254 for RPA.

A small 7×7 configuration calculation was performed to check the sensitivity of the lower $\pi\text{-}\pi^*$ to the size of the active space. The results for the 6 lowest allowed states are qualitatively the same as those in Table 4-1 being generally 400cm^{-1} higher in energy with differences in oscillator strength less than ten percent.

The results for the low energy portion of MgP are found in Table 4-2. The major features of the spectrum consist of a weak degenerate Q band followed by an intense degenerate B band. The Mg is set 0.4 Å above the ring as suggested by X-ray structures [71]. With the addition of the metal atom new features appear in the spectrum, namely the forbidden or nearly forbidden charge transfer bands. The positions of these bands are very sensitive to the Mg out-of-plane coordinate which is easily perturbed. Similarly to H₂P, several forbidden $\pi \rightarrow \pi^*$ transitions are calculated to fall between the B and N bands.

Discussion

Calculations using the RPA procedure yield an explanation of the Soret region for H₂P that conforms to experiment without invoking vibrational coupling to explain the predicted pattern of oscillator strengths or scaling excitation energies in a least squares manner. While the RPA formalism only ensures equivalence between length and velocity oscillator strengths in a complete HF basis the utility of the procedure to deal with transition moments in a balanced fashion is again demonstrated. This balance of transition moments afforded by the RPA is important if properties such as optical rotary strength in addition to oscillator strength are to be calculated. With the CIS procedure the two moments are very different as already noted by others [66]. In addition the RPA oscillator strengths are in better accord with experiment [70]. The experimental B band oscillator

strengths are estimated to be 1.1 as predicted here. The experimental oscillator strengths for the Q bands are less than 0.1 with $Q_{\perp} > Q_{\parallel}$ as predicted by both the CIS and RPA calculation. The PPP Hamiltonian has to be modified in order to reproduce this result [65, 67]. The experimental N band occurs on the shoulder of the high energy side of the intense B band with experimental oscillator strength much less than that of the B band. This fact is inferred by the RPA results but not CIS.

Both the CIS and RPA procedures predict the correct ordering of the Q and B bands for H₂P as deduced from polarization experiments [64]. In addition both procedures predict the splitting of the Q bands in accord with experiment. The splitting from the CIS procedure is 2860cm⁻¹ and from the RPA 4010cm⁻¹. For gas phase H₂P the experimental splitting is 3610cm⁻¹ [69]. For the B band the RPA calculation yields a splitting of 360cm⁻¹ which is in excellent accord with the original low temperature splitting of 240cm⁻¹. The failure to reproduce this splitting theoretically led to the suggestion that this splitting was due to a vibrational progression and that the second "B" band actually appeared as "N", leaving unexplained the reasons for the sharp B_{||} and broad B_⊥(N) [66]. Even for the 1060 configuration active space the CIS procedure predicts a splitting as large as 1000cm⁻¹.

These calculations therefore support the interpretation that the Soret band for H₂P consists of two nearly degenerate transitions of roughly equal oscillator

strength. The N band consists of $\pi-\pi^*$ beyond the four model. No evidence is found to suspect the presence of $n-\pi^*$ below 38000cm^{-1} or that other allowed $\pi-\pi^*$ are present in the Soret region.

No new observations can be attached the MgP spectrum aside from the ability of the RPA to balance transition moments for oscillator strength. As noted previously, the frequencies calculated by the RPA method are generally lower than those calculated from the CIS treatment. Both calculations are in very good accord with experiment.

The ability of the INDO/RPA method to represent a balanced treatment of transition moments has been established through these calculations and those in Chapter 3. The correspondence with experimentally observed transition moments yields confidence in the method to predict and interpret spectra. The INDO/RPA method has also been shown to not degenerate with molecular size so that very large systems can be studied with confidence.

CHAPTER 5

THE INDO/RPA CALCULATION OF NMR CHEMICAL SHIELDING

The Concept of Chemical Shift

The ability to quantitate and establish the nature of “chemical shift” as it relates to magnetic resonance spectroscopy has been, and is, of great interest in quantum chemistry. The phenomenological Hamiltonian most often used for this purpose is usually attributed to Ramsey [72, 73] and most commonly takes the form of a perturbative expansion of the energy of a system with respect to an external magnetic field and the field of the nuclei of interest [74]. The perturbation is small with respect to the total energy of most chemical systems; therefore, the perturbative expansion can be truncated at low order and is usually assumed to be linear. Many empirical and semiempirical models have been developed to predict specific chemical shift in terms of the chemical properties of the atoms of interest and the specific bonding environment [75, 76]. These models and rules are very useful in interpreting the nature of the local chemical environment in a molecule. Direct nonempirical calculations of chemical shift have met with only modest success and normally requires very large basis sets to obtain quantitative accuracy [77]. The failure of smaller basis sets is usually attributed to their inability to represent the gauge invariance of the origin of the externally applied

field. As a result, in the last few years methods to minimize the effect of gauge variance have been developed with much success [78–81].

In this Chapter the local orbital, local origin method of Hansen and Bouman [81] for the calculation of isotropic shielding of the atoms in a closed shell molecule is developed for the INDO/S Hamiltonian. This method is chosen because it utilizes the unique properties of the RPA already discussed, and because the results obtained are easily analyzed in terms of the chemically useful concept of localized effects in molecules.

The magnetic energy of interaction of a nucleus in an external magnetic field can be expressed as [82]

$$U = -\vec{\mu} \cdot \vec{B} \quad (5-1)$$

where $\vec{\mu}$ is the magnetic moment of the nucleus and \vec{B} is the external magnetic field. The magnetic moment of the nucleus is quantized. The operator form of $\vec{\mu}$ is

$$\vec{\mu} = \gamma \vec{P}, \quad |\vec{P}| = \hbar[I(I-1)]^{1/2} \quad (5-2)$$

where \vec{P} is the angular momentum operator and γ is the gyromagnetic ratio of the specific nucleus. For an oriented molecule in an external field of magnitude B aligned along the z axis and with m_I the magnetic quantum number of the nucleus we can express the interaction energy

$$U_z = -\gamma \hbar m_I B \quad (5-3)$$

Differences in magnetic quantum numbers represent differences in interaction energy. The absolute difference in energy for a change of one quantum number is then

$$\Delta U_z = h\nu = |\gamma\hbar|B \quad (5-4)$$

the frequency of which is

$$\nu = \left| \frac{\gamma}{2\pi} \right| B = K_\gamma B \quad (5-5)$$

Therefore, in the absence of any other factors, energy differences for unit changes in magnetic quantum number are linearly dependent on the external magnetic field and are a function of the specific nuclei only. It is this difference in energy with applied field that is measured in a magnetic resonance experiment. If no other factors were involved, a single measurement of γ for a type of nucleus would be sufficient to describe all situations dealing with the same nucleus and NMR would be of very little interest in chemistry. Nuclei are not normally isolated, however, but in the presence of electrons. The external field induces a current in the electrons. This current in turn creates a magnetic field that is in opposition to the applied field. The net field (B) at the nucleus of interest is less than the applied field (B_0). Different electronic environments will modify the total field differently. Each chemically unique environment for a given type of atom in a molecule at

fixed external field strength will thus result in a different frequency. The induced field of the electrons is also linearly dependent on the external field so that

$$\begin{aligned}\nu_j &= K_\gamma B_0(1 - \sigma_j) = \nu_0(1 - \sigma_j) \Rightarrow \\ \sigma_j &= \frac{\nu_0 - \nu_j}{\nu_0}\end{aligned}\tag{5-6}$$

σ_j is the unitless shielding constant for environment j with respect a bare nucleus and represents the effect of the electrons in said environment. With respect to an arbitrary reference environment we define relative chemical shift parameters

$$\delta'_j = \sigma_{\text{ref}} - \sigma_j = \frac{\nu_j - \nu_{\text{ref}}}{\nu_0}\tag{5-7}$$

Since $|\nu_j - \nu_{\text{ref}}| \ll \nu_0$ and $\nu_0 \approx \nu_{\text{ref}}$ relative chemical shift is usually tabulated in terms of parts per million

$$\delta_j(\text{ppm}) = 10^6 \frac{\nu_j - \nu_{\text{ref}}}{\nu_{\text{ref}}}\tag{5-8}$$

In this formalism positive values of relative chemical shift represent an environment that is less shielded than the reference environment.

Theory

We seek a quantum mechanical description of σ which, in general, is dependent on the directional components of the applied field and the components of the nuclear magnetic moment. Equation (5-1) is modified to read

$$\begin{aligned}U &= -\vec{\mu} \cdot [\vec{1} - \tilde{\sigma}] \cdot \vec{B} = -\vec{\mu} \cdot \vec{B} + \vec{\mu} \cdot \tilde{\sigma} \cdot \vec{B} \\ &= U_0 + U_1\end{aligned}\tag{5-9}$$

U represents the total energy of interaction and U_1 the electronic perturbation.

A magnetic field can be expressed in terms of a vector potential that must be incorporated into the Hamiltonian of the system [17]. The kinetic energy portion of Equation (2-1) is modified to read

$$\hat{H} = \frac{1}{2} \sum_{i=1}^n [-i\vec{\nabla}_i + \frac{1}{c}\vec{A}_i] \cdot [-i\vec{\nabla}_i + \frac{1}{c}\vec{A}_i] + V \quad (5-10)$$

where c is the velocity of light and \vec{A} is the magnetic vector potential. The vector potential for a uniform magnetic field is

$$\vec{A}_i^B = \frac{1}{2}\vec{B} \times [\vec{r}_i - \vec{R}] \quad (5-11)$$

with arbitrary gauge origin \vec{R} . All coordinates are relative to the nucleus of interest. The vector potential associated with the magnetic dipole moment of the nucleus is expressed [20]

$$\vec{A}_i^N = \frac{\vec{\mu} \times \vec{r}_i}{r_i^3} \quad (5-12)$$

We choose the coulomb gauge so that $\vec{\nabla} \cdot \vec{A} = 0$ and expand Equation (5-10) according to Equations (5-11) and (5-12)

$$\begin{aligned}
 \hat{H} &= \hat{H}^0 + \hat{H}' \\
 \hat{H}' &= \sum_{i=1}^n -\frac{i}{2c} \left[\vec{B} \times (\vec{r}_i - \vec{R}) + 2 \frac{\vec{\mu} \times \vec{r}_i}{r_i^3} \right] \cdot \vec{\nabla}_i \\
 &\quad + \sum_{i=1}^n \frac{1}{2c^2} \left[\frac{1}{2} \vec{B} \times (\vec{r}_i - \vec{R}) + \frac{\vec{\mu} \times \vec{r}_i}{r_i^3} \right]^2 \\
 &= \sum_{i=1}^n -\frac{i}{2c} \left[\vec{B} \cdot \{(\vec{r}_i - \vec{R}) \times \vec{\nabla}_i\} + 2 \frac{\vec{\mu} \cdot (\vec{r}_i \times \vec{\nabla}_i)}{r_i^3} \right] \\
 &\quad + \sum_{i=1}^n \frac{1}{2c^2} \left[\frac{1}{2} \vec{B} \times (\vec{r}_i - \vec{R}) + \frac{\vec{\mu} \times \vec{r}_i}{r_i^3} \right]^2
 \end{aligned} \tag{5-13}$$

where $[\]^2$ is a shorthand notation for $[\] \cdot [\]$. The last equality in Equation (5-13) represents the perturbation Hamiltonian of interest here. The terms quadratic in field are dropped due to the observation that shielding is practically linear with field according to Equation (5-9). The final expression for the perturbation is then

$$\begin{aligned}
 \hat{H}' &= \sum_{i=1}^n -\frac{i}{2c} \left[\vec{B} \cdot \{(\vec{r}_i - \vec{R}) \times \vec{\nabla}_i\} + 2 \frac{\vec{\mu} \cdot (\vec{r}_i \times \vec{\nabla}_i)}{r_i^3} \right] \\
 &\quad + \sum_{i=1}^n \frac{1}{2c^2} \left[\frac{[\vec{B} \times (\vec{r}_i - \vec{R})] \cdot [\vec{\mu} \times \vec{r}_i]}{r_i^3} \right] \\
 &= \hat{H}'(1) + \hat{H}'(2) = \hat{H}'_B(1) + \hat{H}'_\mu(1) + \hat{H}'(2)
 \end{aligned} \tag{5-14}$$

Perturbations to molecular energies due to the presence of a magnetic field are small so a low order expansion of the perturbation Hamiltonian is adequate.

To second order with a Hartree-Fock reference wavefunction [19]

$$E' = E^1 + E^2 = \langle \psi_{\text{HF}} | \hat{H}' | \psi_{\text{HF}} \rangle + \sum_{k=1}^{\infty} \frac{\langle \psi_{\text{HF}} | \hat{H}' | \psi_k \rangle \langle \psi_k | \hat{H}' | \psi_{\text{HF}} \rangle}{E_{\text{HF}} - E_k} \quad (5-15)$$

where the ψ_k represent excited states of energy E_k . Placing Equation (5-14) into (5-15) yields

$$\begin{aligned} E^1 = & -\frac{i}{2c} \sum_{i=1}^n \{ \vec{B} \cdot \langle \psi_{\text{HF}} | (\vec{r}_i - \vec{R}) \times \vec{\nabla}_i | \psi_{\text{HF}} \rangle \\ & + 2\vec{\mu} \cdot \langle \psi_{\text{HF}} | \frac{\vec{r}_i \times \vec{\nabla}_i}{r_i^3} | \psi_{\text{HF}} \rangle \} \\ & + \sum_{i=1}^n \frac{1}{2c^2} \langle \psi_{\text{HF}} | \frac{[\vec{B} \times (\vec{r}_i - \vec{R})] \cdot [\vec{\mu} \times \vec{r}_i]}{r_i^3} | \psi_{\text{HF}} \rangle \\ & = E^1(1) + E^1(2) \end{aligned} \quad (5-16)$$

and

$$\begin{aligned} & \langle \psi_{\text{HF}} | \hat{H}' | \psi_k \rangle \langle \psi_k | \hat{H}' | \psi_{\text{HF}} \rangle = \\ & \langle \psi_{\text{HF}} | \hat{H}'(1) + \hat{H}'(2) | \psi_k \rangle \langle \psi_k | \hat{H}'(1) + \hat{H}'(2) | \psi_{\text{HF}} \rangle \\ & = \langle \psi_{\text{HF}} | \hat{H}'(1) | \psi_k \rangle \langle \psi_k | \hat{H}'(1) | \psi_{\text{HF}} \rangle + \langle \psi_{\text{HF}} | \hat{H}'(2) | \psi_k \rangle \langle \psi_k | \hat{H}'(2) | \psi_{\text{HF}} \rangle \\ & + \langle \psi_{\text{HF}} | \hat{H}'(1) | \psi_k \rangle \langle \psi_k | \hat{H}'(2) | \psi_{\text{HF}} \rangle + \langle \psi_{\text{HF}} | \hat{H}'(2) | \psi_k \rangle \langle \psi_k | \hat{H}'(1) | \psi_{\text{HF}} \rangle \end{aligned} \quad (5-17)$$

Recalling Equation (5-9) we seek terms that are linear in both external and nuclear field. It is conventional to interpret experiments in terms of the phenomenological Hamiltonian of Equation (5-9), therefore is convenient to gear this development to yield numbers comparable to the interpretation of these experiments. It would be more systematic, however, to calculate the observed experimental spectrum directly and would make a logical project for the future. The first term in Equation

(5-16) is only linear in a single field and can be dropped. In Equation (5-17) all terms involving $\hat{H}'(2)$ are quadratic or higher in field. Dropping these terms leaves

$$\begin{aligned}
 & \langle \psi_{\text{HF}} | \hat{H}'(1) | \psi_k \rangle \langle \psi_k | \hat{H}'(1) | \psi_{\text{HF}} \rangle = \\
 & \langle \psi_{\text{HF}} | \hat{H}'_{\text{B}}(1) + \hat{H}'_{\mu}(1) | \psi_k \rangle \langle \psi_k | \hat{H}'_{\text{B}}(1) + \hat{H}'_{\mu}(1) | \psi_{\text{HF}} \rangle = \\
 & \langle \psi_{\text{HF}} | \hat{H}'_{\text{B}}(1) | \psi_k \rangle \langle \psi_k | \hat{H}'_{\text{B}}(1) | \psi_{\text{HF}} \rangle + \langle \psi_{\text{HF}} | \hat{H}'_{\mu}(1) | \psi_k \rangle \langle \psi_k | \hat{H}'_{\mu}(1) | \psi_{\text{HF}} \rangle + \\
 & \langle \psi_{\text{HF}} | \hat{H}'_{\text{B}}(1) | \psi_k \rangle \langle \psi_k | \hat{H}'_{\mu}(1) | \psi_{\text{HF}} \rangle + \langle \psi_{\text{HF}} | \hat{H}'_{\mu}(1) | \psi_k \rangle \langle \psi_k | \hat{H}'_{\text{B}}(1) | \psi_{\text{HF}} \rangle
 \end{aligned} \tag{5-18}$$

Collecting those terms in Equation (5-18) that are of the proper form leaves

$$\begin{aligned}
 U_1 = & \frac{1}{2c^2} \langle \psi_{\text{HF}} | \sum_{i=1}^n \frac{[\vec{B} \times (\vec{r}_i - \vec{R})] \cdot [\vec{\mu} \times \vec{r}_i]}{r_i^3} | \psi_{\text{HF}} \rangle - \\
 & \frac{1}{c^2} \sum_{k=1}^{\infty} \frac{\langle \psi_{\text{HF}} | \sum_{i=1}^n \frac{\vec{\mu} \cdot [\vec{r}_i \times \vec{\nabla}_i]}{r_i^3} | \psi_k \rangle \langle \psi_k | \sum_{i=1}^n \vec{B} \cdot [(\vec{r}_i - \vec{R}) \times \vec{\nabla}_i] | \psi_{\text{HF}} \rangle}{E_{\text{HF}} - E_k}
 \end{aligned} \tag{5-19}$$

The second term in Equation (2-19) has the proper form as suggested by Equation (5-9). Through vector identities the first term can be rearranged and Equation (5-19) reads

$$\begin{aligned}
 U_1 = & \vec{\mu} \cdot \left\{ \frac{1}{2c^2} \langle \psi_{\text{HF}} | \sum_{i=1}^n \frac{(\vec{I})[(\vec{r}_i - \vec{R}) \cdot \vec{r}_i] - (\vec{r}_i - \vec{R}) \cdot \vec{r}_i}{r_i^3} | \psi_{\text{HF}} \rangle - \right. \\
 & \left. \frac{1}{c^2} \sum_{k=1}^{\infty} \frac{\langle \psi_{\text{HF}} | \sum_{i=1}^n \frac{[\vec{r}_i \times \vec{\nabla}_i]}{r_i^3} | \psi_k \rangle \langle \psi_k | \sum_{i=1}^n [(\vec{r}_i - \vec{R}) \times \vec{\nabla}_i] | \psi_{\text{HF}} \rangle}{E_{\text{HF}} - E_k} \right\} \cdot \vec{B} \\
 & = \vec{\mu} \cdot \vec{\sigma} \cdot \vec{B}
 \end{aligned} \tag{5-20}$$

identifying the form of shielding desired. Let $\vec{\varepsilon}_\mu$ be a unit vector along the direction of the nuclear magnetic moment and $\vec{\varepsilon}_B$ along the applied field.

$$\begin{aligned} \sigma_{\mu B} = & \frac{1}{2c^2} \langle \psi_{\text{HF}} | \sum_{i=1}^n \frac{[\vec{\varepsilon}_B \times (\vec{r}_i - \vec{R})] \cdot [\vec{\varepsilon}_\mu \times \vec{r}_i]}{r_i^3} | \psi_{\text{HF}} \rangle + \\ & \frac{1}{c^2} \sum_{k=1}^{\infty} \frac{\langle \psi_{\text{HF}} | \sum_{i=1}^n \frac{\vec{\varepsilon}_\mu \cdot [\vec{r}_i \times \vec{\nabla}_i]}{r_i^3} | \psi_k \rangle \langle \psi_k | \sum_{i=1}^n \vec{\varepsilon}_B \cdot [(\vec{r}_i - \vec{R}) \times \vec{\nabla}_i] | \psi_{\text{HF}} \rangle}{E_k - E_{\text{HF}}} \end{aligned} \quad (5-21)$$

Equation (5-21) is the basic equation for the calculation of chemical shielding [73]. The first term can be interpreted as that shielding created by the induced current around the nuclei of interest and is known as the diamagnetic component of shielding (σ^d). The second term is known as the paramagnetic component of shielding (σ^p) and can be interpreted as the degree to which the specific chemical environment quenches the induced current around the nucleus. The two components are opposite in sign and a delicate balance must be achieved in order to obtain even qualitative results as compared to experiment.

The transition matrix elements in the paramagnetic portion are over anti-Hermitian one-electron operators. Being one-electron operators the sum can be truncated at single excitations only. Transition moments for anti-Hermitian operators according to the analysis in Chapter 2 for a closed shell reference are expressed

$$\begin{aligned} \langle \psi_{\text{HF}} | \hat{O}_A^\mu | \psi_k \rangle &= \sqrt{2} \sum_{\gamma c} \langle \phi_\gamma | \hat{O}_A^\mu | \phi_c \rangle [X - Y]_{\gamma c, k} \\ \langle \psi_k | \hat{O}_A^B | \psi_{\text{HF}} \rangle &= \sqrt{2} \sum_{\delta d} [X - Y]_{\delta d, k}^\dagger \langle \phi_d | \hat{O}_A^B | \phi_\delta \rangle \end{aligned} \quad (5-22)$$

The energy in the denominator is the transition energy for the excitation (E_K).

Pre and post multiplication of Equation (2-45) yields,

$$\begin{aligned} (A - B)^{-1} // (A - B)(X - Y) &= (X + Y)E_K // E_K^{-1} \\ (X - Y)E_K^{-1} &= (A - B)^{-1}(X + Y) // (X^\dagger - Y^\dagger) \\ (X - Y)E_K^{-1}(X^\dagger - Y^\dagger) &= (A - B)^{-1} \end{aligned} \quad (5-23)$$

Incorporation of Equations (5-22) and (5-23) into the paramagnetic shielding term yields

$$\sigma_{\mu B}^P = \frac{2}{c^2} \sum_{\gamma c \delta d} \langle \phi_\gamma | \hat{O}_A^\mu | \phi_c \rangle (A - B)_{\gamma c, \delta d}^{-1} \langle \phi_d | \hat{O}_A^B | \phi_\delta \rangle \quad (5-24)$$

Let R_γ be the location vector of occupied orbital γ relative to the nucleus of interest. The field dependent transition integral in Equation (5-24) becomes

$$\begin{aligned} \langle \phi_d | \hat{O}_A^B | \phi_\delta \rangle &= \langle \phi_d | (\vec{r} - \vec{R}) \times \vec{\nabla} | \phi_\delta \rangle \cdot \vec{\epsilon}_B \\ &= [\langle \phi_d | (\vec{r} - \vec{R}_\gamma) \times \vec{\nabla} | \phi_\delta \rangle + \langle \phi_d | (\vec{R}_\gamma - \vec{R}) \times \vec{\nabla} | \phi_\delta \rangle] \cdot \vec{\epsilon}_B \\ &= [\langle \phi_d | (\vec{r} - \vec{R}_\gamma) \times \vec{\nabla} | \phi_\delta \rangle + (\vec{R}_\gamma - \vec{R}) \times \langle \phi_d | \vec{\nabla} | \phi_\delta \rangle] \cdot \vec{\epsilon}_B \end{aligned} \quad (5-25)$$

so that

$$\begin{aligned} \sigma_{\mu B}^P &= \frac{2}{c^2} \sum_{\gamma c \delta d} \langle \phi_\gamma | \hat{O}_A^\mu | \phi_c \rangle (A - B)_{\gamma c, \delta d}^{-1} \langle \phi_d | (\vec{r} - \vec{R}_\gamma) \times \vec{\nabla} | \phi_\delta \rangle \cdot \vec{\epsilon}_B \\ &\quad + \frac{2}{c^2} \sum_{\gamma c \delta d} \langle \phi_\gamma | \hat{O}_A^\mu | \phi_c \rangle [(\vec{R}_\gamma - \vec{R}) \times [(A - B)_{\gamma c, \delta d}^{-1} \langle \phi_d | \vec{\nabla} | \phi_\delta \rangle]] \cdot \vec{\epsilon}_B \end{aligned} \quad (5-26)$$

According to Equation (2-27) and the properties of the RPA equations in a complete Hartree Fock basis

$$(A - B)_{\gamma c, \delta d}^{-1} \langle \phi_d | \vec{\nabla} | \phi_\delta \rangle = -\langle \phi_c | \vec{r} | \phi_\gamma \rangle \quad (5-27)$$

The paramagnetic term becomes

$$\begin{aligned}\sigma_{\mu B}^P &= \frac{2}{c^2} \sum_{\gamma c \delta d} \langle \phi_\gamma | \hat{O}_A^\mu | \phi_c \rangle (A - B)_{\gamma c, \delta d}^{-1} \langle \phi_d | (\vec{r} - \vec{R}_\gamma) \times \vec{\nabla} | \phi_\delta \rangle \cdot \vec{\varepsilon}_B \\ &\quad - \frac{2}{c^2} \sum_{\gamma c} \langle \phi_\gamma | \hat{O}_A^\mu | \phi_c \rangle [(\vec{R}_\gamma - \vec{R}) \times \langle \phi_c | \vec{r} | \phi_\gamma \rangle] \cdot \vec{\varepsilon}_B\end{aligned}\quad (5-28)$$

where all references to the global gauge origin are contained in the second sum.

For a closed shell reference and local origins the diamagnetic portion of shielding becomes

$$\begin{aligned}\sigma_{\mu B}^d &= \frac{1}{c^2} \sum_{\gamma} \langle \phi_\gamma | \frac{[\vec{\varepsilon}_B \times (\vec{r} - \vec{R}_\gamma)] \cdot [\vec{\varepsilon}_\mu \times \vec{r}]}{r^3} | \phi_\gamma \rangle \\ &\quad + \frac{1}{c^2} \sum_{\gamma} [\vec{\varepsilon}_B \times (\vec{R}_\gamma - \vec{R})] \cdot \langle \phi_\gamma | \frac{[\vec{\varepsilon}_\mu \times \vec{r}]}{r^3} | \phi_\gamma \rangle\end{aligned}\quad (5-29)$$

where again all references to the global origin are contained in the second sum.

Combining the origin dependent sums of Equations (5-28) and (5-29) and using the vector relation $A \cdot (B \times C) = C \cdot (A \times B)$ yields for the global origin dependent term

$$\begin{aligned}\sigma_{\mu B}(\vec{R}) &= \frac{1}{c^2} \sum_{\gamma} [\vec{\varepsilon}_B \times (\vec{R}_\gamma - \vec{R})] \cdot \langle \phi_\gamma | \frac{[\vec{\varepsilon}_\mu \times \vec{r}]}{r^3} | \phi_\gamma \rangle \\ &\quad - \frac{2}{c^2} \sum_{\gamma c} \langle \phi_\gamma | \frac{\vec{\varepsilon}_\mu \cdot [\vec{r} \times \vec{\nabla}]}{r^3} | \phi_c \rangle \langle \phi_c | \vec{r} | \phi_\gamma \rangle \cdot [\vec{\varepsilon}_B \times (\vec{R}_\gamma - \vec{R})]\end{aligned}\quad (5-30)$$

Utilizing the orbital completeness relation [23]

$$\begin{aligned}\sum_{\gamma} |\phi_\gamma\rangle \langle \phi_\gamma| + \sum_c |\phi_c\rangle \langle \phi_c| &= 1 \\ \sum_c |\phi_c\rangle \langle \phi_c| &= 1 - \sum_{\gamma} |\phi_\gamma\rangle \langle \phi_\gamma|\end{aligned}\quad (5-31)$$

gives for the origin dependent term

$$\begin{aligned}
\sigma_{\mu B}(\vec{R}) &= \frac{1}{c^2} \sum_{\gamma} [\vec{\varepsilon}_B \times (\vec{R}_{\gamma} - \vec{R})] \cdot \langle \phi_{\gamma} | \frac{[\vec{\varepsilon}_{\mu} \times \vec{r}]}{r^3} | \phi_{\gamma} \rangle \\
&- \frac{2}{c^2} \sum_{\gamma} \langle \phi_{\gamma} | \left\{ \frac{\vec{\varepsilon}_{\mu} \cdot [\vec{r} \times \vec{\nabla}]}{r^3} \right\} \{ [\vec{\varepsilon}_B \times (\vec{R}_{\gamma} - \vec{R})] \cdot [\vec{r} | \phi_{\gamma}] \} \rangle \\
&+ \frac{2}{c^2} \sum_{\gamma \delta} \langle \phi_{\gamma} | \frac{\vec{\varepsilon}_{\mu} \cdot [\vec{r} \times \vec{\nabla}]}{r^3} | \phi_{\delta} \rangle \langle \phi_{\delta} | \vec{r} | \phi_{\gamma} \rangle \cdot [\vec{\varepsilon}_B \times (\vec{R}_{\gamma} - \vec{R})]
\end{aligned} \tag{5-32}$$

The second sum can be rearranged

$$\begin{aligned}
&2 \langle \phi_{\gamma} | \left\{ \frac{\vec{\varepsilon}_{\mu} \cdot [\vec{r} \times \vec{\nabla}]}{r^3} \right\} \{ [\vec{\varepsilon}_B \times (\vec{R}_{\gamma} - \vec{R})] \cdot [\vec{r} | \phi_{\gamma}] \} \rangle \\
&= [\vec{\varepsilon}_B \times (\vec{R}_{\gamma} - \vec{R})] \cdot 2 \langle \phi_{\gamma} | \left\{ \frac{\vec{\varepsilon}_{\mu} \cdot [\vec{r} \times \vec{\nabla}]}{r^3} \right\} [\vec{r} | \phi_{\gamma}] \rangle \\
&= [\vec{\varepsilon}_B \times (\vec{R}_{\gamma} - \vec{R})] \cdot \left[\langle \phi_{\gamma} | \left\{ \frac{\vec{\varepsilon}_{\mu} \cdot [\vec{r} \times \vec{\nabla}]}{r^3} \right\} [\vec{r} | \phi_{\gamma}] \rangle - [\langle \phi_{\gamma} | \vec{r} | \left\{ \frac{\vec{\varepsilon}_{\mu} \cdot [\vec{r} \times \vec{\nabla}]}{r^3} \right\} | \phi_{\gamma} \rangle] \right] \\
&= [\vec{\varepsilon}_B \times (\vec{R}_{\gamma} - \vec{R})] \cdot \langle \phi_{\gamma} | \left[\frac{\vec{\varepsilon}_{\mu} \cdot [\vec{r} \times \vec{\nabla}]}{r^3}, \vec{r} \right] | \phi_{\gamma} \rangle
\end{aligned} \tag{5-33}$$

and combined with the first sum

$$\begin{aligned}
\sigma_{\mu B}(\vec{R}) &= \frac{1}{c^2} \sum_{\gamma} [\vec{\varepsilon}_B \times (\vec{R}_{\gamma} - \vec{R})] \cdot \langle \phi_{\gamma} | \frac{1}{r^3} \{ [\vec{\varepsilon}_{\mu} \times \vec{r}] - [\vec{\varepsilon}_{\mu} \cdot [\vec{r} \times \vec{\nabla}], \vec{r}] \} | \phi_{\gamma} \rangle \\
&+ \frac{2}{c^2} \sum_{\gamma \delta} \langle \phi_{\gamma} | \frac{\vec{\varepsilon}_{\mu} \cdot [\vec{r} \times \vec{\nabla}]}{r^3} | \phi_{\delta} \rangle \langle \phi_{\delta} | \vec{r} | \phi_{\gamma} \rangle \cdot [\vec{\varepsilon}_B \times (\vec{R}_{\gamma} - \vec{R})]
\end{aligned} \tag{5-34}$$

Consider the general relationship

$$\begin{aligned}
\vec{\epsilon}_j \cdot (\vec{r} \times \vec{\nabla})[(\vec{\epsilon}_i \cdot \vec{r})|\psi\rangle] &= \vec{\epsilon}_j \cdot \vec{r} \times [\vec{\nabla}(\vec{\epsilon}_i \cdot \vec{r})|\psi\rangle] \\
&= \vec{\epsilon}_j \cdot \vec{r} \times [\vec{\epsilon}_i|\psi\rangle + (\vec{\epsilon}_i \cdot \vec{r})\vec{\nabla}|\psi\rangle] \\
&= (\vec{\epsilon}_j \times \vec{r}) \cdot (\vec{\epsilon}_i|\psi\rangle) + (\vec{\epsilon}_j \times \vec{r}) \cdot [(\vec{\epsilon}_i \cdot \vec{r})\vec{\nabla}|\psi\rangle] \Rightarrow \\
(\vec{\epsilon}_j \times \vec{r}) \cdot (\vec{\epsilon}_i|\psi\rangle) &= \vec{\epsilon}_j \cdot (\vec{r} \times \vec{\nabla})[(\vec{\epsilon}_i \cdot \vec{r})|\psi\rangle] - (\vec{\epsilon}_i \cdot \vec{r})(\vec{\epsilon}_j \times \vec{r}) \cdot [\vec{\nabla}|\psi\rangle] \\
&= \vec{\epsilon}_j \cdot (\vec{r} \times \vec{\nabla})[(\vec{\epsilon}_i \cdot \vec{r})|\psi\rangle] - (\vec{\epsilon}_i \cdot \vec{r})(\vec{\epsilon}_j \cdot \vec{r}) \times [\vec{\nabla}|\psi\rangle] \\
&\quad \left\{ (\vec{\epsilon}_j \times \vec{r}) \cdot \vec{\epsilon}_i - [\vec{\epsilon}_j \cdot (\vec{r} \times \vec{\nabla}), (\vec{\epsilon}_i \cdot \vec{r})] \right\} |\psi\rangle = 0
\end{aligned} \tag{5-35}$$

the last line of which indicates that the first sum in Equation (5-34) vanishes.

The indices of summation for the remaining term are over all occupied orbitals

and can be rewritten as

$$\begin{aligned}
\sigma_{\mu B}(\vec{R}) &= \frac{1}{c^2} \sum_{\gamma\delta} \left\{ \langle \phi_\gamma | \frac{\vec{\epsilon}_\mu \cdot [\vec{r} \times \vec{\nabla}]}{r^3} | \phi_\delta \rangle \langle \phi_\delta | \vec{r} | \phi_\gamma \rangle \cdot [\vec{\epsilon}_B \times (\vec{R}_\gamma - \vec{R})] \right. \\
&\quad \left. + \langle \phi_\delta | \frac{\vec{\epsilon}_\mu \cdot [\vec{r} \times \vec{\nabla}]}{r^3} | \phi_\gamma \rangle \langle \phi_\gamma | \vec{r} | \phi_\delta \rangle \cdot [\vec{\epsilon}_B \times (\vec{R}_\delta - \vec{R})] \right\} \\
&= \frac{1}{c^2} \sum_{\gamma\delta} \langle \phi_\gamma | \frac{\vec{\epsilon}_\mu \cdot [\vec{r} \times \vec{\nabla}]}{r^3} | \phi_\delta \rangle \langle \phi_\delta | \vec{r} | \phi_\gamma \rangle \cdot [\vec{\epsilon}_B \times (\vec{R}_\gamma - \vec{R}_\delta)]
\end{aligned} \tag{5-36}$$

where all references to an external gauge origin have been eliminated from the expression for the shielding.

The final working expression for shielding becomes

$$\begin{aligned}
 \sigma_{\mu B} = & \frac{1}{c^2} \sum_{\gamma} \langle \phi_{\gamma} | \{ (\vec{\varepsilon}_{\mu} \cdot \vec{\varepsilon}_B) (\vec{r} - \vec{R}_{\gamma}) \cdot \vec{r} - \vec{\varepsilon}_{\mu} \cdot (\vec{r} - \vec{R}_{\gamma}) (\vec{\varepsilon}_B \cdot \vec{r}) \} r^{-3} | \phi_{\gamma} \rangle \\
 & + \frac{2}{c^2} \sum_{\gamma c \delta d} \vec{\varepsilon}_{\mu} \cdot \langle \phi_{\gamma} | \frac{\vec{r} \times \vec{\nabla}}{r^3} | \phi_c \rangle (A - B)_{\gamma c, \delta d}^{-1} \langle \phi_d | (\vec{r} - \vec{R}_{\gamma}) \times \vec{\nabla} | \phi_{\delta} \rangle \cdot \vec{\varepsilon}_B \\
 & + \frac{1}{c^2} \sum_{\gamma \delta} \vec{\varepsilon}_{\mu} \cdot \langle \phi_{\gamma} | \frac{\vec{r} \times \vec{\nabla}}{r^3} | \phi_{\delta} \rangle [(\vec{R}_{\gamma} - \vec{R}_{\delta}) \times \langle \phi_{\delta} | \vec{r} | \phi_{\gamma} \rangle] \cdot \vec{\varepsilon}_B
 \end{aligned} \tag{5-37}$$

The problem is resolved into the choice of orbital origins, the evaluation of various property integrals and the construction and inversion of the RPA (A-B) matrix [81].

The expression for shielding is a 3x3 matrix that is a function of the orientation of the molecule and the external field. With the principle exception of solid state NMR, the orientation of molecules with respect to an external field is random and shielding becomes an average of the principle components of the shielding matrix. It is this isotropic value in which we are immediately interested. The following discussion is for ^{13}C isotropic shielding. ^{13}C is chosen for study because the range of normal shielding values is 200 ppm and is a well characterized experimental quantity.

Localization and Integral Evaluation

The occupied orbitals are localized according to the criteria of Foster and Boys [83]. A symmetric transformation of the orbitals is chosen such that the sum of the squares of the pairwise differences in their locations is a maximum. In other words,

$$\max (R = \sum_{\gamma\delta} |\vec{R}_\gamma - \vec{R}_\delta|^2) \quad (5-38)$$

$$\vec{R}_\gamma = [\langle \phi_\gamma | X | \phi_\gamma \rangle, \langle \phi_\gamma | Y | \phi_\gamma \rangle, \langle \phi_\gamma | Z | \phi_\gamma \rangle]$$

An iterative process of successive two by two rotations is performed until all successive pairs are stable within a given threshold [84]. Local orbitals obtained in this fashion are easily identified as bonds between atoms and nonbonding orbitals. Double and triple bonds are represented by tau or banana bonds. These are identified by the program and are selectively delocalized to yield the more familiar local sigma and pi bonds. The property integrals and RPA matrices in Equation (5-37) are first evaluated in the canonical molecular orbital basis via transformation from the appropriate atomic integrals and subsequently transformed to the local basis.

Three choices of local origins in the calculation of molecular shielding are evaluated. The first is the coupled HF (CHF) approximation in which all orbitals are assumed to be located at the nucleus of interest. The second choice assigns all local orbitals to be at their centroid location. As defined by Hansen and Bouman

[81] this is known as the full local orbital, local origin method (FLORG). The final choice, intermediate between the first two, assigns all local orbitals that are bonded to an atom to be at said nucleus and all other orbitals are assumed to be at their centroid location (LORG). Since in a complete basis the results are invariant to the choice of origins, the difference between results in a finite basis tests the sensitivity of the results to the basis type and choice of origins.

There are many atomic integrals necessary for the evaluation of Equation (5-37) that are not normally associated with those required to perform an SCF procedure. Fortunately all integrals of the type used here can be put in the form of a normal overlap integral or a nuclear attraction integral that are easily evaluated. For atomic basis functions of the form [85]

$$|\chi_A\rangle = N_A |n_x, n_y, n_z, \vec{R}_A\rangle = N_A |x_A^{n_x} y_A^{n_y} z_A^{n_z} \exp(-\zeta_A r_A^2)\rangle \quad (5-39)$$

located at center A, dipole integrals, velocity integrals, and angular momentum integrals can be evaluated with overlap routines. The X component of each is outlined below. For dipole,

$$\begin{aligned} \langle \chi_A | X | \chi_B \rangle &= \langle \chi_A | X_B + x_B | \chi_B \rangle \\ &= X_B \langle \chi_A | \chi_B \rangle + N_B \langle \chi_A | n_x + 1, n_y, n_z, \vec{R}_B \rangle \end{aligned} \quad (5-40)$$

and for velocity.

$$\begin{aligned} \langle \chi_A | \nabla_x | \chi_B \rangle &= N_B n_x \langle \chi_A | n_x - 1, n_y, n_z, \vec{R}_B \rangle \\ &\quad - 2\zeta_B N_B \langle \chi_A | n_x + 1, n_y, n_z, \vec{R}_B \rangle \end{aligned} \quad (5-41)$$

The angular momentum integrals are particularly easy to evaluate once the velocity integrals are formed.

$$\begin{aligned}
 \langle \chi_A | (\vec{R} \times \vec{\nabla})_x | \chi_B \rangle &= \langle \chi_A | ((\vec{R}_B + \vec{r}_B) \times \vec{\nabla})_x | \chi_B \rangle \\
 &= \langle \chi_A | (\vec{R}_B \times \vec{\nabla})_x | \chi_B \rangle + \langle \chi_A | (\vec{r}_B \times \vec{\nabla})_x | \chi_B \rangle \\
 &= Y_B \langle \chi_A | \nabla_z | \chi_B \rangle - Z_B \langle \chi_A | \nabla_y | \chi_B \rangle + \\
 &\quad \langle \chi_A | (Y_B \nabla_z - Z_B \nabla_y) | \chi_B \rangle \\
 &= Y_B \langle \chi_A | \nabla_z | \chi_B \rangle - Z_B \langle \chi_A | \nabla_y | \chi_B \rangle + \\
 &\quad + N_B n_z \langle \chi_A | n_x, n_y + 1, n_z - 1, \vec{R}_B \rangle - N_B n_y \langle \chi_A | n_x, n_y - 1, n_z + 1, \vec{R}_B \rangle
 \end{aligned}
 \tag{5-42}$$

The last line of Equation (5-42) includes only renormalized overlap functions of the original basis.

The field integrals associated with the diamagnetic shielding term can be evaluated with nuclear attraction integrals. Most integral packages do not evaluate nuclear attraction integrals explicitly since the sum over all such operators is the desired quantity in an SCF calculation. Modification of the integral routines to obtain information about specific centers is necessary. To obtain the necessary integrals relative to center C consider the following operation on an arbitrary

basis function [86].

$$\begin{aligned}
 \langle \chi_A | \nabla_x \frac{1}{r_c} | \chi_B \rangle &= -\frac{x_c}{r_c^3} \langle \chi_B | + \frac{1}{r_c} \langle \nabla_x \chi_B | \\
 \langle \chi_A | \frac{x_c}{r_c^3} | \chi_B \rangle &= \langle \chi_A | \left[\frac{1}{r_c}, \nabla_x \right] | \chi_B \rangle \\
 &= \langle \chi_A | \frac{1}{r_c} | \nabla_x \chi_B \rangle + \langle \nabla_x \chi_A | \frac{1}{r_c} | \chi_B \rangle
 \end{aligned} \tag{5-43}$$

The gradient of the basis functions is evaluated as with the velocity integrals above. The other components of diamagnetic shielding follow similarly.

$$\begin{aligned}
 \langle \chi_A | \frac{x_c^2}{r_c^3} | \chi_B \rangle &= \langle \chi_A | \frac{x_c(X_B - X_c + x_B)}{r_c^3} | \chi_B \rangle \\
 (X_B - X_c) \langle \chi_A | \frac{x_c}{r_c^3} | \chi_B \rangle &+ N_B \langle \chi_A | \frac{x_c}{r_c^3} | n_x + 1, n_y, n_z, \vec{R}_B \rangle \\
 \langle \chi_A | \frac{x_c y_c}{r_c^3} | \chi_B \rangle &= \langle \chi_A | \frac{(X_B - X_c + x_B) y_c}{r_c^3} | \chi_B \rangle \\
 (X_B - X_c) \langle \chi_A | \frac{y_c}{r_c^3} | \chi_B \rangle &+ N_B \langle \chi_A | \frac{y_c}{r_c^3} | n_x + 1, n_y, n_z, \vec{R}_B \rangle
 \end{aligned} \tag{5-44}$$

Finally the magnetic dipole integral can be evaluated.

$$\begin{aligned}
 \langle \chi_A | \frac{(\vec{r}_c \times \vec{\nabla})_x}{r_c^3} | \chi_B \rangle &= \langle \chi_A | \frac{y_c \nabla_z - z_c \nabla_y}{r_c^3} | \chi_B \rangle \\
 &= \langle \chi_A | \frac{y_c}{r_c^3} | \nabla_z \chi_B \rangle - \langle \chi_A | \frac{z_c}{r_c^3} | \nabla_y \chi_B \rangle \\
 &= \langle \nabla_y \chi_A | \frac{1}{r_c} | \nabla_z \chi_B \rangle + \langle \chi_A | \frac{1}{r_c} | \nabla_y \nabla_z \chi_B \rangle \\
 &\quad - \langle \nabla_z \chi_A | \frac{1}{r_c} | \nabla_y \chi_B \rangle - \langle \chi_A | \frac{1}{r_c} | \nabla_z \nabla_y \chi_B \rangle \\
 &= \langle \nabla_y \chi_A | \frac{1}{r_c} | \nabla_z \chi_B \rangle - \langle \nabla_z \chi_A | \frac{1}{r_c} | \nabla_y \chi_B \rangle
 \end{aligned} \tag{5-45}$$

Reduced Linear Equations

The construction and inversion of the (A–B) matrix is a formidable task for more than about seventy basis functions since the whole single excitation space must be considered. For greater than seventy basis functions, the size of the singles space surpasses that which can be handled with normal computing facilities. The result of the intermediate sum below is a vector of the dimension of the singly excited space.

$$\begin{aligned}
 & \sum_{\delta d} (A - B)_{\gamma c, \delta d}^{-1} \langle \phi_d | (\vec{r} - \vec{R}_\gamma) \times \vec{\nabla} | \phi_\delta \rangle = \\
 & \sum_{\delta d} (A - B)_{\gamma c, \delta d}^{-1} [\langle \phi_d | \vec{r}_{\text{global}} \times \vec{\nabla} | \phi_\delta \rangle - (\vec{R} - \vec{R}_\gamma) \times \langle \phi_d | \vec{\nabla} | \phi_\delta \rangle] = \\
 & \sum_{\delta d} (A - B)_{\gamma c, \delta d}^{-1} \langle \phi_d | \vec{r}_{\text{global}} \times \vec{\nabla} | \phi_\delta \rangle \\
 & - (\vec{R} - \vec{R}_\gamma) \times [\sum_{\delta d} (A - B)_{\gamma c, \delta d}^{-1} \langle \phi_d | \vec{\nabla} | \phi_\delta \rangle]
 \end{aligned} \tag{5-46}$$

If the product of $(A-B)^{-1}$ and the occupied- virtual block of the components of the global angular momentum operator and the same for the velocity operator is known, the remainder of the paramagnetic term can be evaluated as a dot product. The technique of reduced linear equations [13, 14] can be used to create these six vectors directly avoiding the time consuming step of inversion. Let N represent the square matrix (A–B) and M the column vector of the component of velocity or angular momentum of interest. The product column vector is represented by X such that $N^{-1}M = X$ is the equation to be solved for X.

In order to solve for X consider the expansion of X in a basis of column vectors (X_i) such that with k basis columns

$$X^{(k)} = \sum_{i=1}^k X_i c_i^{(k)}, \quad Y_i = NX_i \quad (5-47)$$

and

$$M = NX = \sum_{i=1}^k Y_i c_i^{(k)} \quad (5-48)$$

For a given k and X_i , define the error vector as

$$E = M - \sum_{i=1}^k Y_i c_i^{(k)} \quad (5-49)$$

with norm

$$\delta^{(k)} = M^\dagger M - 2M^\dagger \sum_{i=1}^k Y_i c_i^{(k)} - \sum_{i,j} Y_i^\dagger Y_j c_i^{(k)} c_j^{(k)} \quad (5-50)$$

which we wish to minimize with respect to the expansion coefficients.

$$\frac{\partial \delta^{(k)}}{\partial c_1^{(k)}} = 2M^\dagger Y_1 - 2 \sum_{i=1}^k c_i^{(k)} Y_i^\dagger Y_1 = 0 \quad (5-51)$$

For each Y_1

$$M^\dagger Y_1 = \left(\sum_{i=1}^k c_i^{(k)} Y_i^\dagger \right) Y_1, \quad Y_1^\dagger M = Y_1^\dagger \left(\sum_{i=1}^k c_i^{(k)} Y_i \right) \quad (5-52)$$

Let Y be the matrix of all Y_i and C^k the vector of all coefficients then

$$Y^\dagger M = Y^\dagger Y C^{(k)} \Rightarrow C^{(k)} = (Y^\dagger Y)^{-1} Y^\dagger M \quad (5-53)$$

gives the best possible coefficients for a given set of basis vectors. The inversion in Equation (5-53) is only of the order k . The problem reduces to a choice of X_i such that with minimal k the norm of the error defined by Equation (5-50) is below some threshold tolerance.

Given k vectors the $X_{(k+1)}$ vector should be chosen such that the error vector is zero. According to Equation (5-49) then

$$\begin{aligned} E = 0 &= M - N \sum_{i=1}^k X_i c_i^{(k)} - N X_{k+1} \\ X_{k+1} &= N^{-1} (M - N \sum_{i=1}^k X_i c_i^{(k)}) = N^{-1} (M - \sum_{i=1}^k Y_i c_i^{(k)}) \end{aligned} \quad (5-54)$$

which requires the full inversion of N which is to be avoided. If N^{-1} can be reasonably approximated, however, the next vector can be chosen and the process repeated until convergence is achieved. The matrix N can be partitioned into a diagonal matrix (a) and a matrix that represents the remainder of N (D). The matrix identity

$$N^{-1} = (a + D)^{-1} = a^{-1} - a^{-1} D (a + D)^{-1} \quad (5-55)$$

defines a series in a^{-1} and D . If N is diagonally dominant then the inverse of N may be approximated by the inverse of the diagonal and used in Equation (5-54). Recall that N represents $(A-B)$ the diagonal of which is

$$(A - B)_{\gamma c, \gamma c} = \varepsilon_c - \varepsilon_\gamma + \langle \gamma c | c \gamma \rangle - \langle \gamma c | \gamma c \rangle \quad (5-56)$$

If the molecular two electron integrals have been formed the full diagonal may be used and rapid convergence is usually achieved.

The formation of N involves a very large transformation of integrals from the atomic to the molecular basis. The dimension of N grows with the square of the number of basis functions thus requiring repeated disk IO in order to form products of N and the basis vectors necessary to solve the system of reduced linear equations. The transformation of the integrals and the storage of N may be avoided by performing the product of N and X directly from the atomic orbital basis [14]. Let (a) be the diagonal matrix of differences in orbital eigenvalues. We want

$$Y_i = NX_i = (a + D)X_i = aX_i + DX_i \quad (5-57)$$

where D contains all two-electron integrals. The (a) contribution to Y_i is trivial.

The general matrix element from the contribution from D is given by

$$\begin{aligned} [Y_i^D]_{\gamma c} &= \sum_{\delta d} [\langle c\gamma | \delta d \rangle - \langle d\gamma | c\delta \rangle] [X_i]_{\delta d} \\ &= \sum_{i,j} C_{ic} C_{j\gamma} \left[\sum_{k,l} [\langle ij | lk \rangle - \langle kj | il \rangle] \left[\sum_{\delta d} C_{kd} [X_i]_{\delta d} C_{l\delta} \right] \right] \end{aligned} \quad (5-58)$$

and has been reduced to a series of intermediate sums. The first sum transforms the basis vector into a square matrix the same dimension as the atomic basis.

$$[Y_i^D]_{\gamma c} = \sum_{i,j} C_{ic} C_{j\gamma} \left[\sum_{k,l} [\langle ij | lk \rangle - \langle kj | il \rangle] X_{k,l} \right] \quad (5-59)$$

The second sum is accomplished by making a single pass through the atomic two electron integrals to target a square matrix also of the same dimension as the basis set.

$$[Y_i^D]_{\gamma c} = \sum_{i,j} C_{ic} C_{j\gamma} T_{i,j} \quad (5-60)$$

The final sum targets the vector Y_i .

Through the use of reduced linear equations the inversion of large matrices is avoided. By directly building the matrix products in the atomic basis the entire process can be maintained in core except for the possibility of a single pass through the atomic two-electron integrals which may be on disk. The efficiency of this procedure allows the calculation of atomic shielding to be accomplished for any molecule for which an SCF can be performed. The slowest step becomes the evaluation of the many integrals that have to be calculated and stored by center over the complete atomic basis.

Diamagnetic Shielding in Molecules

Although specific contributions to atomic shielding in molecules can not be directly observed, it is of benefit to consider their contributions from a theoretical point of view. Diamagnetic shielding is a function only of the orbitals occupied in the ground state. In Equation (5-37) the first term can be interpreted as the orbital or bond contribution to diamagnetic shielding. In a local basis the third

term can be interpreted as a bond-bond contribution to diamagnetic shielding. In the CHF approximation the third term vanishes.

Chemical intuition and accurate ab initio calculations suggest that the diamagnetic shielding is primarily a function of the atom of interest and, to a lesser extent, the nearest neighbor bonds [87]. In order to study the effect of local origin choice on the calculation and interpretation of diamagnetic shielding, the specific bond and bond-bond contributions for octane have been calculated and tabulated in Table 5-1.

The local contributions to diamagnetic shielding are essentially constant for all model choices of local origins. The CHF remote contributions, however, are large and varied. They would also suggest that remote contributions are more important than the local contributions. It is demonstrated that the LORG and FLORG methods essentially dampen all remote contributions to diamagnetic shielding in accord with intuition and accurate calculations. For the LORG model the specific local bond terms are tabulated in Table 5-2. These data suggest that diamagnetic shielding may be an additive function of bond type.

In order to test the nature of bond contributions to diamagnetic shielding and to test the effect of electronegative substituents, a series of compounds containing fourteen valence electrons have been calculated. The results are tabulated in Table 5-3. With increasing electronegative substituents the density around the carbon

Table 5-1 Diamagnetic shielding in octane (ppm).

CARBON /MODEL	LOCAL σ^d (bond)	REMOTE σ^d (bond)	LOCAL σ^d (bond-bond)	REMOTE σ^d (bond-bond)	TOT. σ^d
1 CHF	88.75	94.51	—	—	183.3
1 LORG	88.75	0.77	—	0.30	89.8
1 FLORG	18.00	0.77	39.26	0.60	58.6
2 CHF	89.09	116.96	—	—	206.0
2 LORG	89.09	1.37	—	1.76	92.2
2 FLORG	18.33	1.37	40.04	2.12	61.9
3 CHF	89.12	129.68	—	—	218.8
3 LORG	89.12	1.50	—	1.39	92.0
3 FLORG	18.22	1.50	39.63	1.84	61.2
4 CHF	89.14	134.70	—	—	223.8
4 LORG	89.14	1.46	—	1.40	92.0
4 FLORG	18.23	1.46	39.59	1.85	61.1

is reduced, therefore reducing the total diamagnetic shielding. The contribution from the C-H bonds is increased through the inductive effect created by the electronegative substituent while the contribution from the substituent bond is diminished by the same effect. It is noted, however, that the range of diamagnetic shielding is only a few ppm, whereas the total shielding range is roughly sixty

Table 5-2 LORG bond contributions to diamagnetic shielding in octane.

CARBON	C-H(1)	C-H(2)	C-C(1)	C-C(2)
1	22.08	22.11x2	22.44	—
2	—	22.15x2	22.35	22.45
3	—	22.15x2	22.38	22.43
4	—	22.15x2	22.41	22.42

Table 5-3 LORG bond analysis of substituent effects on diamagnetic shielding.

COMPOUND	C-H	C-X	TOTAL
CH ₃ -CH ₃	22.11	22.38	90.00
CH ₃ -NH ₂	22.16	22.21	89.78
CH ₃ -OH	22.25	21.57	88.85
CH ₃ -F	22.37	20.48	87.37

ppm for the same series of compounds. This fact supports the observation that chemical shift is primarily a paramagnetic effect.

The INDO/RPA Method for Chemical Shift

Chemical shift cannot be described by diamagnetic shielding alone. Chemical shift is a sum of both the diamagnetic and paramagnetic terms. Since the range of diamagnetic shielding is small the full range of chemical shift is controlled by the paramagnetic term. In order to study paramagnetic effects two categories of environment have been identified for study. The first is the effect of the number

and type of bonds. This is basically a study of hybridization and its effect on chemical shift. The second effect is that of substituents.

A series of representative small compounds containing single, double, and triple bonds have been selected for study. Benzene and pyridine are also included to study aromatic effects. Since chemical shift is reported with respect to a reference standard, methane is chosen to represent zero shift in this study. The calculated and theoretical values for isotropic chemical shift for the test compounds are included in Table 5-4.

The FLORG model works very well for all test bond environments. The LORG model works well for all bond environments except the triple bond. The CHF method does not work well at all. Since in a complete basis all methods are equivalent, the very different results reflects the sensitivity of the method to the size of the basis. For ab initio calculations very large basis sets are necessary in order to obtain near equivalence of the methods. The utility of the FLORG method in dampening the effects of basis size is demonstrated.

Total shielding values for the molecules used to test the effect of electronegative substituents on diamagnetic shielding have been calculated and tabulated in Table 5-5 relative to ethane. Standard substituent effects relative to a methyl group are included. Only the FLORG model is even qualitatively correct with respect to experiment. It does not, however, approach the known substituent effect

Table 5-4 Calculated and experimental ^{13}C chemical shifts.

CARBON(*)	SHIFT			
	EXP ^a (ppm)	FLORG	LORG	CHF
CH ₄	0.0	0.0	0.0	0.0
C ₂ H ₆	14.2	11.84	6.22	-5.73
CH ₂ CH-C*H ₃	26.	13.41	8.03	-13.34
C ₂ H ₂	74.3	66.26	2.27	3.74
C*H ₂ CH-CH ₃	123.	108.08	74.78	56.55
Pyridine-meta	125.	109.49	79.32	40.52
C ₂ H ₄	130.	113.09	80.26	71.63
Benzene	131.	117.19	84.23	41.47
Pyridine-para	137.	121.29	85.18	40.92
CH ₂ C*H-CH ₃	142.	125.46	87.68	64.94
Pyridine-ortho	155.	144.00	109.67	79.74
CH ₂ O	196.	160.61	125.23	116.60
Correlation Coef.	—	0.9956	0.9573	0.9249

^a Ref. [88]

for such groups. It is here that the small basis is the most severe approximation. The cancelation of the global gauge dependent term in the development of the expression for the total shielding expression depends twice on the properties of a complete HF basis. The first instance occurs in Equation (5-27). In this equation the equivalence relation between length and velocity is invoked. Although only valid in a complete basis, the results obtained for oscillator strength for calculated

Table 5-5 Calculated chemical shifts relative to ethane.

COMPOUND	FLORG(ppm)	LORG	CHF	SUBSTITUENT EFFECT ^a
CH ₃ -CH ₃	0.0	0.0	0.0	0.0
CH ₃ -NH ₂	1.82	-1.3	-3.14	20.
CH ₃ -OH	2.48	-4.91	-14.21	40.
CH ₃ -F	2.70	-9.56	-29.50	60.

^a From a table of additive shifts tabulated from experiment [76].

excitation spectra with the RPA approximation indicate that this approximation is probably sound even with a small basis.

The second use of orbital completeness occurs in the resolution of the identity in Equation (5-31). For a small basis this approximation is severe. The number of virtual orbitals is only seven for ethane and is reduced to four for fluoromethane.. Ab initio calculations for fluoromethanes require triple zeta plus polarization basis sets to approach experimental accuracy. Since the diamagnetic term is only a function of the occupied orbitals it is relatively stable with respect to the quality and size of the basis.

Although the INDO/RPA-FLORG method has some utility for the study of chemical shift the severity of using a minimal basis would be difficult to overcome within the ZDO approximation. The localization methods do, however, dampen the effect of remote contributions to shielding even for the small basis

utilized. Since substituent effects are tabulated for many types of compounds, a combination of empirical formulations for substituent effects could be incorporated into the calculated results to obtain quantitative agreement with experiment. Perhaps the best approach would be to develop an extended valence form of ZDO Hamiltonians to allow a more accurate treatment of all sum over state properties.

CHAPTER 6

A CHARGE DEPENDENT HAMILTONIAN FOR ATOMIC PROPERTIES

Impetus

It is well accepted that ab initio minimal basis set calculations in quantum chemistry at the self consistent field (SCF) level are of limited reliability. One problem with minimal basis set calculations is that the effective valence exponents are fixed so that the electronic density around an atom cannot contract or expand as the atom loses or gains charge. The basis functions should, however, have the flexibility to expand or contract as necessitated by the environment of an atomic center in the molecule. In ab initio theories this implies that the exponents in the basis functions should also be optimized according to the variation principle along with the orbital coefficients. The optimization of orbital exponents is a complex nonlinear problem that is also highly dependent on the form of the basis set functions in its implementation. This problem is alleviated in ab initio theory calculations by use of multiple-zeta basis sets. Instead of a single basis function with a fixed exponent for an orbital, orbitals are represented as a sum of basis functions with differing exponents. In this way the nonlinear optimization of exponents in a minimal basis calculation is linearized. Due to the fact that ab

initio calculations grow as N^4 , the use of multiple-zeta basis sets further restricts the size of systems that can be studied.

The reliability of semiempirical theories, which are most often minimal basis set formalisms, is aided by experimentally calibrated parameters. These theories are less reliable, however, when bonds are highly polar in nature. For example, the calculation of electronic spectra of carbonyls appears to require a different set of two-center parameters than molecules in which the atoms remain primarily neutral in order to get transition energies that match experiment [89, 7]. We are not free to apply the variational principle to optimize effective exponents in semiempirical theories since we have not explicitly dealt with the core electrons. Core-valence potentials are built into the one-electron parameters but without restraining the valence exponents to remain in the valence space, optimizing these exponents will result in a collapse of the valence orbitals into the core [44].

In this Chapter a functional form of charge dependent parameters for atoms is developed. The experimental determination of the one-center integrals is maintained, but the restriction that these parameters are constants is removed. Instead they will be expressions dependent on the charge of the atom. In other words, we envision our orbitals contracting and expanding with charge and proceed to determine the effect this would have on the parameterized integrals. For specific cases, such as when dealing with anions or polar bonds, parameters designed to reproduce properties for neutral species fail to yield accurate results.

In the next Section the link between experiment and the parameters that are currently in use is reviewed. In the following Section some of the approximations that are used in developing atomic-based parameters are removed. The assumption is still made that atomic properties can be accurately modeled with a valence orbital MBS formalism, but the parameters that arise from this assumption no longer need be constants for a given atom. By design, the new parameters developed in this Chapter will reproduce atomic energies and in this way also reproduce the energy differences necessary for describing atomic promotion energies, ionization potentials, and electron affinities. As a consequence of reproducing ionization potentials and electron affinities, orbital electronegativities and absolute hardness values are also obtained. The ability of the new model to accurately duplicate these data is demonstrated while exposing the inability of current models to perform as well.

Atomic Parameterization

Empirically parameterized atomic integrals are sought. Use of experimental data to fit these parameters has three positive results. The first is to give a feel for the impact the terms in the model have on calculated properties. The second is that use of experimental data in the model moderates the approximations invoked. In other words, a balance is achieved between losing accuracy due to the neglected terms, and maintaining in the model the essential physics that is

necessary to determine electronic structure in a meaningful fashion. A third benefit that arises is that parameterized models may perform more accurately than an exact implementation of the theory used.

The following discussion is limited to atoms whose valence-shell consists of only s and p type orbitals. The average valence electronic energy for an atom with a fixed number of s and p electrons can be calculated from experimental data. The valence energy is calculated via a weighted average of the term energies arising from a given configuration. The term energies are weighted by their degree of degeneracy determined from the term S and L quantum numbers. Total degeneracy for a term energy would be $(2S+1)(2L+1)$ [46].

$$\bar{E}(\text{atom}, n_s, n_p) = \frac{\sum_{\text{term}} (2S_{\text{term}} + 1)(2L_{\text{term}} + 1)E_{\text{term}}}{\sum_{\text{term}} (2S_{\text{term}} + 1)(2L_{\text{term}} + 1)} \quad (6-1)$$

The average configuration energy can be expressed as a sum of one-center core terms (U_{ss} and U_{pp}) and a sum of average pair energies [45]. The core terms consist of the electron kinetic energy, the attraction of the electron to the core, and the core-valence potential energy.

$$U_{\mu\nu} = (\mu | -\frac{\nabla^2}{2} - \frac{Z_{\text{core}}}{R} - \hat{E}_c | \nu) = U_{\mu\mu} \delta_{\mu\nu} \quad (6-2)$$

The average pair energies are composed of two-electron coulomb and exchange integrals of the type

$$(\chi_\mu \chi_\nu | \chi_\lambda \chi_\sigma) = \int d\tau_1 d\tau_2 \chi_\mu^*(1) \chi_\nu(1) \frac{1}{r_{12}} \chi_\lambda^*(2) \chi_\sigma(2) \quad (6-3)$$

One can integrate over the angular part of the two-electron coulomb and exchange integrals that are not zero by symmetry and express these as a function of Condon-Shortley integrals [46]. These integrals will become the empirical parameters. We further simplify the equations by assuming the effective exponents for valence s and p orbitals are the same for a given atom. We can now write down expressions for one-center two-electron integrals.

$$J_{ss} = J_{sp_\mu} = (ss | ss) = (ss | p_\mu p_\mu) = F^0 \quad (6-4)$$

$$K_{sp_\mu} = (sp_\mu | sp_\mu) = \frac{1}{3}G^1 \quad (6-5)$$

$$K_{p_\mu p_\nu} = (p_\mu p_\nu | p_\mu p_\nu) = \frac{3}{25}F^2 \quad (6-6)$$

$$J_{p_\mu p_\mu} = (p_\mu p_\mu | p_\mu p_\mu) = F^0 + \frac{4}{25}F^2 \quad (6-7)$$

$$J_{p_\mu p_\nu} = (p_\mu p_\mu | p_\nu p_\nu) = F^0 - \frac{2}{25}F^2 \quad (6-8)$$

F^0 , G^1 , and F^2 are the Condon-Shortley parameters of interest. By averaging over all term energy expressions for a fixed valence configuration and then expressing all two-electron integrals in terms of the above parameters we obtain [45],

$$\begin{aligned} \bar{E}(Z, n_s, n_p) = & n_s U_{ss} + n_p U_{pp} + \frac{1}{2}(n_s + n_p)(n_s + n_p - 1)F^0 \\ & - \frac{1}{6}n_s n_p G^1 - \frac{1}{25}n_p(n_p - 1)F^2 \end{aligned} \quad (6-9)$$

This equation is our working model for atomic parameterization. Standard values for G^1 , and F^2 derived from atomic spectroscopy have been available in the literature for many years [90, 91]. Ionization potentials (IP's) [92] and electron affinities (EA's) [93] are also available for both s and p electrons for most atoms. Standard parameterizations assume that $U_{\mu\mu}$, F^0 , G^1 , and F^2 are fixed values for any given atom. One can then use Equation (6-9) to calculate expressions for U_{ss} and U_{pp} in terms of known IP's or EA's. As an example, Pople's original parameterization for $U_{\mu\mu}$ in the CNDO was derived on the basis of IP's alone [41].

$$U_{2s2s} = -IP_s - (n_s + n_p - 1)F^0 + \frac{1}{6}n_p G^1 \quad (6-10)$$

$$U_{2p2p} = -IP_p - (n_s + n_p - 1)F^0 + \frac{1}{6}n_s G^1 + \frac{2}{25}(n_p - 1)F^2 \quad (6-11)$$

This has been the parameterization of choice for many programs currently in use. Another popular choice uses the average of IP's and EA's to evaluate the $U_{\mu\mu}$'s [42]. The only remaining quantity is F^0 which is generally calculated theoretically using Slater s-type atomic functions with exponents derived from empirical rules for screening constants such as those of Slater [49] or Clementi and Raimondi [94].

A New Atomic Parameterization

The Condon-Shortley exchange parameters available in the literature are examined first [90]. The values available are for atomic cations as well as for neutral atoms. The parameters are assumed to be a function of charge and atomic number. The experimental data is examined to see if any pattern emerges that would suggest a specific functional form. At this point the data is fit in a least squares fashion to the model. A plot of the data for elements Be through F for both F^2 and G^1 are included in Figures 6–1 and 6–2 according to the number of valence electrons. Lines have been drawn through the experimental data representing isoelectronic curves. In this way the functional dependence of these parameters with respect to charge and atomic number is evident. The regularity of the data has allowed for the fitting of a single model for each parameter for these elements that incorporates both charge and atomic number. In all cases the models are linear in net charge (Q) once the valence core charge (Z) is fixed [91]. For elements Be-Ne we obtain,

$$F^2(\text{eV}) = (-2.1972 + 1.9950Z - 0.0249Z^2 - 0.0086Z^3) \\ + (0.2294 + 0.2047Z)Q \quad (6-12)$$

$$\text{STD}(\text{standard deviation}) = 0.323\text{eV}$$

$$G^1(\text{eV}) = (0.4004 + 1.7549Z) + 0.8509Q \\ \text{STD} = 0.323\text{eV} \quad (6-13)$$

and for Na-Ar,

$$F^2(\text{eV}) = (15.4738 - 9.9474Z + 2.2126Z^2 - 0.1430Z^3) \\ + (11.5939 - 4.4603Z + 0.5035Z^2 - 0.0134Z^3)Q \quad (6-14)$$

$$\text{STD} = 0.143\text{eV}$$

$$G^1(\text{eV}) = (-8.9073 + 8.8572Z - 1.8726Z^2 + 0.1204Z^3) \\ + (-4.4977 + 1.9760Z - 0.1706Z^2 + 0.0007Z^3)Q \quad (6-15)$$

$$\text{STD} = .415\text{eV}$$

Tables 6-1 through 6-4 compare some of the experimental values for F^2 and G^1 with those calculated from Equations (6-12) through (6-15).

Of immediate interest here is the strong dependence on these integrals with charge for a given atom. For a fixed minimum basis these values would be considered constant. Moderate deviations between calculated and experimental F^2 and G^1 integrals will have a negligible effect on the total energy in Equation (6-9) in that they contribute the smallest proportion to the total energy.

Having now formulas for F^2 and G^1 we turn our attention to U_{ss} , U_{pp} , and F^0 . As previously discussed these parameters have been estimated in the past as charge independent constants determined via ionization potentials, or ionization potentials and electron affinities. Karlsson and Zerner [45] proposed calculating the core terms from the spectroscopic data alone for neutrals by fitting Equation (6-9) to total valence energies determined from multiple ionization energies and valence promotion energies. In their proposal the value for F^0 continues to be

calculated theoretically over Slater functions using exponents determined from Slater's rules. It is not possible to uniquely determine U_{ss} , U_{pp} , and F^0 from a linear least squares fit of Equation (6-9) due to the inter-dependence of the variables that are coupled. It must be further pointed out that any reasonable form chosen for F^0 can be used and the fitting procedure applied successfully. Since all parameters can not be varied freely in the fit, a form for F^0 is chosen that has a simple interpretation. The fit was performed using two such F^0 's that have been used successfully in semiempirical calculations. Firstly the theoretical form for F^0 is chosen in a fashion consistent with Slater's rules. In this form F^0 is linear with respect to the exponential factor (ζ_n) in the Slater basis.

$$F^0(s, s) = F^0(s, p) = F^0(p, p) = K(n)\zeta_n = (nsns|nsns)$$

$$K(1) = 0.6250\text{au} = 17.0075\text{eV}$$

$$K(2) = 0.3633\text{au} = 9.8856\text{eV}$$

$$K(3) = 0.2581\text{au} = 7.0244\text{eV}$$
(6-16)

From Slater's rules for minimal basis set calculations $\zeta = (Z_{\text{nucl}} - \sigma)/n$. From these rules we derive for F^0 , in electron volts,

$$F^0(1s, 1s) = 5.1023 + 11.9053Z + 5.1023Q$$

$$F^0(2s, 2s) = 3.2128 + 3.2128Z + 1.7300Q$$

$$F^0(3s, 3s) = 3.6293 + 1.5220Z + 0.8195Q$$
(6-17)

where $Z = Z_{\text{valence}} = (Z_{\text{nucl}} - \# \text{ inner electrons})$ and Q is the net charge for the center. Although Slater's rules are frequently used in semiempirical calculations

to evaluate F^0 , it is often convenient to evaluate F^0 via Pariser's observation [47], especially in the calculation of electronic spectra. Pariser's observation is to set F^0 equal to the ionization potential minus the electron affinity for neutral atoms. The values from Pariser's formulation can be fit with a simple A+BZ model for each row and combined with the slope term in charge from Slater's rules above to obtain,

$$\begin{aligned} F^0(1s, 1s) &= 0.9447 + 11.9053Z + 5.1023Q \\ F^0(2s, 2s) &= 3.7271 + 1.5736Z + 1.7300Q \\ F^0(3s, 3s) &= 2.1443 + 1.3239Z + 0.8195Q \end{aligned} \quad (6-18)$$

Now that general expressions for the Slater-Condon integrals are available, a generalization of the core terms is sought in a similar fashion by fitting Equation (6-9) not only for neutral, but also cationic and anionic valence configuration energies determined from multiple ionization energy data. If E_{term} in Equation (6-1) is replaced with the spectral transition energy for that specific term from the ground state, an equation is obtained for the calculation of the promotion energy (E_{prom}) from the ground state of the atom to its average valence configuration energy. The valence configuration energy of an atom can now be expressed in terms of experimentally known quantities.

$$\bar{E}(Z, n_s, n_p) = \sum_{i=1}^{n_s+n_p} -IP_i + \bar{E}_{\text{prom}}(Z, n_s, n_p) \quad (6-19)$$

In this equation, a scale of 0 energy is assumed for the atomic core with all valence electrons separated. In this way the energy of the core is maintained as a constant. Each addition of a valence electron thus lowers the atomic energy by the negative of the corresponding ionization potential. Additionally, electron affinity data can be used to add electrons beyond the neutral atom. In order to obtain E_{prom} energies for anions, the promotion energies [95] of atoms with the same valence configuration in terms of atomic number are extrapolated since these data are not readily available for anions. The correlation coefficients for the interpolation of E_{prom} 's with atomic number are essentially 1.000 for a simple linear model in all cases. The extrapolated values for the lowest valence states are usually small as would be expected for orbitals on an atom of loosely held electrons. Using these experimental data and the modeled Slater-Condon integrals, the core integrals can be successfully modeled. Using Slater F^0 's the core terms obtained in electron volts are,

$$U_{1s1s} = (26.7674 - 40.3624Z) + (-0.4781 + 0.0103Z)Q \quad (6-20)$$

$$\begin{aligned} U_{2s2s} &= (1.6381 - 3.8614Z - 3.1275Z^2) \\ &+ (1.6649 - 0.9632Z - 0.0065Z^2)Q + (0.6291 + 0.0088Z)Q^2 \\ U_{2p2p} &= (1.1008 - 1.7462Z - 3.0980Z^2) \\ &+ (1.2714 - 0.6043Z - 0.0016Z^2)Q + (0.2392 + 0.0045Z)Q^2 \end{aligned} \quad (6-21)$$

$$\begin{aligned}
U_{3s3s} &= (0.7922 - 4.6810Z - 1.5215Z^2) \\
&+ (0.5146 - 0.6326Z + 0.0089Z^2)Q + (0.2017 + 0.0255Z)Q^2 \\
U_{3p3p} &= (3.0984 - 4.2000Z - 1.4512Z^2)
\end{aligned} \tag{6-22}$$

$$+ (0.8865 - 0.3162Z - 0.0004Z^2)Q + (0.2945 - 0.0183Z)Q^2$$

and using the modified Pariser's approximation for F^0 the core terms are,

$$U_{1s1s} = (24.6886 - 38.2836Z) + (-2.5569 + 0.0103Z)Q \tag{6-23}$$

$$\begin{aligned}
U_{2s2s} &= (1.8954 - 4.9381Z - 2.3079Z^2) \\
&+ (1.9221 - 1.7828Z - 0.0065Z^2)Q + (0.6291 + 0.0088Z)Q^2
\end{aligned} \tag{6-24}$$

$$\begin{aligned}
U_{2p2p} &= (1.3580 - 2.8229Z - 2.2784Z^2) \\
&+ (1.5286 - 1.4239Z - 0.0016Z^2)Q + (0.2392 + 0.0045Z)Q^2 \\
U_{3s3s} &= (0.0497 - 4.0375Z - 1.4224Z^2) \\
&+ (-0.2279 - 0.7316Z + 0.0089Z^2)Q + (0.2017 + 0.0255Z)Q^2
\end{aligned} \tag{6-25}$$

$$U_{3p3p} = (2.3559 - 3.5566Z - 1.3522Z^2)$$

$$+ (0.1440 - 0.4153Z - 0.0004Z^2)Q + (0.2945 - 0.0183Z)Q^2$$

The number of parameters included in the fit for a row is 16 once the two electron integral forms are specified. The number of atomic states included in the fit for row 1 is 80 and for row 2, 58. The standard deviation for row 1 is 0.24eV, while that for row 2 is 0.32eV. A summary of the results obtained by

using these equations in calculating average configuration energies of neutral and singly ionized atoms is given in Tables 6-5 through 6-8. The data for aluminum, silicon, phosphorus, and sulfur are shown in Figures 6-3 through 6-6 where they are compared with results using INDO/1 atom fixed parameters. Three possible energies are available for an atom of a given charge depending on the promoted state of the atom. These are s^2p^N , s^1p^{N+1} , and s^0p^{N+2} . The INDO/1 parameters are based on Slater- F^0 's for neutrals and Equations (6-10) and (6-11) for the core terms.

Analysis

Several important observations can be made from Figures 6-3 through 6-6. In all cases the new parameterization is able to reproduce the experimental values quite well. Since one can obtain total atomic energies by adding a constant to the valence energies the new model is capable of reproducing total energies as well. The INDO/1 average energies not only do a poorer job as might be expected, but shifts the minimum of the curve to the right. Since the position of the minimum determines the charge at which atoms are most stable, this shift of minimum cannot account for the fact that most anions are more stable than neutrals. In addition, the use of fixed two-electron repulsion integrals causes the slope of the energy to increase too rapidly as the atom becomes anionic in INDO/1. The curve for sulfur is a dramatic example of this effect. In this curve, the slope of the experimental

data is much “softer” than that of the INDO/1 data. It is again pointed out that the new parameterization takes into effect the “softening” of the repulsion integrals as atoms become anions and reproduces the experimental data well.

A second observation one can make from the Figures is that of the differences in slope of the curves of the neutral species for the two parameterizations. The slope of atomic energy with respect to the number of electrons is directly related to the electronegativity of the atom. In the early sixties workers fit empirical quadratic formulas to atomic multiple ionization potentials and electron affinities and used these formulas to calculate empirical slopes [96]. These slopes correlate quite well with Mulliken’s electronegativity scale [97, 98]. Hinze and Jaffe [95] developed a similar model based on the use of spectroscopic energies to fit a quantum mechanical expression similar to the one used in this Chapter but with charge independent parameters. With their model as well as the one proposed here electronegativities for atoms are reproduced well. As can be seen in the graphs, the slopes for the INDO/1 data are much too small for neutral atoms to reproduce atomic electronegativities. If the derivative of Equation (6–9) is taken with respect to the number of p electrons, the negative of the electronegativity of p type electrons for atoms in an average valence state is obtained. These derivatives have a particular significance in density functional theory [99, 100]. Mulliken electronegativities are calculated as the average of the valence state ionization energy and electron affinity for the atom in its ground state. To compare

Mulliken electronegativities in the literature and the model used here it is necessary to correct the literature values for the use of average configuration energies used to fit Equation (6–9). Tables 6–9 and 6–10 are provided for this comparison. Electronegativities can be calculated in closed form for anions and cations as well as neutrals for all elements in a row with a single formula. Reasonable estimates can be obtained even if ionization potential and electron affinity information is not readily available.

Finally the concept of absolute orbital hardness is considered as it relates to hard and soft acids and bases [101] and density functional theory [102]. Recent studies have associated analytic second derivatives of the energy with respect to the number of electrons with an absolute hardness scale in much the same way as the absolute electronegativity is defined above. A finite difference value for absolute hardness is obtained by [103],

$$\text{HARDNESS} = 0.5 \left(\frac{\partial^2 E}{\partial N^2} \right) \approx 0.5(\text{IP} - \text{EA}) \quad (6-26)$$

As in the case of electronegativity analytic derivatives for hardness can be obtained. The hardness values can easily be estimated in this way for anions, which are difficult to obtain experimentally. Tables 6–11 and 6–12 compare some hardness values obtained by finite differences and by the present model. The agreement is outstanding as expected from the manner in which these values are obtained.

Table 6-1 F² experimental and modeled values

ELEMENT	Z	Q	EXP ^a (eV)	MODEL(eV)
Be	2	0	2.6564	2.6251
B	3	0	3.4809	3.3337
C	4	+1	5.8986	5.8856
C	4	0	4.5100	4.8376
N	5	0	6.4596	6.0858
O	6	+1	8.8866	8.4841
O	6	0	6.9029	7.0268
F	7	+1	9.1718	9.2711
Ne	8	+2	11.363	11.514

^a Ref. [90]

Table 6-2 G¹ experimental and modeled values.

ELEMENT	Z	Q	EXP ^a (eV)	MODEL(eV)
Be	2	0	3.8282	3.9104
B	3	0	5.4015	5.6653
C	4	2	9.2959	9.1220
C	4	1	8.3779	8.2712
C	4	0	6.8979	7.4203
N	5	2	11.036	10.877
N	5	1	10.087	10.026
N	5	0	8.9585	9.1752
O	6	2	12.666	12.632
O	6	1	11.500	11.781
O	6	0	11.816	10.930
F	7	2	14.196	14.387
F	7	1	13.850	13.536
Ne	8	3	16.813	16.993
Ne	8	2	15.788	16.142

^a Ref. [90]

Table 6-3 F² experimental and modeled values.

ELEMENT	Z	Q	EXP ^a (eV)	MODEL(eV)
Mg	2	0	3.2732	3.2851
Al	3	+1	4.1721	4.0662
Al	3	0	1.6025	1.6831
Si	4	+1	2.5913	2.8834
Si	4	0	2.2627	1.9317
P	5	+2	3.6390	3.5841
P	5	0	2.9477	3.1729
S	6	+3	4.7796	4.7415
S	6	+2	4.7517	4.6772
S	6	+1	4.7145	4.6129
S	6	0	4.5379	4.5485
Cl	7	+3	6.3759	6.5427
Cl	7	+2	6.1156	6.0953
Cl	7	+1	5.6878	5.6478
Ar	8	+3	8.1830	8.0937
Ar	8	+2	6.7510	6.8193

^a Ref. [90]

Table 6-4 G¹ experimental and modeled values.

ELEMENT	Z	Q	EXP ^a (eV)	MODEL(eV)
Mg	2	0	2.4765	2.2802
Al	3	+1	4.1532	3.9771
Al	3	0	3.3591	4.0627
Si	4	+2	5.5782	5.7141
Si	4	+1	4.9299	4.9909
Si	4	0	4.8124	4.2677
P	5	+3	6.8469	7.2426
P	5	+2	6.4385	6.0344
P	5	+1	4.7748	4.8262
S	6	+3	7.6545	6.9577
S	6	+1	3.6452	4.2009
S	6	0	3.0757	2.8360
Cl	7	+2	4.3299	5.0938
Cl	7	+1	4.0863	3.8690
Ar	8	+3	6.0301	6.0607
Ar	8	+2	5.5273	5.2956

^a Ref. [90]

Table 6-5 Total valence energies (eV) for ground state (s^2p^n).

Elem	Net valence charge.					
	Q=-1		Q=0		Q=+1	
	Exp. ^a	Model	Exp.	Model	Exp.	Model
H	-14.349	-14.349	-13.595	-13.595	—	—
He	—	—	-79.002	-79.002	-54.415	-54.415
Li	-6.021	-6.121	-5.392	-5.351	—	—
Be	-27.534	-27.207	-27.534	-27.551	-18.211	-18.236
B	-71.367	-71.414	-71.384	-71.542	-63.087	-62.861
C	-147.87	-147.99	-147.42	-147.55	-136.75	-136.69
N	-266.26	-266.07	-264.70	-264.82	-251.51	-251.44
O	-434.63	-434.61	-432.22	-432.46	-416.38	-416.34
F	-662.33	-662.37	-658.91	-659.37	-640.25	-640.36
Ne	—	—	-954.36	-954.24	-932.74	-932.64

^a Ref. [104]

Table 6-6 Total valence energies (eV) for the excited configuration (s^1p^{n+1}).

	Net valence charge.			
	Q=0		Q=+1	
Elem	Exp. ^a	Model	Exp.	Model
Li	-3.544	-3.743	—	—
Be	-24.171	-24.392	-14.252	-14.479
B	-65.654	-65.734	-57.339	-57.549
C	-138.80	-138.69	-127.98	-128.05
N	—	—	-239.12	-239.06
O	-415.53	-416.02	-399.84	-399.71
F	-638.03	-638.24	-618.73	-619.00
Ne	—	—	-905.88	-905.66

^a Ref. [104]

Table 6-7 Total valence energies (eV) for ground state (s^2p^n).

Elem	Net valence charge.					
	Q=-1		Q=0		Q=+1	
	Exp. ^a	Model	Exp.	Model	Exp.	Model
Na	-5.685	-5.816	-5.139	-5.410	—	—
Mg	-22.681	-22.083	-22.681	-22.638	-15.035	-15.118
Al	-53.485	-53.695	-53.296	-53.219	-47.277	-46.924
Si	-103.48	-103.94	-102.71	-103.09	-94.937	-94.827
P	-177.52	-177.23	-175.79	-175.83	-165.65	-165.99
S	-278.74	-278.43	-276.09	-276.05	-264.49	-264.40
Cl	-412.65	-412.29	-409.98	-408.72	-395.26	-394.92
Ar	—	—	-577.99	-578.43	-562.14	-562.53

^a Ref. [104]Table 6-8 Total valence energies (eV) for the excited configuration (s^1p^{n+1}).

Elem	Net valence charge.			
	Q=0		Q=+1	
	Exp. ^a	Model	Exp.	Model
Na	-3.036	-2.553	—	—
Mg	-19.561	-19.469	-10.607	-10.596
Al	—	—	-41.937	-42.005
Si	—	—	-87.762	-88.297
P	-169.00	-168.92	-157.04	-157.66
Cl	—	—	-383.70	-383.77

^a Ref. [104]

Table 6-9 Electronegativities for first row elements.

Elem.	Q	$\chi^a(\text{ev}/Q)$	χ^b	χ^c
B	0	3.70	4.14	4.29
B	-1	-3.38		
C	+1	17.20	17.53	
C	0	5.08	5.56	6.27
C	-1	-3.63		
N	+1	20.55	20.96	
N	0	6.76	7.38	7.27
N	-1	-3.71	-3.05	
O	+1	24.18	24.52	
O	0	8.59	9.13	7.53
O	-1	-3.75	-2.84	
F	+1	27.92	28.21	
F	0	10.43	11.04	10.41
F	-1	-3.90		
Ne	+1	31.63	32.11	
Ne	0	12.10		

^a $\chi = -(\partial E / \partial N_p)_{Z, N_s}$ from Equation (6-9).

^a $\chi = .5(\text{IP} + \text{EA})$ corrected for average configuration energies.

^a $\chi = .5(\text{IP} + \text{EA})$ from ground state.

Table 6-10 Electronegatives for second row elements.

Elem.	Q	$\chi^a(\text{eV}/Q)$	χ^b	χ^c
Al	0	3.31	3.10	3.21
Al	-1	-2.28		
Si	+1	12.26	12.05	
Si	0	4.41	4.27	4.76
Si	-1	-2.55		
P	+1	14.46	14.64	
P	0	5.42	5.94	5.62
P	-1	-2.42		
S	+1	16.74	16.95	
S	0	6.79	7.13	6.22
S	-1	-1.82	-1.73	
Cl	+1	19.36	19.50	
Cl	0	8.46	8.70	7.31
Cl	-1	-1.09		
Ar	+1	22.09	22.15	
Ar	0	9.92		

^a $\chi = -(\partial E / \partial N_p)_{Z, N_s} = (\text{eV per charge})$ from Equation (6-9).

^b $\chi = .5(\text{IP} + \text{EA})$ corrected for average configuration energies.

^c $\chi = .5(\text{IP} + \text{EA})$ from ground state.

Table 6-11 Hardness values (eV/Q²) for first row elements.

Elem.	Q	HARD ^a	HARD ^b	HARD ^c
B	0	4.40	4.16	4.01
B	-1	2.67		
C	+1	6.91	6.86	
C	0	5.21	5.11	5.00
C	-1	3.51		
N	+1	7.23	7.77	
N	0	6.07	5.82	7.27
N	-1	4.41	4.61	
O	+1	8.60	8.68	
O	0	6.98	6.72	6.06
O	-1	5.36	5.25	
F	+1	9.54	9.55	
F	0	7.96	7.62	7.01
F	-1	6.37		
Ne	+1	10.54	10.49	
Ne	0	8.99		

^a $\text{HARD} = .5(\partial^2 E / \partial N_p^2)_{Z, N_s}$ from Equation (6-9).

^b $\text{HARD} = .5(\text{IP-EA})$ corrected for average configuration energies.

^c $\text{HARD} = .5(\text{IP-EA})$ from ground state.

Table 6-12 Hardness values (eV/Q²) for second row elements.

Elem.	Q	HARD ^a	HARD ^b	HARD ^c
Al	0	2.91	2.88	2.77
Al	-1	2.69		
Si	+1	4.15	4.28	
Si	0	3.70	3.50	3.38
Si	-1	3.25		
P	+1	4.82	4.50	
P	0	4.22	4.21	4.86
P	-1	3.62		
S	+1	5.31	5.35	
S	0	4.64	4.48	4.12
S	-1	3.97	4.38	
Cl	+1	5.79	5.78	
Cl	0	5.11	5.03	4.70
Cl	-1	4.44		
Ar	+1	6.40	6.30	
Ar	0	5.77		

^a HARD = $.5(\partial^2 E / \partial N_p^2)_{Z, N_s}$ from Equation (6-9).

^b HARD = $.5(\text{IP-EA})$ corrected for average configuration energies.

^c HARD = $.5(\text{IP-EA})$ from ground state.

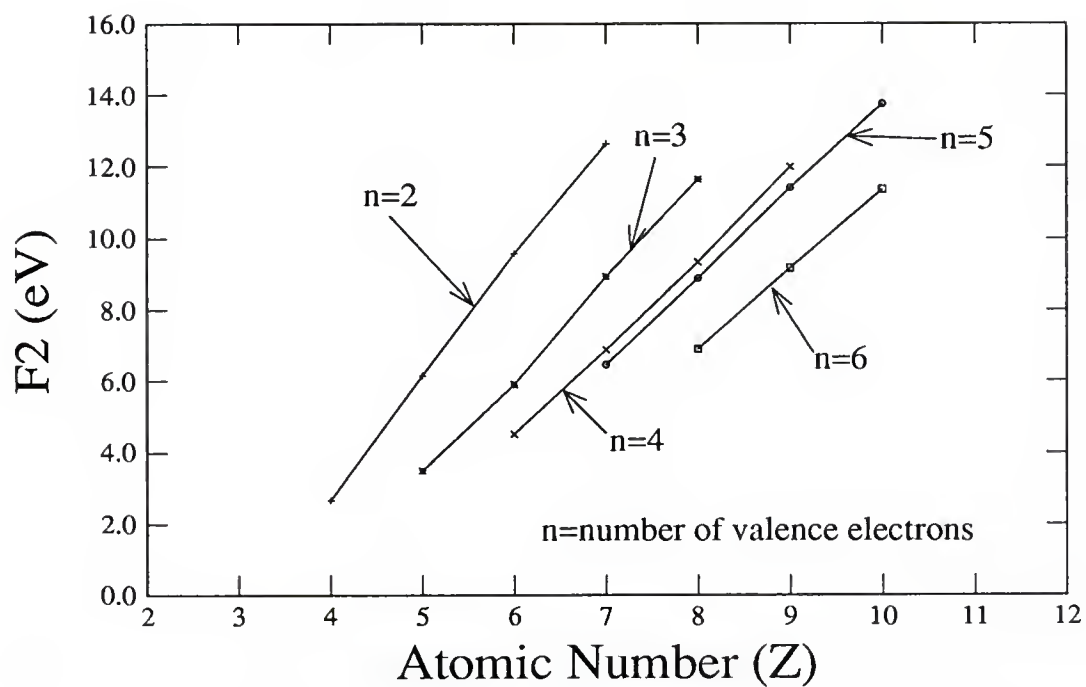


Figure 6-1 F^2 (eV) values as a function of atomic occupation.

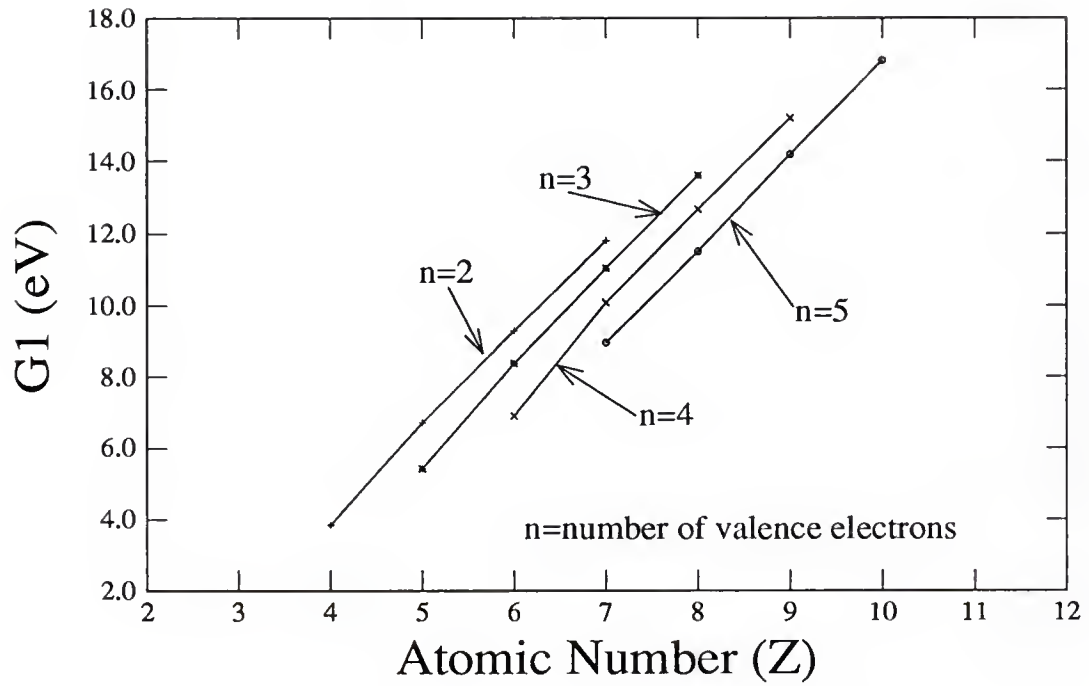


Figure 6-2 G^1 (eV) values as a function of atomic occupation.

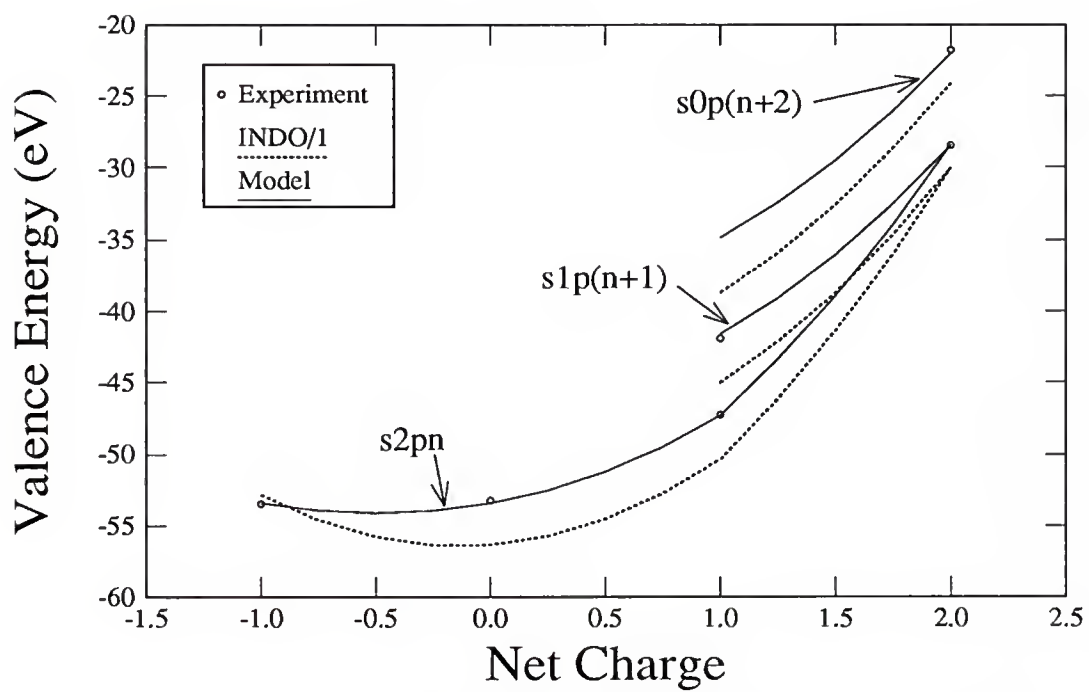


Figure 6-3 Aluminum: Average valence configuration energies (eV) vs. charge.

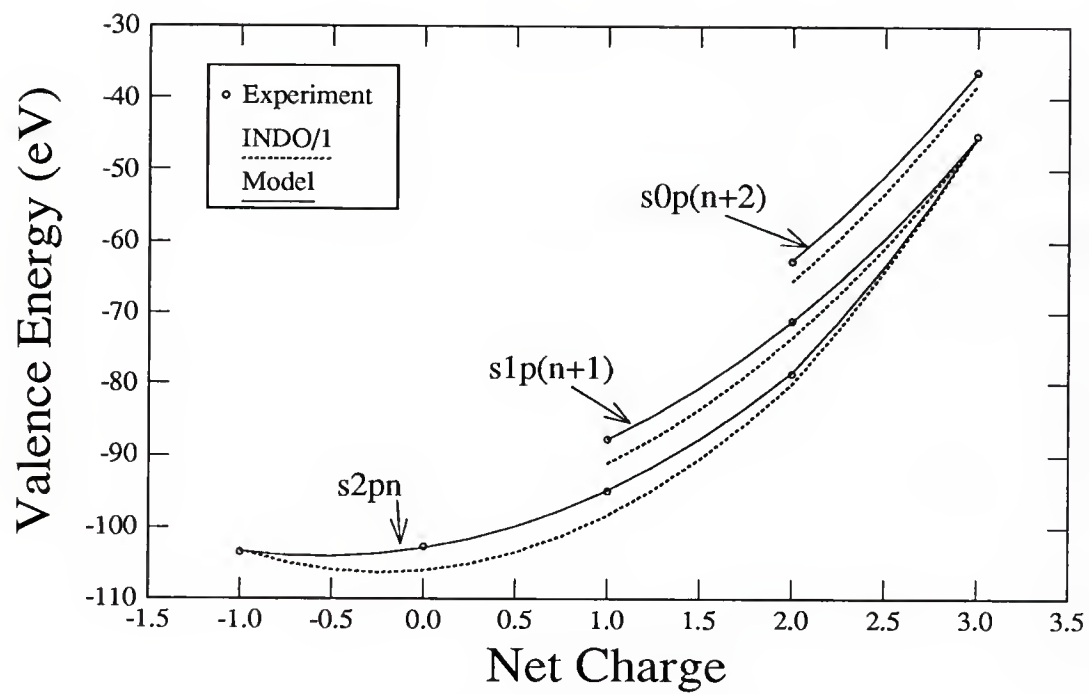


Figure 6-4 Silicon: Average valence configuration energies (eV) vs. charge.

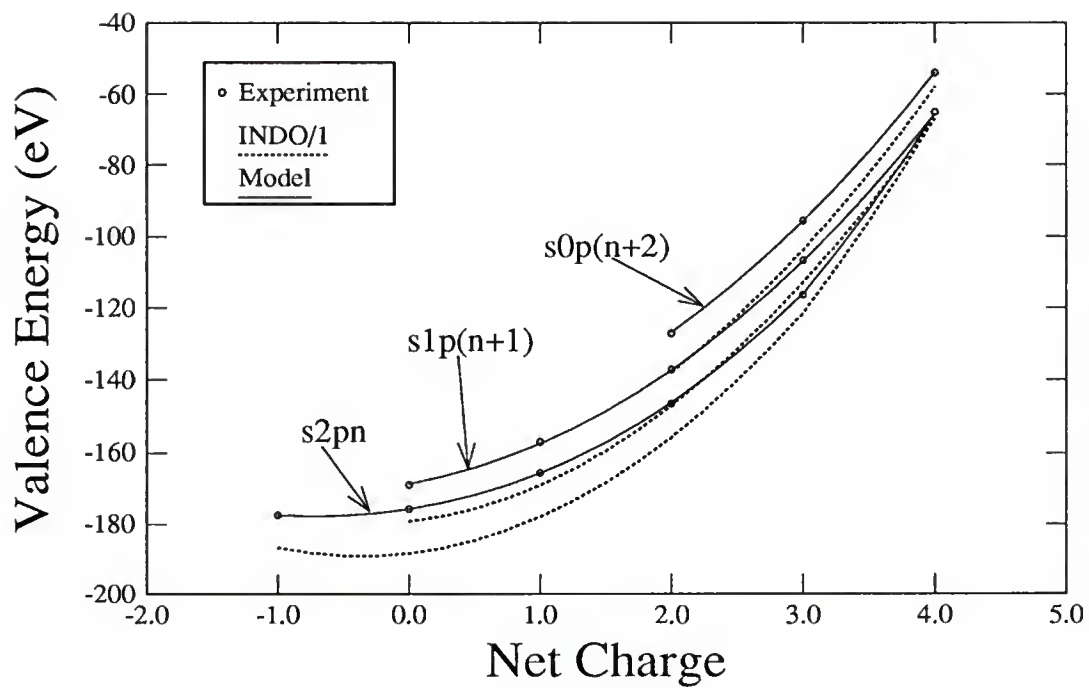


Figure 6-5 Phosphorus: Average valence configuration energies (eV) vs. charge.

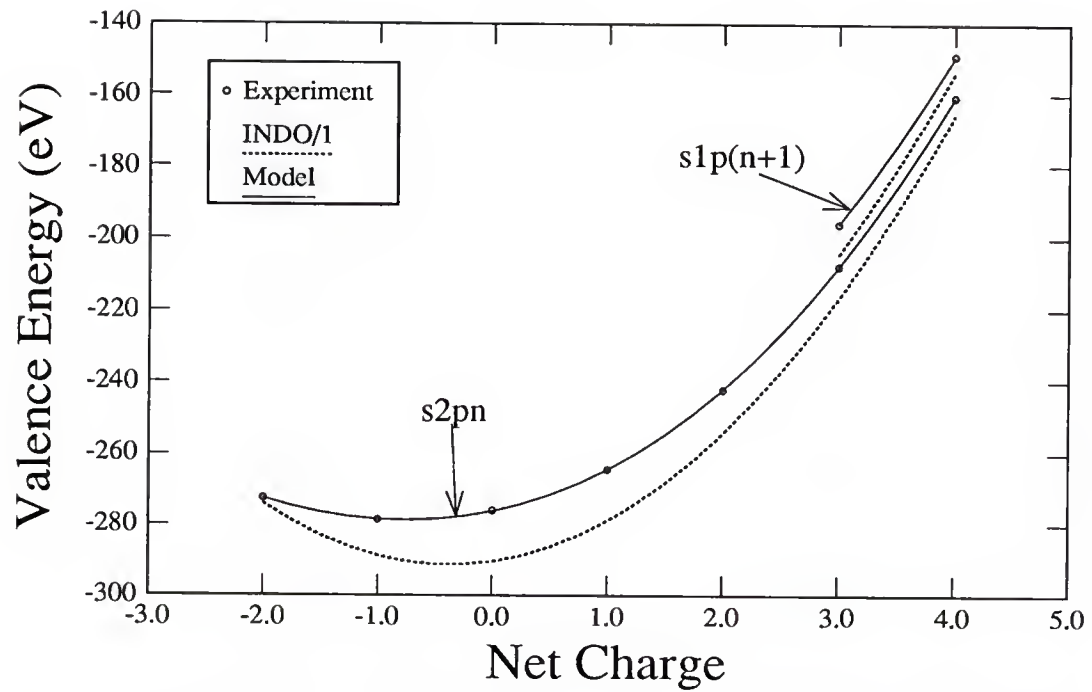


Figure 6-6 Sulfur: Average valence configuration energies (eV) vs. charge.

CHAPTER 7
A DENSITY PARTITIONED HAMILTONIAN
FOR MOLECULAR ELECTRONIC SPECTRA

Density Partitioning

Borrowing from concepts that seem natural in density functional theory [16], the atomic parameters that enter into most semiempirical Hamiltonians are reexamined. Density functional theory will suggest atomic parameters that are functions of charge and atomic number. In this chapter such parameters are developed and utilized in a fashion appropriate for the calculation of electronic excitations and ionizations. Due to the success of the spectroscopic version of the Intermediate Neglect of Differential Overlap (INDO/S) approximation in the prediction of electronic properties, the basic form of this Hamiltonian is maintained.

The total atomic energy (E) is expanded in a Taylor series with respect to the total number of electrons N

$$E(N, Z) = E(Z, Z) + (N - Z) \frac{\partial E}{\partial N} + .5(N - Z)^2 \frac{\partial^2 E}{\partial N^2} + \text{higher terms} \quad (7-1)$$

Utilizing generalized formalizations of hardness [101] and electronegativity or chemical potential [98, 99]

$$\text{HARDNESS} = \eta \equiv .5 \left(\frac{\partial^2 E}{\partial N^2} \right) \quad (7-2)$$

$$\text{ELECTRONEG.} = \chi \equiv -\left(\frac{\partial E}{\partial N}\right) = -\text{CHEM. POT.} \quad (7-3)$$

allows Equation (7-1) to be rewritten. In terms of net atomic charge (Q),

$$E(Q, Z) = E(0, Z) + Q\chi + Q^2\eta + \dots \quad (7-4)$$

On the other hand, the energy for the average configuration of an atom containing only s and p electrons in the valence shell is according to Equation (6-9),

$$E(n_s, n_p, Z) = n_s U_s + n_p U_p + .5(n_s + n_p)(n_s + n_p - 1)F^0 \\ - \frac{1}{6}n_s n_p G^1 - \frac{1}{25}n_p(n_p - 1)F^2 \quad (7-5)$$

in which U_s and U_p are the one-electron energies for s and p electrons and F^0 , G^1 and F^2 are the Condon-Shortley two-electron integrals. In Equation (7-5) it is assumed that $F^0 = F^0(ss) = F^0(sp) = F^0(pp)$.

Parameters in the INDO Hartree-Fock model represent integrals. Once these integrals are chosen via computation in an appropriate atomic basis, or in this case parameterization, the solution of the molecular problem proceeds along well established lines whether the theory is Hartree-Fock or correlated. In a normal HF procedure the charge density is varied until self consistency is obtained. The integrals are fixed and therefore it is through fixed integrals that the HF procedure sees the potential created by the centers in the molecule. In large basis set calculations linear combinations of these integrals over the basis allows the effective potential to vary with molecular environment. This degree of flexibility

is never present in any minimal basis set calculation, and it is this deficiency that needs correction.

In the previous Chapter, a method for obtaining total energy from experimental data is reviewed and used to develop an empirical atomic parameterization that is fully charge dependent and is capable of modeling atomic energies very accurately, although it remains in a MBS formalism. As a result of predicting energies accurately, orbital electronegativities and hardness values are also reproduced. This approach is being denoted "energy partitioning" since the total atomic energy is modeled. This procedure is most appropriate for the calculation of energy based properties such as molecular conformations. Energy partitioning, however, requires that derivatives of the parameters be taken with respect to Q as part of the total energy derivatives in order to reproduce atomic potentials. The HF procedure within a MBS restriction does not include this effect.

In the present treatment a slightly different approach is pursued. Once the electronic occupation of an atom in a molecule is defined, the atomic parameters for that center are fixed such that the slope and curvature of the atomic energy of interest is maintained with frozen parameters. If the atomic occupations change then the atomic parameters of interest are adjusted and again frozen to reflect the new slope and curvature of the energy at that occupation. Parameters chosen in this way are being denoted "density partitioning" since parameters are adjusted to reflect the instantaneous chemical potential and hardness at a given occupation

or density of a center. Density partitioning of atomic energies allows the HF procedure to “see” the bare atom potentials directly.

The idea of introducing charge dependent parameters into approximate electronic structure theories for molecules is, of course, not a new one [105–110], and dates back to the work of Wheland and Mann [105] who convincingly demonstrated its utility. In work with motivation related to this treatment Singerman and Jaffe [110] recognized that it was difficult to reproduce the spectra of sulfur containing compounds using the CNDO/S [89, 111] method without creating charge dependent parameters for the sulfur d orbitals. The present approach differs from others in that the concept of charge dependency for the whole Hamiltonian is generalized in a fashion consistent with a more accurate description of the local potential of all the atoms in a molecule and not just to correct for specific cases for which charge dependency is a necessity.

In the following Section the method for obtaining charge dependent atomic parameters in accord with density partitioning is discussed. In the subsequent Sections the concept of charge dependency is extended to the resonance integrals and two-center Coulomb integrals of the INDO molecular Hamiltonian. Finally comparisons are made between INDO/S and the charge iterative approach presented here. The Condon-Shortley integrals G^1 and F^2 developed in the previous Chapter are kept here.

Atomic Hamiltonian

Consider an energy expansion for atoms truncated at second order.

$$E(N, Z) = A(Z) + NB(Z) + N^2C(Z) \quad (7-6)$$

In terms of this expression χ and η can be written as,

$$\chi = -B(Z) - 2NC(Z), \quad \eta = 2C(Z) \quad (7-7)$$

In like manner, derivatives of Equation (7-5) with respect to the number of p electrons to obtain,

$$\begin{aligned} -\chi_p &= \left[\frac{\partial E}{\partial n_p} \right] \\ &= U_p + .5(2n_s + 2n_p - 1)F^0 - \frac{1}{6}n_s G^1 - \frac{1}{25}(2n_p - 1)F^2 \end{aligned} \quad (7-8)$$

and

$$2\eta = \left[\frac{\partial^2 E}{\partial n_p^2} \right] = F^0 - \frac{2}{25}F^2 \quad (7-9)$$

One can now solve for the spherically symmetric Coulomb integral F^0 in Equation (7-9) and note that from finite differences $\eta = .5(IP - EA)$.

$$F^0 = 2\eta + \frac{2}{25}F^2 = \left[\frac{\partial^2 E}{\partial n_p^2} \right] + \frac{2}{25}F^2 \approx (IP - EA) + \frac{2}{25}F^2 \quad (7-10)$$

The F^2 integral is small with respect to the leading term of the ionization potential (IP) less the electron affinity (EA). Ignoring the small F^2 term, the well known

Pariser's approximation for F^0 is recovered. The finite difference approximation for χ_p is $.5(IP+EA)$. Solving for U_p in Equation (7-8) yields,

$$U_p = -\chi_p - .5(2n_s + 2n_p - 1)F^0 + \frac{1}{6}G^1 + \frac{1}{25}(2n_p - 1)F^2 \quad (7-11)$$

Using finite difference approximations for χ_p and F^0 one obtains well known, and, in this case, formally equivalent expressions for U_p , and similar expressions for U_s [45, 6].

$$\begin{aligned} U_p &= -IP - (n_s + n_p - 1)F^0 + \frac{1}{6}n_s G^1 + \frac{2}{25}(n_p - 1)F^2 \\ &= -EA - (n_s + n_p)F^0 + \frac{1}{6}n_s G^1 + \frac{2}{25}n_p F^2 \end{aligned} \quad (7-12)$$

From the above it is clear that if the IP and EA of an atomic orbital is known then the parameters associated with that orbital can be uniquely determined. Alternatively if the instantaneous derivatives of the energy with respect to charge is known, the same analysis can be performed. Implicit in the above derivatives is the assumption of continuously differential charge. With this assumption the experimental energies can be fitted to a least squares polynomial and the derivatives taken explicitly. This is the approach used for the determination of F^0 . There are several benefits to this approach. First of all, only total atomic energies are necessary instead of both IP's and EA's. Electron affinities are not as available as total energies. Secondly, this approach allows the fitting of a single polynomial expression for the atomic energies as a function of atomic number and

charge for a whole row. With a single expression derivatives can be taken for a given atom and charge for which specific atomic information may not be available. Finally, the F^0 's obtained in this way are of the same form as those obtained from Slater type orbitals as developed in the previous Chapter. For principle quantum number $n=2$, 35 total energies were used and for $n=3$, 32 data points were used to fit the energy polynomial. The second derivatives were taken and used to fit F^0 according to Equation (7-10) to obtain,

$$\begin{aligned} n = 2, \quad F^0(\text{eV}) &= 3.04282 + 1.80972Z_v + 3.28219Q \\ n = 3, \quad F^0(\text{eV}) &= 2.70856 + 1.11349Z_v + 1.22155Q \end{aligned} \quad (7-13)$$

Z_v is the valence charge (e.g. C=4) and Q is the net charge. The standard deviation for both $n=2$ and $n=3$ is 0.1eV.

This form of F^0 appeals to our chemical intuition. As charge increases one expects the center to contract and thus repulsions to increase as predicted here. The slope with charge is less for the second row as one would expect for larger more polarizable atoms. An effective exponent for an atom can be obtained that is of the same form as that of Slater's rules and thus one can extract effective screening constants for the model.

The so called core terms, U_s and U_p , are the one-electron energies consisting of kinetic energy, nuclear electronic attraction and a core-valence potential due to the neglect of core electrons. Using single exponent Slater orbitals the kinetic energy and nuclear attraction portion of the core terms can be calculated exactly

as $U = A'(n,l)\zeta^2 - B'(n)\zeta Z_v + \langle V_c \rangle$. A' is a constant dependent on the principle quantum number (n) and angular momentum (l). B' is a constant dependent upon the principal quantum number only and $\langle V_c \rangle$ is the core-valence potential energy. Expanding the exponent as with F^0 one obtains a general form for the core terms.

$$\begin{aligned} U_i &= a + bZ_v + cZ_v^2 + (d + eZ_v)Q + fQ^2 + \langle V_c \rangle \\ &= a' + b'Z_v + c'Z_v^2 + (d' + e'Z_v)Q + f'Q^2 \end{aligned} \quad (7-14)$$

The second equality assumes that the core-valence potential does not in itself generate any higher terms in Z_v or Q .

Since atomic ionizations are of interest Equation (7-12) is chosen to obtain values for the core terms. Only IP's are necessary to perform the analysis as F^0 has already been determined. Fitting in this way reproduces the finite difference approximation for electronegativity which is equivalent to Mulliken's scale [97] and also reproduces Koopmans' approximation for IP's and EA's for atoms. Again data for a whole row is collected to fit Equation (7-14) above so that interpolation for missing data allows core terms to be calculated. The modeled core terms in eV are,

$$\begin{aligned} U_{2s} &= 1.747 - 5.057Z_v - 1.916Z_v^2 + (2.609 - 3.619Z_v)Q + 1.967Q^2 \\ \#pts &= 30, \quad \text{std. dev.} = .21\text{eV} \\ U_{2p} &= .996 - 2.741Z_v - 1.876Z_v^2 + (1.906 - 3.317Z_v)Q + 1.635Q^2 \\ \#pts &= 35, \quad \text{std.dev.} = .18\text{eV} \end{aligned} \quad (7-15)$$

$$\begin{aligned}
 U_{3s} &= .296 - 4.267Z_v - 1.189Z_v^2 + (-.186 - 1.246Z_v)Q + 0.697Q^2 \\
 \#pts &= 23, \quad \text{std.dev.} = .30\text{eV} \\
 U_{3p} &= .761 - 2.356Z_v - 1.242Z_v^2 + (0.152 - 1.080Z_v)Q + .565Q^2 \\
 \#pts &= 36, \quad \text{std.dev.} = .40\text{eV}
 \end{aligned}
 \tag{7-16}$$

It is appealing that the model suggests only a quadratic in Z_v for a fixed charge. Under current methods of parameterization each atom in a row has to be parameterized separately. For a given s, p shell in a row at a fixed charge one would require 16 separate parameters. In this model anions, neutrals, and several levels of positive charge are modeled with just 12 parameters.

For Hydrogen only two useful energy values (neutral and anion) are available for the determination of two unknowns, namely F^0 , and U_s . F^0 is set to $(IP_s - EA_s) = 12.841\text{eV}$, and $U_s = -IP_s = -13.585\text{eV}$.

Molecular Hamiltonian

As discussed in Chapter 3, there are two types of terms that must be addressed in the parameterization of two-center quantities at the INDO level of approximation. Recalling Equation (3-9) the generalized form of many two-center repulsion integrals used in semiempirical theory can be expressed as,

$$\gamma_{AB}(R_{AB}) = \frac{f_g}{\left[\left(\frac{f_g}{\gamma_{AB}(0)} \right)^m + R_{AB}^m \right]^{1/m}}
 \tag{7-17}$$

For this study the one-center limit is calculated exactly using Slater orbitals with atomic exponents obtained from the effective one-center F^0 's discussed in the previous Section. This is a minor modification from previous numerical averages but one which allows a proper united atom limit. The Weiss factor is maintained at 1.2 and $m=1$ as with INDO/S.

Recalling Equation (3-10) the INDO two-center one-electron matrix element denoted β_{AB} is usually expressed as the average of one-center bond parameters weighted by the overlap (S_{ij}) between two Slater orbitals and an appropriate fixed interaction factor (f_{ij}) for the type of orbitals involved.

$$\beta_{AB} = \begin{cases} .5(\beta_A + \beta_B)S_{AB} & \text{for } \beta_{ss} \\ .5(\beta_A + \beta_B)f_{s\sigma}S_{AB} & \text{for } \beta_{sp\sigma} \\ .5(\beta_A + \beta_B)[f_{\sigma\sigma}g_{\sigma}S_{\sigma\sigma} + f_{\pi\pi}g_{\pi}S_{\pi\pi}] & \text{for } \beta_{pp} \end{cases} \quad (7-18)$$

Parameterization of this matrix element involves determining the one-center bond terms and appropriate interaction factors.

Encouraged by the simple form of the core terms in the last Section, parameterization of the atom bond parameters with the same form as Equation (7-14) is sought. Standard practice for the determination of resonance integrals requires separate parameterizations for each atom. This requires reliable molecular information for molecules of each atom in a row. In this study the polynomial for a row is parametrized at once. Molecular ionization potentials and excitation spectra for several compounds were used in order to adjust the bond parameter polynomials

and interaction factors. For the present only Hydrogen through Fluorine has been examined. The quadratic term in charge for principal quantum number two was not included due to the relatively few compounds studied.

$$\beta_{\text{H}}(\text{eV}) = -6.527 - 10.157Q + 5.129Q^2 \quad (7-19)$$

$$\beta_{\text{Li-F}}(\text{eV}) = 2.351 - 2.661Z_v - .6716Z_v^2 + (.503 - 5.066Z_v)Q \quad (7-20)$$

$$f_{s\sigma} = .8976, \quad f_{\sigma\sigma} = 1.166, \quad f_{\pi\pi} = .5283 \quad (7-21)$$

Modified SCF Procedure

A modified self consistent field (SCF) program has been developed to incorporate charge iteration. Initially all atoms in a molecule are assumed to be neutral and all parameters and necessary integrals for performing the SCF are their neutral values. In the first SCF sequence, cycling is performed until the density is adequately converged, and a population analysis is obtained. At this point charges are assigned to centers and compared with the previous charges. If they are the same to within a given tolerance the procedure is terminated, else the SCF integrals are updated and the procedure continued. The final SCF sequence

is stopped at normal convergence on energy or density. Normally only two SCF sequences are necessary to observe stable atomic charges.

The diagonal elements of the Fock matrix include a term that can be evaluated as

$$\sum_{B(\neq A)} (P_{BB} - Z_B) \gamma_{AB} = - \sum_{B(\neq A)} Q_B \gamma_{AB} \quad (7-22)$$

for a basis function on center A in which Q_B is the effective charge at center B seen by center A. Since P_{BB} represents the Löwdin population for center B these are used to define atomic charge. Exponents for the overlap portion of the resonance integrals are those of Slater with the exponent for Hydrogen set at 1.2.

Due to the fact that standard INDO/S calculations usually do a poorer job in estimating $n-\pi^*$ excitation energies for carbonyls relative to $\pi-\pi^*$ a modification to the way the core terms are evaluated has been developed to overcome this problem. Consider the noneffectual modification to Equation (7-5).

$$\begin{aligned} E(n_s, n_p, Z) &= n_s(U_s + A) + n_p(U_p - \frac{n_s}{n_p}A) \\ &+ .5(n_s + n_p)(n_s + n_p - 1)F^0 - \frac{1}{6}n_s n_p G^1 - \frac{1}{25}n_p(n_p - 1)F^2 \quad (7-23) \\ &= n_s U'_s + n_p U'_p + \dots \end{aligned}$$

These modified core terms do not effect atomic properties but they do have an effect on the hybridization of a center in a molecular calculation. By making A positive, one moves the one electron s orbital energies closer to the p orbital energies allowing a stronger mixing of the two. A pronounced effect is observed

on the nonbonding orbital energies relative to those of pi bonding. The use of this scheme is only valid in a charge iterative scheme since the ratio n_s/n_p is also modified during the calculation to maintain equivalence between Equations (7-5) and (7-23). The value of A for Oxygen was set at 7eV. This value was determined as a compromise between correcting for $n-\pi^*$ excitation energies while maintaining an accurate prediction of molecular ionization energies.

Results

The results for model compounds used for electronic excitation spectra are presented in Table 7-1 and compared to INDO/S for seven active occupied and virtual orbitals. The RMS error for INDO/S is 3194cm^{-1} and that for the charge iterative model is 1460cm^{-1} . Most noted is the substantial improvement in $n-\pi^*$ carbonyl excitation energies for the charge iterative model. The results for IP's are presented in Table 7-2. The RMS error for INDO/S and for the charge iterative model is 1.18eV. No quantitative improvement is observed for the Koopmans' IP's for the model compounds for the two parameterizations. Both models maintain correct qualitative ordering for the orbital energies except for pyridine. In this case both models place the nonbonding orbital lower in energy than is observed relative to the occupied pi orbitals. This order is corrected in $\Delta E(\text{SCF})$ calculations or through a CI treatment of the positive ion.

Table 7-1 Electronic Excitation Energies for the Model Compounds.

Molecule	Excitation	Exper.(cm-1)	INDO/S	Char. Iter.
Benzene ^a	$\pi \rightarrow \pi^*$	38090	37797	38060
Benzene	$\pi \rightarrow \pi^*$	48972	48370	48483
Benzene	$\pi \rightarrow \pi^*$	55900	54445	54757
Benzene	$\pi \rightarrow \pi^*$	55900	54445	54757
Pyridine ^a	$n \rightarrow \pi^*$	34771	35500	34337
Pyridine	$\pi \rightarrow \pi^*$	38350	38686	38465
Pyridine	$n \rightarrow \pi^*$	-	43911	45294
Pyridine	$\pi \rightarrow \pi^*$	49750	49430	49807
Pyridine	$\pi \rightarrow \pi^*$	~55000	55761	55819
Pyridine	$\pi \rightarrow \pi^*$	~55000	56432	56510
Croton- aldehyde ^b	$n \rightarrow \pi^*$	30490	24729	28264
Croton- aldehyde	$\pi \rightarrow \pi^*$	45454	47182	45638
Form- aldehyde ^c	$n \rightarrow \pi^*$	33898	25653	30370

^a Ref. [52, 53]^b Ref. [112]^c Ref. [24]

Table 7-2 Koopmans' IP's for Model Compounds.

Molecule	Exper.(eV)	INDO/S	Char. Iter.
Benzene ^a	9.25 π	8.95	9.39
Benzene	11.49 σ	12.47	12.60
BNH ₄ ^b	11.36 π	11.35	11.47
BNH ₄	12.08 σ	12.69	12.52
C ₂ H ₄ ^a	10.51 π	9.99	10.38
C ₂ H ₄	12.85 σ	13.52	13.06
F ₂ ^c	15.83 π	16.91	17.20
F ₂	18.8 π	19.2	19.51
Formaldehyde ^d	10.9 n	10.82	12.22
Formaldehyde	14.5 π	13.44	13.99
H ₂ ^a	15.88 σ	18.87	15.73
Pyridine ^e	9.67 n	10.09	10.49
Pyridine	9.8 π	9.06	9.54
Pyridine	10.5 π	9.89	10.04
Li ₂ ^f	4.96 σ	5.11	4.80

^a Ref. [50]^b Ref. [113]^c Ref. [89]^d Ref. [114]^e Ref. [51]^f Ref. [38]

CHAPTER 8 CONCLUSIONS

Spectroscopy

The utility of the random phase approximation in conjunction with the INDO/S model Hamiltonian has been demonstrated. The INDO/CIS method has been very successful in the prediction of transition energies, but has not been as satisfactory in the prediction of absorption probabilities. The RPA method maintains the ability to predict accurate transition energies but also provides considerable improvement in predicting transition moments that compare with experiment, and with differing formalisms. With the INDO/S Hamiltonian both methods require careful consideration in the selection of the active orbitals in the calculation. This is a consequence of utilizing a model Hamiltonian and not a function of the methods themselves. It is encouraging however that a truncated active space is adequate to obtain predictive results. If it were not, some interesting systems would not be appropriate for calculation. The INDO/S-RPA method therefore meets the criteria set forth of being computational feasible for large systems. No degradation in predictability versus size was found to exist for the systems studied.

These methods applied to the study of free base and magnesium porphyrin demonstrate the power of being able to predict accurate oscillator strengths. CIS methods applied to these molecules have not allowed corroboration with experimental observations due partly to the failure to predict accurate oscillator strengths. The ability and utility of the RPA method to selectively correlate transition moments is also demonstrated by predicting an accurate splitting for the intense B band of free base porphyrin.

The calculation of certain response properties are closely related to the ability to accurately predict excitation energies and transition moments. NMR chemical shift is one such property. The ability to present a balanced treatment of transition moments in a finite basis, however, does not imply adherence to the orbital completeness relations which are necessary to accurately predict such properties. The use of a local basis minimizes the effect of long range contributions. Long range contributions usually deteriorate calculated results when utilizing a finite basis. The full magnitude of the paramagnetic term, however, requires a much more complete manifold of states than can be derived from a minimal basis in order to be predictive of experiment. Other response properties, such as polarizability [14], also suffer from the same problem when utilizing MBS formalisms. If semiempirical theories are to be predictive of such properties then extended valence formalisms must be developed and tested. The extension of the MBS formalisms of the INDO Hamiltonian to allow for orbital relaxation in

Chapters 6 and 7 is a step towards modeling extended basis sets for the occupied orbitals. Extending the number and quality of virtual orbitals is a project for the future.

Development of a Better Model

An atom in a molecule gains or loses charge to its neighbors. Although quantum mechanical methods to measure a non-observable like atomic charge are somewhat ambiguous, the observation that the electronic distribution about an atom expands or contracts with gain or loss of electrons is not. Minimum basis set calculations choosing basis sets from neutral atoms are handicapped in this regard. They have fixed extent.

To accommodate electron gain or depletion, orbital exponents can be varied, or linear combinations of different sized orbitals can be used, and either of these refinements leads to major improvements in results. As the former nonlinear variation is much more difficult than the linear optimization of multiple-zeta functions, and, in fact is not as flexible in accommodating differing size for differing molecular orbitals, variation of exponents in molecular calculations is seldom performed. On the other hand, approximate molecular orbital theories are nearly always based on a MBS formalism to preserve simplicity. Accommodation of charge can therefore only be accommodated through the SCF equations, and

this is not enough. If it were, then MBS ab initio calculations would be as effective as multiple-zeta.

In this work two approaches are developed to accommodate orbital relaxation in a fashion that will correct for the major deficiencies of a MBS formalism. The major effects of expansion and contraction of the electronic distribution are accommodated in such a way that both atomic and molecular properties are reproduced with high accuracy.

An atomic model is presented that is capable of reproducing atomic energetics very accurately. The emphasis of this work, however, is methods for spectroscopy. It is demonstrated that improvements to the basic model for molecules can be accomplished through the use of charge dependent formalisms. While maintaining the quality of π - π^* transitions, the simple and physically intuitive strategy for improving n - π^* excitation energies for carbonyl's is possible.

In addition to improving agreement with molecular electronic spectra the information content of atomic parameters is increased while simplifying their structure. By fitting for a whole row at once for all available charges, both the one-center Coulomb integrals and one-electron core integrals are easily obtained with total atomic energies, or total energies and ionization potentials. It is not necessary to obtain orbital electron affinities as is necessary for the use of Pariser's approximation for Coulomb integrals. Since the parameters are constrained to be

at most quadratic in atomic number interpolation for sparse atomic data occurs naturally as does extrapolation to atomic anions. The extension of the form of the one-center core terms to the one-center resonance terms greatly simplifies the parameterization at the molecular level. Much smaller data bases of molecular data can be employed to obtain parameters. If no charge dependence for the resonance integrals is needed, one could define the resonance integrals for a whole row by specifying only three values (preferably the atoms at the ends and one in the middle).

The analysis of the atomic parameters in terms of the chemically useful concepts of orbital hardness and electronegativity provides a connection to the areas of density functional theory. This type of analysis allows the probing of forces within molecules necessary for the description of chemical activity and in this case, orbital energies and electronic spectra.

BIBLIOGRAPHY

1. R. G. Parr, *The Quantum Theory of Molecular Electronic Structure*, W. A. Benjamin, Inc., New York, 1963.
2. R. Pariser and R. G. Parr, *J. Chem. Phys.* **21**, 466 (1953).
3. R. Pariser and R. G. Parr, *J. Chem. Phys.* **21**, 767 (1953).
4. J. A. Pople, *Trans. Faraday Soc.* **49**, 1375 (1953).
5. R. Hoffmann, *J. Chem. Phys.* **39**, 1397 (1963).
6. J. A. Pople, D. L. Beveridge, and P. A. Dobosh, *J. Chem. Phys.* **47**, 2026 (1967).
7. J. Ridley and M. Zerner, *Theor. Chim. Acta* **32**, 111 (1973).
8. J. Linderberg and N. Y. Ohrn, *Propagators in Quantum Chemistry*, Academic, London, 1973.
9. J. C. Y. Chen, *J. Chem. Phys.* **40**, 615 (1964).
10. A. E. Hansen and T. D. Bouman, *Mol. Phys.* **37**, 1713 (1979).
11. J. Oddershede, *Adv. Quantum Chem.* **11**, 275 (1978).
12. E. Dalgaard, *Phys. Rev. A* **26**, 42 (1982).
13. G. D. Purvis and R. J. Bartlett, *J. Chem. Phys.* **75**, 1284 (1981).
14. W. A. Parkinson and M. C. Zerner, *J. Chem. Phys.* **90**, 5606 (1989).

15. T. D. Bouman and A. E. Hansen, *Chem. Phys. Lett.* **149**, 510 (1988).
16. R. G. Parr and W. Yang, *Density-Functional Theory of Atoms and Molecules*, Oxford, New York, 1989.
17. E. Merzbacher, *Quantum Mechanics*, John Wiley and Sons, New York, 1970.
18. I. N. Levine, *Molecular Spectroscopy*, John Wiley and Sons, New York, 1975.
19. I. N. Levine, *Quantum Chemistry*, Allyn and Bacon, Inc., Boston, MA, 1983.
20. J. D. Jackson, *Classical Electrodynamics*, John Wiley and Sons, New York, 1975.
21. A. E. Hansen and T. D. Bouman, *Adv. Chem. Phys.* **44**, 545 (1980).
22. D. J. Griffiths, *Introduction to Electrodynamics*, Prentice-Hall, Inc., New Jersey, 1981.
23. A. Szabo and N. S. Ostlund, *Modern Quantum Chemistry*, Macmillan, New York, 1982.
24. H. Suzuki, *Electronic Absorption Spectra and Geometry of Organic Molecules*, Academic, New York, 1967.
25. L. D. Barron, *Molecular Light Scattering and Optical Activity*, Cambridge, New York, 1982.
26. E. Charney, *The Molecular Basis of Optical Activity*, John Wiley and Sons, New York, 1979.
27. P. Jorgensen and J. Simons, *Second Quantization-Based Methods in Quantum Chemistry*, Academic, New York, 1981.
28. H. F. Schaefer, editor, *Methods of Electronic Structure Theory*, volume 3, Plenum, New York, 1977.

29. C. C. J. Roothaan, *Rev. Mod. Phys.* **23**, 69 (1951).
30. P. O. Lowdin, *J. Chem. Phys.* **18**, 365 (1950).
31. C. W. McCurdy, T. N. Rescigno, D. L. Yeager, and V. McKow, *Methods of Electronic Structure Theory*, volume 3, Plenum, New York, 1977.
32. R. Harris, *J. Chem. Phys.* **50**, 3947 (1969).
33. A. E. Hansen, *Mol. Phys.* **13**, 425 (1967).
34. D. J. Rowe, *Rev. Mod. Phys.* **40**, 153 (1968).
35. N. Ullah and J. Rowe, *Nucl. Phys. A* **163**, 257 (1971).
36. N. S. Ostlund, *J. Chem. Phys.* **57**, 2994 (1972).
37. A. E. Hansen and T. D. Bouman, *Chem. Phys. Lett.* **45**, 326 (1977).
38. J. A. Pople and D. L. Beveridge, *Approximate Molecular Orbital Theory*, McGraw-Hill, New York, 1970.
39. J. A. Pople, D. P. Santry, and D. P. Segal, *J. Chem. Phys.* **43**, S129 (1965).
40. J. A. Pople and G. A. Segal, *J. Chem. Phys.* **43**, S136 (1965).
41. J. A. Pople and G. A. Segal, *J. Chem. Phys.* **44**, 3289 (1966).
42. D. P. Santry and G. A. Segal, *J. Chem. Phys.* **47**, 158 (1967).
43. J. Sadlej, *Semi-Empirical Methods of Quantum Chemistry*, Wiley, New York, 1979.
44. M. Zerner, *Mol. Phys.* **23**, 963 (1972).
45. G. Karlsson and M. Zerner, *Int. J. Quantum Chem.* **7**, 35 (1973).

46. J. C. Slater, Quantum Theory of Atomic Structure, volume 1, McGraw-Hill, New York, 1960.
47. R. J. Pariser, J. Chem. Phys. **21**, 568 (1953).
48. N. Mataga and K. Nishimoto, Z. Physick. Chem. (Frankfurt) **13**, 140 (1953).
49. J. C. Slater, Phys. Rev. **36**, 57 (1930).
50. J. W. Rabalais, Principles of Ultraviolet Photoelectron Spectroscopy, Wiley, New York, 1977.
51. C. R. Brundle, M. B. Robin, and N. A. Kuebler, J. Am. Chem. Soc. **94**, 1466 (1972).
52. J. E. Parkin and K. K. Innes, J. Mol. Spectry. **15**, 407 (1965).
53. K. K. Innes, J. P. Byrne, and I. G. Roos, J. Mol. Spectry. **22**, 125 (1967).
54. G. A. George and G. C. Morris, J. Mol. Spectry. **26**, 67 (1968).
55. H. Baba and I. Yamazaki, J. Mol. Spectry. **44**, 118 (1972).
56. D. Dolphin, editor, The Porphyrins, Part A, Academic, London, 1978.
57. G. D. Dorough, J. R. Miller, and F. M. Huennekens, J. Am. Chem. Soc. **73**, 4315 (1951).
58. H. Kuhn, J. Chem. Phys. **17**, 1198 (1949).
59. W. T. Simpson, J. Chem. Phys. **17** (1949).
60. J. W. Weigl, J. Mol. Spectry. **1**, 133 (1957).
61. C. Rimington, S. F. Mason, and O. Kennard, Spectrochim. Acta **12**, 65 (1958).

62. M. Gouterman, *J. Mol. Spectry.* **6**, 138 (1961).
63. M. Gouterman, G. H. Wagniere, and L. C. Snyder, *J. Mol. Spectry.* **11**, 108 (1963).
64. B. G. Anex and R. S. Umans, *J. Am. Chem. Soc.* **86**, 5026 (1964).
65. C. Weiss, H. Kobayashi, and M. Gouterman, *J. Mol. Spectry.* **16**, 415 (1965).
66. A. J. McHugh, M. Gouterman, and C. Weiss, *Theor. Chim. Acta* **24**, 346 (1972).
67. M. Sundbom, *Acta Chem. Scand.* **22**, 1317 (1968).
68. J. Petke, G. Maggiora, L. Shipman, and R. Christoffersen, *J. Mol. Spectry.* **71**, 64 (1978).
69. L. Edwards, D. H. Dolphin, M. Gouterman, and A. D. Adler, *J. Mol. Spectry.* **38**, 16 (1971).
70. L. Edwards, D. H. Dolphin, and M. Gouterman, *J. Mol. Spectry.* **35**, 90 (1970).
71. W. D. Edwards and M. C. Zerner, *Int. J. Quantum Chem.* **23**, 1407 (1983).
72. N. F. Ramsey, *Phys. Rev.* **78**, 699 (1950).
73. N. F. Ramsey, *Phys. Rev.* **86**, 243 (1952).
74. A. J. Sadlej, *Int. J. Quantum Chem.* **23**, 147 (1983).
75. J. A. Pople, *J. Chem. Phys.* **37**, 53 (1962).
76. G. C. Levy, R. L. Lichter, and G. L. Nelson, *Carbon-13 Nuclear Magnetic Resonance Spectroscopy*, John Wiley and Sons, New York, 1980.

77. G. Boucekkine-Yaker, A. Boucekkine, and G. Berthier, *Int. J. Quant. Chem. Symp.* **18**, 369 (1984).
78. C. M. Rohlfing, L. C. Allen, and R. Ditchfield, *Chem. Phys.* **87**, 9 (1984).
79. M. Schindler and W. Kutzelnigg, *J. Chem. Phys.* **76**, 1919 (1982).
80. B. Levy and J. Ridard, *Mol. Phys.* **44**, 1099 (1981).
81. A. E. Hansen and T. D. Bouman, *J. Chem. Phys.* **82**, 5035 (1985).
82. R. K. Harris, *Nuclear Magnetic Resonance Spectroscopy*, Pitman, London, 1983.
83. J. M. Foster and S. F. Boys, *Rev. Mod. Phys.* **32**, 300 (1960).
84. T. D. Bouman, B. Voigt, and A. E. Hansen, *J. Am. Chem. Soc.* **101**, 550 (1979).
85. H. Taketa, S. Huzinaga, and K. O-Ohata, *J. Phys. Soc. Jap.* **21**, 2313 (1966).
86. L. E. McMurchie and E. R. Davidson, *J. Comput. Phys.* **26**, 218 (1978).
87. J. Facelli, D. Grant, T. Bouman, and A. Hansen, *J. Comput. Chem.* **11**, 32 (1990).
88. M. Schindler and W. Kutzelnigg, *J. Am. Chem. Soc.* **105**, 1360 (1983).
89. J. D. Bene and H. H. Jaffe, *J. Chem. Phys.* **48**, 1807 (1968).
90. J. Hinze and H. H. Jaffe, *J. Chem. Phys.* **38**, 1834 (1963).
91. H. A. Skinner and H. O. Prichard, *Trans. Faraday Soc.* **49**, 1254 (1953).
92. C. E. Moore, *Atomic Energy Levels*; NBS Circular 467, volume I, National Bureau of Standards, Washington, DC, 1949.

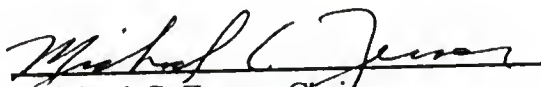
93. J. Huheey, *Inorganic Chemistry*, Harper and Row, New York, 1983.
94. E. Clementi and D. L. Raimondi, *J. Chem. Phys.* **38**, 2686 (1963).
95. J. Hinze and H. H. Jaffe, *J. Am. Chem. Soc.* **84**, 540 (1962).
96. R. P. Iczkowski and J. L. Margrave, *J. Am. Chem. Soc.* **83**, 3547 (1961).
97. R. S. Mulliken, *J. Chem. Phys.* **2**, 782 (1934).
98. H. O. Pritchard and H. A. Skinner, *Chem. Rev* **55**, 745 (1955).
99. R. G. Parr, R. A. Donnelly, M. Levey, and W. E. Palke, *J. Chem. Phys.* **68**, 3801 (1978).
100. R. G. Parr and L. J. Bartolotti, *J. Am. Chem. Soc.* **104**, 3801 (1982).
101. R. G. Pearson, *J. Chem. Educ.* **64**, 561 (1987).
102. M. Berkowitz, S. K. Ghosh, and R. G. Parr, *J. Am. Chem. Soc.* **107**, 6811 (1985).
103. R. G. Parr and R. G. Pearson, *J. Am. Chem. Soc.* **105**, 7512 (1983).
104. J. B. Baker and M. C. Zerner, *J. Phys. Chem.* **94**, 2866 (1990).
105. G. W. Wheland and D. E. Mann, *J. Chem. Phys.* **17**, 264 (1949).
106. R. D. Brown and M. L. Heffernan, *Trans. Faraday Soc.* **54**, 757 (1958).
107. J. M. Parks and R. G. Parr, *J. Chem. Phys.* **32**, 1657 (1960).
108. R. Iffert and K. Jug, *Theor. Chim. Acta* **72**, 373 (1987).
109. I. Kovesdi, *THEOCHEM* **152**, 341 (1987).

- 110. J. A. Singerman and H. H. Jaffe, *J. Am. Chem. Soc.* **103**, 1358 (1981).
- 111. R. L. Ellis, G. Kuehnlenz, and H. H. Jaffe, *Theor. Chim. Acta* **26**, 131 (1972).
- 112. N. S. Bayliss and E. G. McRae, *J. Phys. Chem.* **58**, 1006 (1954).
- 113. N. P. Westwood and N. H. Werstiuk, *J. Am. Chem. Soc.* **108**, 891 (1986).
- 114. Y. Ohrn and G. Born, *Adv. Quantum Chem.* **13**, 1 (1981).

BIOGRAPHICAL SKETCH

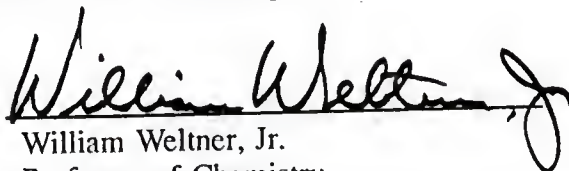
David Baker was born in Lancaster, South Carolina, on October 25, 1961, to John and Margaret who reside there to this day. He has one brother, Philip, who lives in North Carolina with his wife Crystal. He attended the University of South Carolina, majored in chemistry, and graduated in 1982. He worked for Owens-Corning Fiberglas for four years during which time he acquired a wife which he adores and a cat which he very often does not. His wife, Rebecca, is the daughter of Herbert and Billie Corbitt of Columbia, South Carolina. For the last 4.5 years he has attended the University of Florida studying quantum chemistry with Dr. Michael C. Zerner associated with the Quantum Theory Project. His commitment to his church and faith is of paramount importance to him. He aspires to be in academics.

I certify that I have read this study and that in my opinion it conforms to acceptable standards of scholarly presentation and is fully adequate, in scope and quality, as a dissertation for the degree of Doctor of Philosophy.



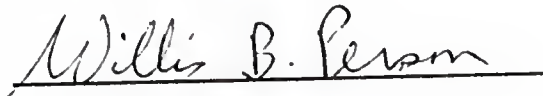
Michael C. Zerner, Chair
Professor of Chemistry and
Physics

I certify that I have read this study and that in my opinion it conforms to acceptable standards of scholarly presentation and is fully adequate, in scope and quality, as a dissertation for the degree of Doctor of Philosophy.



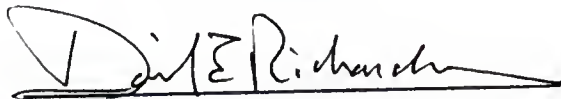
William Weltner, Jr.
Professor of Chemistry

I certify that I have read this study and that in my opinion it conforms to acceptable standards of scholarly presentation and is fully adequate, in scope and quality, as a dissertation for the degree of Doctor of Philosophy.



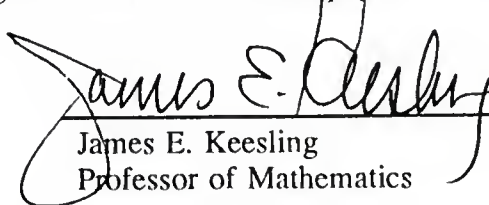
Willis B. Person
Professor of Chemistry

I certify that I have read this study and that in my opinion it conforms to acceptable standards of scholarly presentation and is fully adequate, in scope and quality, as a dissertation for the degree of Doctor of Philosophy.



David E. Richardson
Associate Professor of Chemistry

I certify that I have read this study and that in my opinion it conforms to acceptable standards of scholarly presentation and is fully adequate, in scope and quality, as a dissertation for the degree of Doctor of Philosophy.


James E. Keesling
Professor of Mathematics

This dissertation was submitted to the Graduate Faculty of the Department of Chemistry in the College of Liberal Arts and Sciences and to the Graduate School and was accepted as partial fulfillment of the requirements for the degree of Doctor of Philosophy.

May 1991

Dean, Graduate School

UNIVERSITY OF FLORIDA



3 1262 08285 456 2